Flow Science Incorporated
420 Neff Avenue, Suite 230, Harrisonburg, VA 22801
(540) 442-8433 • FAX (540) 442-8863

Water Purification Demonstration Project: Limnology and Reservoir Detention Study of San Vicente Reservoir – Nutrient and Algae Modeling Results

Prepared for
City of San Diego
600 B Street, Suite 600,
San Diego, CA 92101

Prepared By
Li Ding, Ph.D., P.E. (VA)
Senior Engineer

Reviewed By
Imad A. Hannoun, Ph.D., P.E. (VA)
President

Reviewed By
E. John List, Ph.D., P.E. (CA)
Principal Consultant

FSI V094005
May 01, 2012

Table of Contents

List of Tables

List of Figures

SUMMARY

San Vicente Reservoir (SVR) is located near Lakeside, California, and is used as a source of drinking water supply by the City of San Diego (City), its owner and operator. The reservoir currently has a capacity of about 90,000 acre-feet (see Figure 1). It is undergoing an expansion that will raise the dam 117 feet (ft) and increase the reservoir's storage to 247,000 acre-feet at the spillway level (or 242,000 acre-feet at the maximum operation level). The City is considering an option to augment SVR supply by bringing advanced purified recycled water (*i.e.*, purified water) from the advanced water purification facility to SVR. The purified water would be blended with other water in the reservoir. The current project – the Water Purification Demonstration Project (Demonstration Project) – will not actually put any purified water into the reservoir; rather it will study and model the reservoir augmentation process. A component of the Demonstration Project is the Limnology and Reservoir Detention Study of San Vicente Reservoir (Limnology Study).

As part of the Limnology Study, Flow Science Incorporated (FSI) has developed a three-dimensional water quality model that is used to evaluate hydrodynamic and water quality effects of using purified water to augment SVR. After the model was developed, its results were compared to existing field data and documented in a Technical Memorandum (TM #1) submitted to the City in 2010 (FSI, 2010). The TM #1 has been peer-reviewed by the National Water Research Institute Independent Advisory Panel (NWRIIAP) that was assembled for the review of the City's Demonstration Project. After implementing suggestions proposed by the NWRIIAP, the model was deemed by NWRIIAP to be "an effective and robust tool, for 1) simulating thermoclines and hydrodynamics of the San Vicente Reservoir; 2) assessing biological water quality for nutrients; 3) assessing options for the purified water inlet location" (NWRIIAP, 2010).

Upon completion of the SVR model calibration and validation, FSI conducted simulations of purified water delivery to the expanded SVR under various projected future operating conditions using the calibrated/validated model. The simulation results and findings are presented in two separate Technical Memorandums (TM #2 and TM #3). The TM #2 summarizes the hydrodynamic aspects of the modeling results and was submitted to the City on November 28, 2011. This report, TM #3, focuses on the water quality aspects of the modeling results and findings, with emphasis on nutrients (phosphorus and nitrogen), dissolved oxygen (DO), and algal concentration levels. The water quality parameters evaluated include chlorophyll *a* (a surrogate measure of algal growth), DO, pH, nitrate as N, ammonia as N, Total Nitrogen (TN), Soluble Reactive Phosphorus (SRP), Total Phosphorus (TP) and Secchi depth.

The goal of this work is to determine the effects of purified water delivery on the reservoir's water quality under anticipated future conditions in the expanded reservoir.

Because both the reservoir expansion and augmentation with purified water are expected to affect the reservoir water quality, a two-step approach was taken in this study to examine the water quality effects caused by the reservoir expansion and argumentation, respectively.

RESERVOIR EXPANSION

First, the SVR model was used to determine the effects of the reservoir expansion on water quality, without the introduction of any purified water. This was accomplished by performing a simulation (referred to as Expanded Reservoir Case) that uses the same reservoir conditions (climate, inflow and outflow volumes and concentrations etc.) as the 2006 - 2007 calibration simulation (*i.e.*, Existing Case), except for using a higher initial reservoir volume that is set at 155,000 acre-feet (median expected future storage). The results from the Expanded Reservoir Case were compared against those from the Existing Case. The differences between the results of these two simulations demonstrate the effects of the expansion on the reservoir's water quality in the absence of any purified water discharge to the reservoir.

Based on the results of these two simulations, the following conclusions and observations on the effects of the reservoir expansion can be made:

- As evidenced in **Table S-1**, the reservoir expansion is predicted to extend the duration of the hypolimnetic anoxia by an average of 27 days per year (from 189 days per year to 216 days per year) and enlarge the volume of water under anoxic condition by at least two fold.

- The reservoir expansion will produce lower surface chlorophyll *a* concentrations and higher Secchi depths *(i.e.*, better water clarity) in the reservoir. It is predicted that the annual average chlorophyll *a* concentration will decrease from 5.8 micrograms per liter (µg/L) to 3.4 µg/L and the annual average Secchi depth will increase from 3.2 meters (m) to 4.7 m after the expansion.

- Based on a nutrient loading calculation, the internal nutrient loadings *(i.e.*, nutrients released from sediment) are larger than all external loadings combined over the two-year modeling period for both the Existing Case and Expanded Reservoir Case. Meanwhile, the reservoir expansion is predicted to lead to a significant increase in sediment nutrient release, likely due to the larger hypolimnetic bottom area and extended hypolimnetic anoxia period. However, despite the significantly higher sediment release, surface TN concentrations are actually lower after the reservoir expansion, a result of the significantly larger volume of water for the Expanded Reservoir Case. The resulting lower nutrient concentrations are believed to be one of the main factors that lead to lower surface

chlorophyll *a* concentrations for the Expanded Reservoir Case (compared to the Existing Reservoir Case).

Table S-1. Summary of Bottom Anoxia[1] Occurrence for Existing Case and Expanded Reservoir Case

Simulation	Days Under Anoxia: Total Days (Percentage)[2]	Average Surface Chlorophyll *a* (µg/L)	Average Secchi Depth (m)
Existing Case	189 (52%)	5.8	3.2
Expanded Reservoir Case	216 (59%)	3.4	4.7

Notes:1. Anoxia is defined here as the bottom DO less than 0.5 mg/L
2. Both the total number of days and percentage under anoxia are yearly values averaged over the two-year simulation period.

FUTURE OPERATING CONDITIONS

After the effects of the reservoir expansion were determined, the model was used to examine the water quality in the expanded reservoir under future operating conditions both with and without purified water augmentation. Specifically, the following two future scenarios were simulated:

- Base Case (includes purified water inflow) ---- This scenario considered an expanded reservoir under median expected storage and expected future operations. The initial reservoir volume for the Base Case is set at 155,000 acre-feet. The following annual flow rates were assumed: for aqueduct inflow 3,000 acre-feet/year (a-f/y); runoff 4,500 a-f/y; purified water inflow 15,000 a-f/y; and dam withdrawal 19,000 a-f/y, with no water transfers from Sutherland Reservoir into SVR.

- No Purified Water ---- The inputs for this scenario are similar to those for the Base Case scenario, except for no purified water additions and an equal reduction in reservoir outflow. The initial reservoir volume for this scenario is set at 155,000 acre-feet. The annual flow rates for aqueduct inflow, runoff, purified water inflow and dam withdrawal are 3,000, 4,500, 0 and 4,000 acre-feet/year respectively. There are no water transfers from Sutherland Reservoir into SVR.

Results from the Base Case and No Purified Water scenarios were compared against those obtained from the Existing Case simulations (*i.e*., no reservoir expansion). Based on the simulation results, the following conclusions and observations on the effects of the purified water and future operating conditions are made:

- The hypolimnetic anoxia period is predicted to last an average of 189 days per year for the Existing Case (**Table S-2**). For the No Purified Water scenario, the hypolimnetic anoxia period is predicted to increase to 207 days per year, an addition of 18 days per year. Adding purified water into the reservoir under future operating conditions (*i.e.*, Base Case) will further extend the average duration of the hypolimnetic anoxia period by 8 days, to a total of 215 days per year.

- The No Purified Water scenario produces lower algae levels *(i.e.*, lower surface chlorophyll *a* concentrations) and higher Secchi depths (*i.e.*, better water clarity) compared to the Existing Case. For example, the annual average chlorophyll *a* concentration and Secchi depth are predicted to be 5.8 µg/L and 3.2 m respectively for the Existing Case (**Table S-2**). By comparison, the annual average chlorophyll *a* concentration and Secchi depth are predicted to be 3.1 µg/L and 4.8 m, respectively, for the No Purified Water scenario in the expanded reservoir. This is a reduction of 2.7 µg/L for the average chlorophyll *a* concentration and an increase of 1.6 m for the average Secchi depth compared to the Existing Case.

- The Base Case scenario also produces lower algae levels *(i.e.*, lower surface chlorophyll *a* concentrations) and higher Secchi depths (*i.e.*, better water clarity) compared to the Existing Case. The Base Case is predicted to produce 3.7 µg/L for the annual average chlorophyll *a* concentration and 4.3 m for the annual average Secchi depth (**Table S-2**). This is a reduction of 2.1 µg/L for the average chlorophyll *a* concentration and an increase of 1.1 m for the average Secchi depth compared to the Existing Case.

- Nutrient loading calculations show that nutrient sediment release constitutes a significant portion of all nutrient loadings into SVR for all future scenarios as well as the Existing Case. The future operating scenarios (*i.e.*, Base Case and No Purified Water) produce sediment nutrient loadings significantly larger than those for the Existing Case, likely a result of the larger hypolimnetic bottom area and extended hypolimnetic anoxia period. However, despite the significantly higher sediment release for the future operating scenarios, surface TN concentrations are actually lower for the future scenarios compared to the Existing Reservoir Case, a result of the larger volume of water in the expanded reservoir. The resulting

lower nutrient concentrations are believed to be one of the main factors that lead to lower surface chlorophyll *a* concentrations for the future operating scenarios (compared to the Existing Reservoir Case).

- Nutrient limitation in SVR can be affected by various factors including the nutrient loadings from all the inflows and the sediments. As a result, nutrient limitation at any point may vary based on existing conditions. However, note that the N:P ratio of the purified water is expected to reach about 159, indicating that algal growth in the future reservoir may tend to become more phosphorus-limited.

Table S-2. Summary of Simulated DO, Chlorophyll *a* and Secchi Depth for Modeling Scenarios

Operating Scenarios	Days Under Anoxia[1]: Total Days (Percentage)[2]	Average Surface Chlorophyll *a* (µg/L)	Average Secchi Depth (m)
Existing Case	189 (52%)	5.8	3.2
No Purified Water	207 (57%)	3.1	4.8
Base Case	215 (59%)	3.7	4.3

Notes: 1. Anoxia is defined here as the bottom DO less than 0.5 mg/L.
2. Both the total days and percentage under anoxia are yearly values averaged over the two-year simulation period.

1. INTRODUCTION

1.1 BACKGROUND

San Vicente Reservoir (SVR) is located near Lakeside, California, and is used as a drinking water supply by the City of San Diego (City), its owner and operator (**Figure 1**). The reservoir currently has a capacity of about 90,000 acre-feet. It is undergoing an expansion that will raise the dam by 117 feet and increase the reservoir's storage to 247,000 acre-feet at the spillway level (or 242,000 acre-feet at the maximum operation level). The reservoir expansion is scheduled to be completed in 2013.

In the meantime, a water reuse project, entitled Reservoir Augmentation, is being studied by the City. If implemented at full-scale, Reservoir Augmentation would bring advanced purified recycled water (*i.e.*, purified water) from the advanced water purification facility to the expanded SVR via a pipeline. The purified water would be blended with other water in the reservoir. The current project – the Water Purification Demonstration Project (Demonstration Project) – will not actually put any purified water into the reservoir; rather it will study and model the Reservoir Augmentation process. A component of the Demonstration Project is the Limnology and Reservoir Detention Study of San Vicente Reservoir (Limnology Study).

As part of the Limnology Study, Flow Science Incorporated (FSI) has developed a three-dimensional computer model that is used to evaluate hydrodynamic and water quality effects of using purified water to augment SVR. After the model was developed, its results were compared to existing field data and documented in a Technical Memorandum (TM #1) submitted to the City in 2010 (FSI, 2010). The TM #1 has been peer-reviewed by the National Water Research Institute Independent Advisory Panel (NWRIIAP) that was assembled for the review of the City's Demonstration Project. The model was deemed by NWRIIAP, with some fine-tuning, as "an effective and robust tool, for 1) simulating thermoclines and hydrodynamics of the San Vicente Reservoir; 2) assessing biological water quality for nutrients; 3) assessing options for the purified water inlet location" (NWRIIAP, 2010). After the review, all the suggestions by NWRIIAP on fine-tuning the model have been addressed or implemented. Findings and results from the TM #1 that are relevant to the work presented here are summarized in the next section.

Upon completion of the SVR model calibration and validation, FSI conducted simulations of purified water release to the expanded reservoir under various projected future operating conditions using the calibrated/validated model. The simulation results and findings are presented in two separate Technical Memorandums (TM #2 and TM #3). The TM #2 summarizes the hydrodynamic aspects of the modeling results and was submitted to the City on November 28, 2011. The highlights of TM#2 are included in the

next section. This current report, TM #3, focuses on the water quality aspects of the modeling results and findings with emphasis on nutrients (phosphorus and nitrogen), DO, and algal concentration levels. The water quality parameters evaluated include chlorophyll *a* (a surrogate measure of algal growth), DO, pH, nitrate as N, ammonia as N, Total Nitrogen (TN), Soluble Reactive Phosphorus (SRP), Total Phosphorus (TP) and Secchi depth.

This work has been performed by Flow Science Incorporated (FSI) of Pasadena, California, under contract to the City of San Diego, California.

1.2 THE SVR MODEL

1.2.1 General Description of the SVR Model

The three-dimensional SVR model consists of two coupled computer models that simulate both the hydrodynamics and water quality of SVR. These two models are the Estuary Lake and Coastal Ocean DYnamics Model (ELCOM) for hydrodynamic simulation and the Computational Aquatic Ecosystem DYnamics Model (CAEDYM) for water quality simulation. ELCOM requires the user to define boundary conditions, physical inputs, meteorological inputs, and bathymetry in a grid structure. The output from ELCOM consists of predictions for water velocities, temperature, salinity (*i.e.*, conductivity), and concentrations of decaying or conservative tracers in space and time within the body of water. CAEDYM is a suite of water quality modules that compute interactions between biological organisms and the chemistry of their nutrient cycles (**Figure 2**). It is coupled with ELCOM to simulate the biochemical parameters of an aquatic ecosystem including carbon, nitrogen, phosphorus, silicon, organic matter, DO, pH, inorganic suspended solids, metals, carbon, fish and chlorophyll *a*. In this study, we focus on simulation results for nutrients (*i.e.*, nitrogen and phosphorus), DO and algae in the expanded SVR. Detailed information and technical descriptions concerning ELCOM and CAEDYM are included in **Appendix A**.

The SVR modeling domain includes both the existing reservoir as well as the proposed expanded reservoir (**Figure 1**). A grid with a horizontal resolution of 100 × 100 m is used in this study – similar to the grid used in the water quality calibration (**Figure 3**). It should be noted that the horizontal grid used in the water quality simulation is coarser than the grid used in the hydrodynamic simulation (*i.e.*, 50 × 50 m in resolution) in order to ensure a reasonable computational time. The vertical grid used in the water quality simulation is the same as that used in the hydrodynamic simulation, with a grid size of 1.64 ft (0.5 m) near the surface and expanding in size with depth. A test has been conducted (and presented in TM #1) to evaluate the accuracy of the coarse grid in simulating temperature and conductivity. It concluded that using either the fine or coarse grids will result in almost identical predicted conductivity and temperature

profiles. Therefore, it is appropriate to use the coarse grid in the water quality simulation to ensure adequate model resolution and reasonable model run times.

1.2.2 Model Calibration/Validation

The model calibration was conducted for the two-year period of 2006 and 2007. The input data required by the calibration were either based on the measured data or derived from these data. Various comparisons between model and data are presented in the TM #1 and they include temperature, conductivity, DO, pH, nutrients (nitrogen and phosphorus), chlorophyll *a* and Secchi depth. In the following, we discuss the highlights of TM #1.

1.2.2.1 Hydrodynamic (ELCOM) Calibration/Validation

The calibrated/validated ELCOM model shows good agreement with the measured data for both water temperature and conductivity. For example, the onset and duration of thermal stratification as well as the deepening rate of the thermocline were predicted accurately by the model (**Figure 4**). In particular both the field data and model show that winter water temperatures in the fully mixed reservoir were nearly uniform in the vertical direction at a value near 12 ^{o}C to 13 ^{o}C. By April, increased solar radiation warmed the water surface up to 17 ^{o}C to 18 ^{o}C and thermal stratification started to develop. This process intensified and by summer (July through September) the surface temperatures had risen to as high as 28 ^{o}C, while the temperature in the hypolimnion remained nearly unchanged at the winter temperature of 12 ^{o}C to 13 ^{o}C. This large temperature difference between surface and bottom indicates that a strong vertical stratification was established in the lake. The thermocline was well defined and located at a depth ranging from approximately 30 to 40 ft, as shown in **Figure 4** for both the model and the data. In the fall, surface water temperatures steadily decreased due to reduced solar radiation and cooler air temperatures. This generated convective plumes within the reservoir, which combined with more effective wind mixing, deepened the thermocline to a depth of 60 ft by November. The stratification continued to weaken until the reservoir totally destratified and became well mixed at the end of the year, or at the beginning of the following year. The variation of conductivity in the reservoir was also well captured by the model (see Figures 18-20 in TM #1 for the calibration results in conductivity).

After the ELCOM model was calibrated, a validation was performed to compare the model against the results of previous tracer field studies. The validation shows that the model was capable of replicating the main features of the tracer study. This provides verification and assurance that the model performance is reliable and accurate in simulating hydrodynamics in the reservoir.

1.2.2.2 Water Quality (CAEDYM) Calibration

For all the simulated water quality parameters, the calibrated CAEDYM model shows overall good agreement with measured data. For example, both field data and simulation show that DO concentrations at the surface remained high throughout the years as a result of both the supply of oxygen directly from the atmosphere and of oxygen produced by photosynthetic activity near the surface (**Figure 5**). At high rates of photosynthesis, oxygen production by algae exceeded the diffusion of oxygen out of the system and this resulted in occasional oxygen supersaturation in the spring of 2006 and 2007. At the beginning of the simulation period, DO near the bottom of the reservoir was near saturation levels, a result of strong vertical mixing in the winter period. However, during the spring and summer, strong stratification at SVR inhibited vertical mixing and the DO at the bottom was quickly depleted by the decay of organic material (primarily algae cells) settling through the water column and organic matter in the sediments (*i.e.*, Sediment Oxygen Demand or SOD). The water in the hypolimnion became anoxic (defined as DO < 0.5 milligrams per liter [mg/L] herein) in the spring and anoxia lasted through the fall for both years, until the reservoir became destratified in the winter. **Figure 5** shows that the simulated DO concentrations captured the major trends in the measured DO concentrations, including the onset, duration, and magnitude of anoxia in the hypolimnion, the hypolimnetic DO decay rate in the spring, and the high surface DO concentrations resulting from algae blooms.

The available in-reservoir chlorophyll *a* data were qualitatively measured using a fluorometer that had not been calibrated. The calibration of chlorophyll *a* was conducted indirectly through comparisons with measured Secchi depth (**Figure 6**). Note that the formula used to derive Secchi depths using surface chlorophyll *a* concentrations is presented in the figure and this formula was also used in this study to obtain Secchi depths in all scenarios presented here. As shown in **Figure 6**, the Secchi depths from the calibration match fairly well with the measured Secchi depths, indicating a reasonably good calibration for chlorophyll *a*.

In conclusion, the SVR model is capable of capturing both the hydrodynamic features and the water quality variations in the reservoir. The simulation results are generally in good agreement with the field measurements. Thus the model provides "an effective and robust tool, for simulating thermoclines and hydrodynamics of the San Vicente Reservoir" and for "assessing biological water quality for nutrients" (findings from NWRIIAP, 2010). For more details of the calibration/validation refer to TM #1 (FSI, 2010).

1.3 SUMMARY OF HYDRODYNAMIC RESULTS IN TM #2

TM #2 presented the hydrodynamic results of various projected future operating scenarios for the expanded SVR. In particular, simulation results for temperature, conductivity and tracers are included in TM #2 for evaluation of reservoir hydrodynamics. Note that TM #2 has been peer-reviewed by NWRIIAP, which concluded that "the modeling is sufficiently predictive for purposes of evaluating the input of advanced treated recycled water" (NWRIIAP, 2012). In the simulations presented in TM #2, various hypothetical tracers were added to the purified water inflow to illustrate dilution, mixing and transport of the purified water within the reservoir. In particular, decaying tracers were used to study the dilution and inactivation of potential pathogens entering the reservoir; conservative tracers (*i.e.*, non-decaying) were used to simulate potential effects of elevated concentrations of chemical constituents in the purified water entering SVR after "excursion events" at the water purification facility.

Based on the simulation results, several key conclusions for the reservoir hydrodynamics were drawn in TM #2 and are listed here:

- Reservoir expansion will increase the volume of the hypolimnion but will have a negligible effect on overall temperature variation patterns as well as the thermocline depth during stratified periods.

- For all simulated future operating scenarios, decaying tracer concentrations in the reservoir outflow are predicted to achieve a 2-log reduction (100:1 reduction in concentration) in the unstratified period and significantly higher reductions (at least 4 logs; that is, a 10,000:1 reduction) in the stratified period.

- The minimum predicted dilution in the reservoir outflow for conservative tracers is about 900:1 for all simulated future operating scenarios.

- Moving the purified water inlet location closer to the reservoir outlet is predicted to generally (but not always) result in slightly higher values in the reservoir outflow concentrations for both the decaying and conservative tracers during the unstratified period. During the stratified period, different purified water inlet locations have little effect on decaying and conservative tracer concentrations in the reservoir outflow.

1.4 APPROACH AND REPORT ORGANIZATION

The goal of the work presented here is to determine the effects of purified water on the reservoir's water quality under anticipated future operating conditions in the expanded reservoir. Both the reservoir expansion and augmentation with purified water are expected to affect the reservoir water quality. Thus, a two-step approach was taken with the intent of examining the effects caused by each of these two changes. First, water quality effects caused solely by the reservoir expansion are investigated in **Chapter 2** by comparing results from two simulations that are different in the initial reservoir water volume, but otherwise identical. In **Chapter 3**, the water quality of the expanded reservoir under future operating conditions is examined, both with and without purified water augmentation to demonstrate the combined effects of argumentation and expansion under future operating conditions. Finally, conclusions and discussion are provided in **Chapter 4**.

2. EFFECTS OF RESERVOIR EXPANSION

The existing SVR has a capacity of 90,000 acre-feet and is currently undergoing an expansion to a capacity of 247,000 acre-feet that will be completed in 2013. Absent the Reservoir Augmentation project, SVR will be filled with imported water, local runoff, and water transferred from Sutherland Reservoir. Should the Reservoir Augmentation project go forward, the purified water would substitute for some of the imported water. The purified water would be diluted with other water stored in the reservoir. It is expected that the reservoir expansion alone could cause changes in the reservoir water quality. Thus, it is useful to investigate these anticipated changes in order to understand the future baseline conditions in the expanded reservoir. This was accomplished by performing a simulation that uses the same reservoir conditions (climate, inflow and outflow parameters etc.) as the 2006 - 2007 calibration simulation, except for using a higher initial reservoir volume that is set at 155,000 acre-ft (median expected future storage, see **Table 1**). This simulation is referred to herein as the Expanded Reservoir Case and the results from this simulation are compared to those from the original calibration in the unexpanded reservoir (henceforth referred as the Existing Case). The differences between the Existing Case and Expanded Reservoir Case therefore demonstrate the effects of the reservoir's expansion on water quality under the same operating conditions.

It should be noted that the nutrient levels in all the existing inflows to SVR are highly variable. **Figure 7** shows an example of nutrient levels in one of the main inflows to SVR, the aqueduct inflow, during the modeling period. The highest concentration of TN, for example, is almost four times that of the lowest concentration. This is expected to lead to variable nutrient and algae levels in the reservoir.

2.1 COMPARISON OF MODELING RESULTS

Figure 8 shows a comparison of simulated water temperatures from the Existing Case and Expanded Reservoir Case. The depth and deepening rate of the thermocline are fairly similar between these two simulations, indicating that the reservoir expansion will cause no major changes in the thickness of the epilimnion. Note that the volume of the epilimnion is somewhat larger for the Expanded Reservoir Case, mostly a result of the increase in the reservoir's surface area. However, the thickness and volume of the hypolimnion will be significantly larger for the Expanded Reservoir Case. With a larger hypolimnion, the reservoir from the Expanded Reservoir Case is predicted to destratify in the late fall or early winter a few days later than that from the Existing Case.

Table 1. Summary of Bottom Anoxia[1] Occurrence for Existing Case and Expanded Reservoir Case

Simulation	Year	Initial Reservoir Volume (acre-feet)	Bottom Anoxia Period	Days Under Anoxia: Total Days (Percentage)[2]	Average Surface Chlorophyll *a* (µg/L)	Average Secchi Depth (m)
Existing Case	2006	64,000	1/1 – 1/15 7/10 – 12/14	189 (52%)	5.8	3.2
	2007	60,000	6/8 – 12/28			
Expanded Reservoir Case	2006	155,000	1/1 – 1/19 6/21 – 12/23	216 (59%)	3.4	4.7
	2007	149,000	5/21 – 12/31			

Notes:1. Anoxia is defined here as the bottom DO less than 0.5 mg/L
2. Both the total number of days and percentage under anoxia are yearly values averaged over the two-year simulation period.

Figure 9 shows contours of simulated DO from the Existing Case and Expanded Reservoir Case at Station A (see **Figure 1** for Station A location). Time series of simulated surface and bottom DO at the same station are presented in **Figure 10**. As shown, the simulated DO exhibits similar patterns between the Existing Case and Expanded Reservoir Case. At the surface, DO concentrations are relatively high due to the oxygen replenishment from the atmosphere and algal production. At the bottom, DO concentrations steadily decrease during the stratified period because of algae decay and SOD, then rise sharply during the unstratified period as vertical mixing transports surface water with high DO towards the bottom.

Despite the similarities in overall DO profiles, reservoir expansion produces a few changes in DO concentrations in the reservoir as well. First, reservoir expansion significantly increases the volume of water under anoxic condition. **Table 2** lists volumes of water under an anoxic condition on several selected days during the two-year simulation period for both the Existing Case and the Expanded Reservoir Case. It shows that the volume of water under an anoxic condition in the Expanded Reservoir Case is at least twice and sometimes five times, as large as for the Existing Case. Secondly, during the unstratified period, DO concentrations in the Expanded Reservoir Case are predicted to be lower than those in the Existing Case. This is a result of the increased reservoir depth and the somewhat slower destratification rate for the Expanded Reservoir Case. This is one of the factors that lead to the predicted early onset of hypolimnetic anoxia for the Expanded Reservoir Case. For example, the hypolimnetic anoxia period starts on 6/21 in 2006 for the Expanded Reservoir Case compared to 7/10 for the Existing Case. Finally, the reservoir expansion delays destratification and prolongs the duration of hypolimnetic anoxia in the reservoir. In the Existing Case in 2006, the hypolimnetic

anoxia period is predicted to end on 12/14. In the Expanded Reservoir Case, the hypolimnetic anoxia period is predicted to end on 12/23, a delay of 9 days. Overall, the hypolimnetic anoxia period from the Existing Case consists of 52% of the time per year on average, which is equivalent to 189 days per year (**Table 1**). With the reservoir expansion, the reservoir experiences hypolimnetic anoxia for 59% of the time or for 216 days per year on average. Thus, given the same operating conditions the reservoir expansion is predicted to extend the hypolimnetic anoxia period by an average of 27 days per year.

Table 2. Predicted Volume of Water under Anoxic Conditions in the Existing Case and Expanded Reservoir Case

Date	Existing Case (acre-ft)	Expanded Reservoir Case (acre-ft)
8/1/06	15,900	48,000
10/1/06	17,600	64,600
12/1/06	15,900	82,300
8/1/07	25,000	57,600
10/1/07	32,500	66,500
12/1/07	24,000	82,300

Note: The volume of water under an anoxic condition is defined as the layer with DO less than 0.5 mg/L

Predicted time series of ammonia (as N), nitrate (as N), TN, SRP and TP at the surface and bottom of the reservoir are presented in **Figures 11 - 15**. Note that TN (TP) is defined as the sum of all particulate and soluble forms of nitrogen (phosphorus). Except for nitrate, all nutrients behave in a similar fashion. At the surface, nutrient concentrations (nitrogen and phosphorus) are generally low during the spring and summer due to algal consumption, and are generally high during the unstratified period when surface water is mixed with the nutrient-rich hypolimnion. At the bottom, nutrient concentrations (except for nitrate) generally show an opposite trend from surface nutrient concentrations: they rise during the stratified period as a result of sediment nutrient release and fall sharply during the unstratified period after being mixed with the surface water in which nutrients are depleted by algae. For nitrate, variation patterns are different from those displayed by other nutrient components. Nitrate levels are low in the summer and high in the winter at both the surface and the bottom (**Figure 12**). In the summer, algal growth consumes most of surface nitrate and the hypolimnetic anoxic condition leads to the loss of the bottom nitrate through denitrification or conversion to ammonia. In the winter, large influxes of nitrate from surface runoff and aqueduct inflow are mostly responsible for the rise in nitrate concentration at the surface and bottom within the reservoir.

Figure 16 shows predicted time series of surface chlorophyll *a* concentrations and **Figure 17** shows time series of Secchi depths derived from simulated chlorophyll *a*. Both figures indicate that the reservoir expansion will lower surface chlorophyll *a* levels and increases Secchi depth in the reservoir. **Table 1** lists predicted annual averages of surface chlorophyll *a* concentration and Secchi depth. With the expansion, the annual average surface chlorophyll *a* concentration is predicted to decrease from 5.8 µg/L to 3.4 µg/L, a 41% reduction in annual algal growth. This leads to a 47% increase in the annual average Secchi depth after expansion; the annual average Secchi depth increases from 3.2 m for the Existing Case to 4.7 m for the Expanded Reservoir Case.

A comparison of simulated pH between the Existing Case and Expanded Reservoir Case is presented in **Figure 18.** As shown, the pH is fairly similar for both simulations.

2.2 NUTRIENT LOADINGS

Phosphorus and nitrogen loadings have been computed for all inflows to SVR, as well as estimated for sediment release for both the Existing Case and Expanded Reservoir Case (**Tables 3** and **4**). The external nutrient loadings (*i.e.*, loadings from inflows) are calculated as the product of water inflow rate and the associated nutrient concentrations. The model does not directly output the total nutrient loadings from the sediments (*i.e.*, internal loadings). However, an order-of-magnitude estimate was computed for the sediment nutrient loading by multiplying the hypolimnetic volume of the reservoir by the rise in nutrient concentration at the reservoir bottom. Nutrient fluxes by atmospheric deposition are considered to be negligible.

As shown in **Tables 3** and **4**, estimated sediment nutrient loadings constitute a significant portion of the total nutrient loadings to the reservoir. In fact, the reservoir is calculated to receive more nutrients from the sediments than those from all inflows combined over the two-year modeling period. For example, in the Expanded Reservoir Case, the sediments release calculations shows about 26.6 tons TP over the two-year period and the total TP loading from all inflows is calculated to be 9.2 tons over the same period. In the Existing Case, the calculated sediment TP loading and the sum of all inflow TP loadings are 11.7 and 9.2 tons, respectively, over the two-year period.

In general, the limiting factor for algal growth is considered to be nitrogen if N:P < 10 and phosphorus if N:P > 10 (Horne and Goldman, 1994). From **Tables 3** and **4**, the ratios of TN:TP total loadings for the Existing Reservoir and Expanded Reservoir range from 3-6, indicating algal growth is likely limited by nitrogen in the reservoir. Note, however, that the inflow water quality is very variable and depends on both the water source and seasonality so the nutrient limitation at any specific instant may vary.

Tables 3 and **4** also show that the estimated total amount of nutrients released by sediments are generally larger in the Expanded Reservoir Case than in the Existing Case, partly a result of the larger hypolimnetic bottom area and extended hypolimnetic anoxia period for the Expanded Reservoir Case. The sediments are estimated to release a total of 26.6 tons TP over the two-year period in the Expanded Reservoir Case, more than twice of that in the Existing Case (*i.e.*, 11.7 tons TP). For TN, the estimated sediment release in the anoxic period is 80.6 tons for the Expanded Reservoir Case, almost three times the amount for the Existing Case (*i.e.*, 27.6 tons).

In conclusion, the reservoir expansion is predicted to slightly extend the duration of the hypolimnetic anoxia and enlarge the volume of water under anoxic condition. The reservoir expansion also produces lower surface chlorophyll *a* concentrations and higher Secchi depth *(i.e.*, more water clarity). Based on a nutrient loading calculation, the internal nutrient loadings *(i.e.*, sediment release) are larger than all external loadings combined over the two-year modeling period for both the Existing Case and Expanded Reservoir Case. Meanwhile, the reservoir expansion leads to an increase in sediment nutrient release due to the larger hypolimnetic bottom area and extended hypolimnetic anoxia period. However, despite the significantly higher sediment release, surface TN concentrations are actually lower after the reservoir expansion (**Figure 13**), a result of the significantly larger volume of water for the Expanded Reservoir Case. The resulting lower nutrient concentrations are believed to be one of the main factors that lead to lower surface chlorophyll a concentrations for the Expanded Reservoir Case (compared to the Existing Reservoir Case).

Table 3. Estimated Annual Phosphorus Loadings[1] for the Existing and Expanded Reservoir

Sources	SRP				TP			
	Existing Case		Expanded Reservoir Case		Existing Case		Expanded Reservoir Case	
	2006	2007	2006	2007	2006	2007	2006	2007
Purified Water	0	0	0	0	0	0	0	0
Runoff	0.1	0.8	0.1	0.8	2.9	3.3	2.9	3.3
Aqueduct Inflow	0.7	0.5	0.7	0.5	1.7	1.3	1.7	1.3
Sediment Release	9.0	2.6	19.5	7.0	9.0	2.7	19.5	7.1
Total Loadings	9.8	3.9	20.3	8.3	13.6	7.3	24.1	11.7

Note: 1. All units for loadings are in tons/year (*i.e.*, 2000 lbs/year)

Table 4. Estimated Annual Nitrogen Loadings[1] for the Existing and Expanded Reservoir

Sources	(NO_3 +NH_4) as N				TN			
	Existing Case		Expanded Reservoir Case		Existing Case		Expanded Reservoir Case	
	2006	2007	2006	2007	2006	2007	2006	2007
Purified Water	0	0	0	0	0	0	0	0
Runoff	3.4	5.4	3.4	5.4	4.8	7.6	4.8	7.6
Aqueduct Inflow	14.6	15.5	14.6	15.5	22.4	21.1	22.4	21.1
Sediment Release	13.2	14.3	61.8	17.7	13.3	14.3	61.9	18.7
Total Loadings	31.2	35.2	79.8	38.6	40.5	43.0	89.1	46.4

Note: 1. All units for loadings are in tons/year (*i.e.*, 2000 lbs/year)

3. MODELING RESULTS FOR FUTURE CONDITIONS

3.1 MODELING SCENARIOS

Two scenarios have been modeled to evaluate the water quality in the expanded reservoir under future operating conditions. The first scenario considered the expected typical future conditions with purified water at median expected storage and normal expected operations, and is referred to herein as the Base Case. The second scenario addresses the expanded reservoir under future operating conditions but with no added purified water, referred to herein as No Purified Water. This latter case is identical to the Base Case except no purified water is introduced into the reservoir (with a compensating equal reduction in outflow).

The comparison of these two future scenarios enables a quantification of the effects of purified water addition on the expanded reservoir behavior under future operating conditions. The parameters for these two modeling scenarios were determined in collaboration between the City, its consultants, and Flow Science, and are based on information provided by the San Diego County Water Authority (SDCWA) about the expected future operational schemes for SVR. The Base Case utilized the Design Purified Water Inlet Location (see **Figure 1** for the location) as the point of release for purified water inflow into SVR. The two scenarios considered Port #2 at the reservoir outlet tower structure to be the open port for all water withdrawals from the reservoir. It should be noted that hydrodynamic results of the modeling for these two scenarios are included in the TM #2 (FSI, 2011) and are not included here. Only the results of the water quality analyses are presented in this report, focusing on DO, nutrients, chlorophyll *a* and Secchi depth. In the following, details of each of these two modeling scenarios are discussed.

3.1.1 Base Case

The Base Case simulated a two-year period of reservoir operations and used the same 2006 - 2007 meteorological data, aqueduct inflow water quality data, runoff water quality data, and other modeling parameters as used in the Existing Case, except for the initial reservoir volume, introduction of purified water, and modified inflow and outflow rates as discussed below. Note also that the measured wind data used as inputs for the model included several Santa Ana Wind events that occurred in the winter of each simulated year.

The City provided the initial reservoir volume and inflow and outflow rates for the Base Case. The initial reservoir volume for the Base Case is considered to be near the median of the expected future conditions with a volume of 155,000 acre-feet (determined

in conjunction with SDCWA). It is considered that the daily inflows and outflows will be constant throughout each month and it was also assumed that there would be no water transfers from Sutherland Reservoir into SVR in the modeling period. For the Base Case, a new surface inflow, the purified water inflow, was added to represent incoming purified water from the advanced water purification facility at an annual rate of 15,000 a-f/y. The detailed monthly inflow and outflow volumes for each source for the Base Case are listed in **Table 5**. The available withdrawal elevations on the proposed reservoir outlet are listed in **Table 6** and Port #2 was used for all water withdrawals from the reservoir. The multi-year averages of weekly water temperatures at North City Water Reclamation Plant were used to characterize the purified water temperature and the salinity of the purified water was considered to be constant at 100 parts per million (ppm).

The water quality for the purified water inflow was determined by analyzing water quality field data measured in the effluent from the advanced water purification facility (these data are available separately). After consulting with the City and analyzing the effluent data, FSI provided the final values for water quality of purified water used in the simulations. These are listed in **Table 7** as well as the nutrient concentrations for other inflows. Note that particulate and organic nutrients are considered to be negligible in the purified water. Thus, the concentration of TN in the purified water is 0.78 mg/L, the sum of ammonia, nitrate and nitrite in the purified water; the concentration of TP in the purified water is 0.004 mg/L and equal to the concentration of SRP.

3.1.2 No Purified Water Scenario

The data inputs for the No Purified Water scenario are similar to those for the Base Case scenario, except for no purified water additions and an equal reduction in reservoir outflow volume (to obtain similar reservoir storage volumes). The purpose of conducting this simulation was, by comparison with the Base Case, to evaluate the water quality effects of the purified water addition on the expanded SVR. **Table 8** presents the monthly water volumes of inflows and outflow for the No Purified Water scenario.

Table 5. Monthly Reservoir Inflow and Outflow Volumes for Base Case Operating Scenario

Month	Aqueduct Inflow (acre-feet)	Runoff Inflow (acre-feet)	Purified Water Inflow (acre-feet)	Withdrawal (acre-feet)
Jan-Year 1	0	0	1440	0
Feb-Year 1	0	1,500	1590	0
Mar-Year 1	0	1,500	1480	0
Apr-Year 1	1,000	1,500	1350	0
May-Year 1	1,000	0	1230	0
Jun-Year 1	1,000	0	1090	0
Jul-Year 1	0	0	900	2200
Aug-Year 1	0	0	1020	4200
Sep-Year 1	0	0	1090	4200
Oct-Year 1	0	0	1120	4200
Nov-Year 1	0	0	1210	4200
Dec-Year 1	0	0	1480	0
Jan-Year 2	0	0	1440	0
Feb-Year 2	0	1,500	1590	0
Mar-Year 2	0	1,500	1480	0
Apr-Year 2	1,000	1,500	1350	0
May-Year 2	1,000	0	1230	0
Jun-Year 2	1,000	0	1090	0
Jul-Year 2	0	0	900	2200
Aug-Year 2	0	0	1020	4200
Sep-Year 2	0	0	1090	4200
Oct-Year 2	0	0	1120	4200
Nov-Year 2	0	0	1210	4200
Dec-Year 2	0	0	1480	0

Table 6. Available Withdrawal Elevations on Proposed Reservoir Outlet Tower

Port	Withdrawal Elevation
6	733 ft
5	708 ft
4	683 ft
3	653 ft
2	623 ft
1	593 ft

Table 7. Inflow Water Quality Parameters

Water Quality Parameter	Purified Water	Aqueduct Inflow	Runoff
$(NO_3 + NO_2) - N$ (mg/L)	0.64	0.12 – 0.47	0.02 – 3.00
$NH_4 - N$ (mg/L)	0.14	0.02 – 0.09	0.02 – 0.15
TN (mg/L)	0.78	0.17 – 0.68	0.18 – 4.22
SRP (mg/L)	0.004	0.009 – 0.031	0.007 – 0.16
TP (mg/L)	0.004	0.024 – 0.081	0.022 – 0.32

Table 8. Monthly Reservoir Inflow and Outflow Volumes for No Purified Water Scenario

Month	Aqueduct Inflow (acre-feet)	Runoff Inflow (acre-feet)	Purified Water Inflow (acre-feet)	Withdrawal (acre-feet)
Jan-Year 1	0	0	0	0
Feb-Year 1	0	1500	0	0
Mar-Year 1	0	1500	0	0
Apr-Year 1	1000	1500	0	0
May-Year 1	1000	0	0	0
Jun-Year 1	1000	0	0	0
Jul-Year 1	0	0	0	800
Aug-Year 1	0	0	0	800
Sep-Year 1	0	0	0	800
Oct-Year 1	0	0	0	800
Nov-Year 1	0	0	0	800
Dec-Year 1	0	0	0	0
Jan-Year 2	0	0	0	0
Feb-Year 2	0	1500	0	0
Mar-Year 2	0	1500	0	0
Apr-Year 2	1000	1500	0	0
May-Year 2	1000	0	0	0
Jun-Year 2	1000	0	0	0
Jul-Year 2	0	0	0	800
Aug-Year 2	0	0	0	800
Sep-Year 2	0	0	0	800
Oct-Year 2	0	0	0	800
Nov-Year 2	0	0	0	800
Dec-Year 2	0	0	0	0

3.2 COMPARISON OF MODELING RESULTS

In this section, results from the Base Case are compared with those from the Existing Case and No Purified Water scenarios. **Figure 19** provides a comparison of inflow rates among the Existing Case, No Purified Water and Base Case. **Figure 20** shows a comparison of reservoir water volume during the two-year modeling period for these

three scenarios. The main differences in flow rate and water volume among the scenarios are summarized in **Table 9**.

Table 9. Modeled Operating Scenarios

Operating Scenarios	Description	Initial Reservoir Volume (acre-feet)	Annual Purified Water Inflow (acre-feet/year)	Annual Aqueduct inflow (acre-feet/year)	Annual Reservoir Outflow (acre-feet/year)
Existing Case[1] (06/07)	existing conditions during 2006 - 2007	64,000 /60,000	0	27,018 /30,810	28,417 /22,185
No Purified Water[2]	no purified water additions and an equal reduction in reservoir outflow	155,000	0	3,000	4,000
Base Case[2]	median expected storage and normal expected operations	155,000	15,000	3,000	19,000

Notes: 1. The total volume of runoff and water transfers from Sutherland is 1,556 acre-feet for 2006 and 5,902 acre-feet for 2007.
2. Runoff flow rate is 4,500 acre-feet/year and there are no water transfers from Sutherland Reservoir into SVR.

Figure 21 shows a comparison of simulated water temperature among the Existing Case, No Purified Water scenario, and Base Case at Station A. Note that the vertical axis in all figures hereafter is defined as elevation (and not depth) to allow labeling of the reservoir outlet port elevations. The temperature patterns are fairly similar among all three scenarios with similar thermocline development patterns. However, since the reservoir is significantly shallower in the Existing Case, the destratification in the winter appears to occur earlier in that case than in the other two scenarios. A comparison between the Base Case and the No Purified Water scenario shows that the thermocline is slightly deeper for the Base Case (*e.g.*, little less than 3 ft deeper in September), a result of adding purified water in the epilimnion.

A comparison of simulated surface and bottom DO among the Existing Case, No Purified Water, and Base Case is shown in **Figure 22**. **Table 10** lists the hypolimnetic anoxia period of these three scenarios. The hypolimnetic anoxia period is predicted to last an average of 189 days per year (or 52% of the time in a year) for the Existing Case. For the future No Purified Water scenario, the hypolimnetic anoxia period increases to 207 days per year, an addition of 18 days per year. Adding purified water into the reservoir under future operating conditions (*i.e.*, Base Case) further extends the average duration of the hypolimnetic anoxia period by 8 days, to a total of 215 days per year.

Table 10. Summary of Simulated DO, Chlorophyll *a* and Secchi Depth for Modeling Scenarios

Operating Scenarios	Year	Initial Reservoir Volume (acre-feet)	Bottom Anoxia Period	Days Under Anoxia: Total Days (Percentage)[2]	Average Surface Chlorophyll *a* (µg/L)	Average Secchi Depth (m)
Existing Case	2006	64,000	1/1 – 1/15 7/10 – 12/14	189 (52%)	5.8	3.2
	2007	60,000	6/8 – 12/28			
No Purified Water	2006	155,000	1/1 – 1/21 6/25 – 12/23	207 (57%)	3.1	4.8
	2007	155,000	6/5 – 12/31			
Base Case	2006	155,000	1/1 – 1/24 6/23 – 12/31	215 (59%)	3.7	4.3
	2007	155,000	1/1, 6/3 – 12/31			

Notes: 1. Anoxia is defined here as the bottom DO less than 0.5 mg/L.
2. Both the total days and percentage under anoxia are yearly values averaged over the two-year simulation period.

Figures 23 - 27 show comparisons for nitrate, ammonia, TN, SRP and TP among the Existing Case, Base Case and No Purified Water scenarios. In general, the Base Case and No Purified Water scenarios show similarities in variation trends and both are somewhat different from the Existing Case in overall patterns (mostly a result of different inflow/outflow sources and temporal patterns). The Base Case generally shows slightly higher nitrogen concentrations (**Figures 23 - 25**) and slightly lower phosphorus concentrations (**Figures 26** and **27**) than the No Purified Water scenario. This is a result of year-round inflow of purified water with relatively high nitrogen levels and low phosphorus levels.

Comparisons of simulated surface chlorophyll *a* concentrations and derived Secchi depths among the Existing Case, Base Case and No Purified Water are shown in **Figures 28** and **29** respectively. As shown, variation patterns for the Base Case and No Purified Water (*i.e.*, two future operating scenarios) resemble each other and the Base Case shows slightly higher chlorophyll *a* levels and slightly lower Secchi depths. In contrast, the Existing Case features significantly higher algal levels and lower Secchi depths than the Base Case or No Purified Water scenarios. In addition, the temporal variations in chlorophyll *a* concentration and Secchi depth for the Existing Case are different from the future operating scenarios, likely because of significant differences in the timing and magnitude of nutrient loadings between these scenarios.

Annual average surface chlorophyll *a* concentration and Secchi depth are listed in **Table 10** for all three scenarios. The annual chlorophyll *a* concentration and Secchi depth are predicted to be 5.8 µg/L and 3.2 m respectively for the Existing Case. In comparison, the annual average chlorophyll *a* concentration and Secchi depth are 3.1 µg/L and 4.8 m respectively for the No Purified Water scenario. This is a reduction of 2.7 µg/L for the average chlorophyll *a* concentration and an increase of 1.6 m for the average Secchi depth when the operating conditions change from the Existing Case to the No Purified Water scenario in the expanded reservoir. Meanwhile, the Base Case is predicted to produce 3.7 µg/L for the annual average chlorophyll *a* concentration and 4.3 m for the annual average Secchi depth. This is a reduction of 2.1 µg/L for the annual average chlorophyll *a* concentration and an increase of 1.1 m for the annual average Secchi depth compared to the Existing Case. This indicates that both the No Purified Water scenario and Base Case are predicted to produce lower algal levels *(i.e.*, lower surface chlorophyll *a* concentrations) and higher water clarity (*i.e.*, high Secchi depths) compared to the Existing Case.

A comparison of simulated pH among the Existing Case, Base Case and No Purified Water scenarios is presented in **Figure 30.** As shown, the pH is fairly similar for all three runs.

3.3 NUTRIENT LOADINGS

Tables 11 – 14 present, respectively, the nutrient loadings for SRP, TP, the sum of nitrate and ammonia, and TN, for the Existing Case, Base Case and No Purified Water scenarios.

For phosphorus (**Tables 11** and **12**), the loadings from the sediments are generally larger than other loadings and consist of 30 - 90% of all phosphorus loadings into SVR. Both the Base Case and No Purified Water scenarios produce sediment nutrient loadings that are twice as large as those from the Existing Case, likely a result of the larger hypolimnetic bottom area and extended hypolimnetic anoxia period. There is little difference in the sediment releases between the Base Case and No Purified Water scenarios.

For nitrogen (**Tables 13** and **14),** the loadings from the sediments are significant as well and consist of about 30 – 80% of all nitrogen loadings into SVR. Sediment nutrient loadings are generally higher for the future scenarios (*i.e.*, Base Case and No Purified Water scenarios) than the Existing Case.

However, despite the significantly higher sediment release for the future operating scenarios, surface TN concentrations are actually lower for the future scenarios compared to the Existing Reservoir Case (**Figure 25**), a result of the larger volume of water in the

expanded reservoir. The resulting lower nutrient concentrations are believed to be one of the main factors that lead to lower surface chlorophyll a concentrations for the future operating scenarios (compared to the Existing Reservoir Case).

It is noted that the N:P ratio (*i.e.*, calculated as the ratio of the TN loading to TP loading in this case) in the purified water, the major inflow to SVR in the Base Case, is about 159. As shown, this overall ratio for the reservoir can be affected by many factors including the nutrient loadings from inflows as well as sediments. However, given the extremely high N:P ratio of the purified water inflow, algal growth in the future reservoir may tend to become more phosphorus-limited.

Table 11. Annual SRP Loadings[1]

Sources	Existing Case		No Purified Water		Base Case	
	2006	2007	2006	2007	2006	2007
Purified Water	0	0	0	0	0.1	0.1
Runoff	0.1	0.8	0.5	0.5	0.5	0.5
Aqueduct Inflow	0.7	0.5	0.1	0.1	0.1	0.1
Sediment Release[2]	9.0	2.6	19.4	7.0	19.4	7.0
Total Loadings	9.8	3.9	20.0	7.6	20.1	7.7

Note: 1. All units for the loadings are in tons/year *(i.e.*, 2000 lbs/year)

Table 12. Annual TP Loadings[1]

Sources	Existing Case		No Purified Water		Base Case	
	2006	2007	2006	2007	2006	2007
Purified Water	0	0	0	0	0.1	0.1
Runoff	2.9	3.3	0.9	0.9	0.9	0.9
Aqueduct Inflow	1.7	1.3	0.2	0.1	0.2	0.1
Sediment Release[2]	9.0	2.7	19.4	7.0	19.4	7.0
Total Loadings	13.6	7.3	20.5	8.0	20.6	8.1

Note: 1. All units for the loadings are in tons/year *(i.e.*, 2000 lbs/year)

Table 13. Annual (NO_3+NH_4)-N Loadings[1]

Sources	Existing Case		No Purified Water		Base Case	
	2006	2007	2006	2007	2006	2007
Purified Water	0	0	0	0	15.9	15.9
Runoff	3.4	5.4	9.9	6.4	9.9	6.4
Aqueduct Inflow	14.6	15.5	1.1	1.7	1.1	1.7
Sediment Release[2]	13.2	14.3	60.1	14.2	68.9	23.0
Total Loadings	31.2	35.2	71.1	22.3	95.8	47.0

Note: 1. All units for the loadings are in tons/year *(i.e.,* 2000 lbs/year)

Table 14. Annual TN Loadings[1]

Sources	Existing Case		No Purified Water		Base Case	
	2006	2007	2006	2007	2006	2007
Purified Water	0	0	0	0	15.9	15.9
Runoff	4.8	7.6	14.0	9.1	14.0	9.1
Aqueduct Inflow	22.4	21.1	1.3	2.1	1.3	2.1
Sediment Release[2]	13.3	14.3	60.1	14.2	68.9	23.0
Total Loadings	40.5	43.0	75.4	25.4	100.1	50.1

Note: 1. All units for the loadings are in tons/year *(i.e.,* 2000 lbs/year)

4. CONCLUSIONS AND DISCUSSION

The objectives of this study were to use the calibrated and validated SVR ELCOM/CAEDYM water quality model to evaluate the effects of purified water on water quality in the expanded SVR. To achieve these goals, a two-step approach was taken to examine the effects caused by the reservoir expansion and augmentation with purified water, respectively. This work focused on water quality results for nutrients DO, and algal growth.

RESERVOIR EXPANSION

First, the model was used to determine the effects of the reservoir expansion on water quality, without the introduction of any purified water. This was accomplished by performing a simulation that uses the same reservoir conditions (climate, inflow and outflow volumes and concentrations etc.) as the 2006 - 2007 calibration simulation (Existing Case), except for using a higher initial reservoir volume that is set at 155,000 acre-feet (median expected future storage). The results from this simulation (Expanded Reservoir Case) were compared against those obtained from the Existing Case simulation. The differences between the results of these two simulations demonstrate the effects of the expansion on the reservoir's water quality.

Based on the results of these two simulations, the following conclusions and observations on the effects of the reservoir expansion can be made:

- The reservoir expansion is predicted to extend the duration of the hypolimnetic anoxia by an average of 27 days per year (from 189 days per year to 216 days per year) and enlarge the volume of water under anoxic condition by at least two fold.

- The reservoir expansion will produce lower surface chlorophyll *a* concentrations and higher Secchi depths *(i.e.*, better water clarity) in the reservoir. It is predicted that the annual average chlorophyll *a* concentration will decrease from 5.8 µg/L to 3.4 µg/L and the annual average Secchi depth will increase from 3.2 m to 4.7 m after the expansion.

- Based on a nutrient loading calculation, the internal nutrient loadings *(i.e.*, nutrients released from sediment) are larger than all external loadings combined over the two-year modeling period for both the Existing Case and Expanded Reservoir Case. Meanwhile, the reservoir expansion is predicted to lead to a significant increase in sediment nutrient release, likely due to the larger hypolimnetic bottom area and extended hypolimnetic anoxia period. However, despite the significantly higher sediment release, surface TN concentrations are actually lower after the reservoir expansion, a result of the significantly larger

volume of water for the Expanded Reservoir Case. The resulting lower nutrient concentrations are believed to be one of the main factors that lead to lower surface chlorophyll *a* concentrations for the Expanded Reservoir Case (compared to the Existing Reservoir Case).

FUTURE OPERATING CONDITIONS

After the effects of the reservoir expansion were determined, the model was used to examine the water quality in the expanded reservoir under future operating conditions both with and without purified water augmentation. Specifically, the following two future scenarios were simulated:

- Base Case (includes purified water inflow) ---- This scenario considered an expanded reservoir under median expected storage and expected future operations. The initial reservoir volume for the Base Case is set at 155,000 acre-feet. The following annual inflow rates were assumed: for aqueduct inflow 3,000 a-f/y; runoff 4,500 a-f/y; purified water inflow 15,000 a-f/y; and dam withdrawal 19,000 a-f/y, with no water transfers from Sutherland Reservoir into SVR.

- No Purified Water ---- The inputs for this scenario are similar to those for the Base Case scenario, except for no purified water additions and an equal reduction in reservoir outflow. The initial reservoir volume for this scenario is set at 155,000 acre-feet. The annual rates for aqueduct inflow, runoff, purified water inflow and dam withdrawal are 3,000, 4,500, 0 and 4,000 a-f/y respectively. There are no water transfers from Sutherland Reservoir into SVR.

Results from the Base Case and No Purified Water scenarios were compared against those obtained from the Existing Case simulations (*i.e.*, no reservoir expansion). The purpose is to quantify the water quality effects of purified water by comparing the Base Case against the No Purified Water scenario, and to evaluate the effects of future operating conditions in the expanded reservoir (prior to adding purified water) by comparing the No Purified Water scenario against the Existing Case.

Based on the simulation results, the following conclusions and observations on the effects of the purified water and future operating conditions are made:

- The hypolimnetic anoxia period is predicted to last an average of 189 days per year for the Existing Case. For the No Purified Water scenario, the hypolimnetic anoxia period is predicted to increase to 207 days per year, an addition of 18 days per year. Adding purified water into the reservoir under

future operating conditions (*i.e.*, Base Case) will further extend the average duration of the hypolimnetic anoxia period by 8 days, to a total of 215 days per year.

- The No Purified Water scenario produces lower algae levels *(i.e.*, lower surface chlorophyll *a* concentrations) and higher Secchi depths (*i.e.*, better water clarity) compared to the Existing Case. For example, the annual average chlorophyll *a* concentration and Secchi depth are predicted to be 5.8 µg/L and 3.2 m respectively for the Existing Case. By comparison, the annual average chlorophyll *a* concentration and Secchi depth are predicted to be 3.1 µg/L and 4.8 m, respectively, for the No Purified Water scenario in the expanded reservoir. This is a reduction of 2.7 µg/L for the average chlorophyll *a* concentration and an increase of 1.6 m for the average Secchi depth compared to the Existing Case.

- The Base Case scenario also produces lower algae levels *(i.e.*, lower surface chlorophyll *a* concentrations) and higher Secchi depths (*i.e.*, better water clarity) compared to the Existing Case. The Base Case is predicted to produce 3.7 µg/L for the annual average chlorophyll *a* concentration and 4.3 m for the annual average Secchi depth. This is a reduction of 2.1 µg/L for the average chlorophyll *a* concentration and an increase of 1.1 m for the average Secchi depth compared to the Existing Case.

- Nutrient loading calculations show that nutrient sediment release constitutes a significant portion of all nutrient loadings into SVR for all future scenarios as well as the Existing Case. The future operating scenarios (*i.e.*, Base Case and No Purified Water) produce sediment nutrient loadings significantly larger than those for the Existing Case, likely a result of the larger hypolimnetic bottom area and extended hypolimnetic anoxia period. However, despite the significantly higher sediment release for the future operating scenarios, surface TN concentrations are actually lower for the future scenarios compared to the Existing Reservoir Case, a result of the larger volume of water in the expanded reservoir. The resulting lower nutrient concentrations are believed to be one of the main factors that lead to lower surface chlorophyll *a* concentrations for the future operating scenarios (compared to the Existing Reservoir Case).

- Nutrient limitation in SVR can be affected by various factors including the nutrient loadings from all the inflows and the sediments. As a result, nutrient limitation at any point may vary based on existing conditions. However, note that the N:P ratio of the purified water is expected to reach about 159,

indicating that algal growth in the future reservoir may tend to become more phosphorus-limited.

5. REFERENCES

City of San Diego (2008). "IPR Description for BOR Grant 122208 MS," obtained from Jeffery Pasek of the City of San Diego through e-mail on December 23, 2008.

Flow Science Incorporated (2010). "Reservoir Augmentation Demonstration Project: Limnology and Reservoir Detention Study of San Vicente Reservoir – Calibration of the Water Quality Model", FSI Project No. V094005, Pasadena, CA.

Flow Science Incorporated (2011). "Water Purification Demonstration Project: Limnology and Reservoir Detention Study of San Vicente Reservoir – Hydrodynamic Modeling Study", FSI Project No. V094005, Pasadena, CA.

Horne, A.J. and C.R. Goldman (1994). "Limnology (Second Edition)", Published by McGraw-Hill, Inc. ISBN 0-07-023673-9.

National Water Research Institute (2010). "Findings and Recommendations of the Limnology and Reservoir Subcommittee Meeting for the Reservoir Augmentation Demonstration Project's 'Limnology and Reservoir Detention Study of the San Vicente Reservoir' " Memorandum from NWRI Independent Advisory Panel for the City of San Diego's Indirect Potable Reuse/Reservoir Augmentation Demonstration Project, June 7, 2010.

National Water Research Institute (2012). "Findings and Recommendations of the Limnology and Reservoir Subcommittee Meeting for the Reservoir Augmentation Demonstration Project's 'Limnology and Reservoir Detention Study of the San Vicente Reservoir' " Memorandum from NWRI Independent Advisory Panel for the City of San Diego's Indirect Potable Reuse/Reservoir Augmentation Demonstration Project, January 5, 2012.

6. GLOSSARY

Advanced Water Purification Facility: The demonstration facility located at the North City Water Reclamation Plant. The facility is considered "advanced" because of the high level of treatment utilizing reverse osmosis and advanced oxidation.

Blending: Mixing or combining one water source with another such as purified water with raw water sources.

Conductivity: See "Salinity".

Constituent: In water, a constituent is a dissolved chemical element or compound or a suspended material that is carried in the water.

Drought: A defined period of time when rainfall and runoff in a geographic area are much less than average.

Epilimnion: Natural thermal stratification exists for much of the year in almost all temperate lakes and reservoirs and creates three vertical zones. The upper, warmer water is called the epilimnion, the deeper, colder water is called the hypolimnion, whereas the middle portion separating these two layers, where the rate of vertical temperature change is greatest, is called the metalimnion, or thermocline.

Excursion events at the advanced purification facility: Events in which the water quality of the recycled water into the advanced purification facility deviates from the normal or expected conditions. They result in the final outflow from the advanced purification facility may contain chemical constituents at higher level than normal concentrations when no such events occur.

Hypolimnion: See "epilimnion".

Pathogens: Disease-causing organisms. The general groupings of pathogens are viruses, bacteria, protozoa, and fungi.

Periods of mixing: Periods when water temperatures become vertically uniform in the water body and they generally occur in the winter.

Purified water: Recycled water that has been treated to an advanced level beyond tertiary treatment, so that it can be added to water supplies ultimately used for drinking water. The treatment includes membrane filtration with microfiltration or ultrafiltration, reverse osmosis (RO), and advanced oxidation that consists of disinfection with

ultraviolet light (UV) and hydrogen peroxide (H_2O_2). Purified water may be released into a groundwater basin or surface water reservoir that supplies water to a drinking water treatment facility.

Purified water inflow: Purified water that is transported from the advanced purified water treatment facility to SVR.

Purified water inlet: Point of release in SVR for purified water inflow. Note that the purified water is assumed to be released at the surface of SVR.

Recycled water: Water that originated from homes, businesses and drains as municipal wastewater and has undergone a high level of treatment at a reclamation facility so that it can be beneficially reused for a variety of purposes. This is the water that comes into the AWP Facility.

Reservoir: A manmade lake or tank used to collect and store water.

Reservoir augmentation: The process of adding purified water to a surface water reservoir. The purified water undergoes advanced treatment (membrane filtration, reverse osmosis and UV disinfection/advanced oxidation). The purified water is then blended with untreated water in a reservoir. The blended water is then treated and disinfected at a conventional drinking water treatment plant and is distributed into the drinking water delivery system. Also known as "surface water augmentation."

Reservoir outflow: The flow withdrawal through the opening port located at the outlet structure near the dam.

Reservoir outlet: The opening port at the outlet structure near the dam. In this study, the opening port is assumed to be Port #2.

Salinity: The concentration of mineral salts dissolved in water. Salinity may be measured by weight (total dissolved solids or TDS) or by electrical conductivity. Salinity and TDS are both measures of the amount of salt dissolved in water, and the terms are often used interchangeably. Generally, salinity is used when referring to water with a lot of salt (*e.g.*, seawater), whereas TDS is used to refer to water with little salt (*e.g.*, freshwater).

Storage: Water held in a reservoir for later use.

Soluble Reactive Phosphorus (SRP): A measure of orthophosphate, the filterable (soluble, inorganic) fraction of phosphorus, the form directly taken up by plant cells.

Surface water: Water located on the Earth's surface, in a river, stream, lake, pond or surface water reservoir.

Thermocline: See "epilimnion".

Total Nitrogen (TN): A measure of all the forms of nitrogen, dissolved or particulate, that are found in a sample.

Total Phosphorus (TP): A measure of all the forms of phosphorus, dissolved or particulate, that are found in a sample.

Water Purification Demonstration Project (Demonstration Project): The second phase of the City of San Diego's Water Reuse Program. During this test phase the Advanced Water Purification Facility will operate for approximately one year and will produce 1 million gallons of purified water per day. A study of the San Vicente Reservoir is being conducted to test the key functions of reservoir augmentation and to determine the viability of a full-scale project. No purified water will be sent to the reservoir during the demonstration phase.

Water Measurement Terms

Milligrams per liter (mg/L) ***also known as parts per million (ppm):*** A measurement describing the amount of a substance (such as a mineral, chemical or contaminant) in a liter of water; a unit used to measure concentration of water constituents (parts of something per million parts of water). One part per million is equal to one milligram per liter. (This term is becoming obsolete as instruments measure smaller concentrations.) This is equivalent to one drop of water diluted into 50 liters (roughly the fuel tank capacity of a compact car) or about thirty seconds out of a year.

Acre-foot (AF): A unit of water commonly used in the water industry to measure large volumes of water. It equals the volume of water required to cover one acre to a depth of one foot. An acre-foot is 325,851 gallons (43,560 cubic feet) and is considered enough water to meet the needs of two families of four with a house and yard for one year.

Micrograms per liter (µg/L) also known as parts per billion (ppb): A frequently used measurement for water concentration (parts of something per billion parts of water). One part per billion is equivalent to one second of time in 32 years or one drop of water in a swimming pool. One thousand parts per billion is equal to one part per million.

FIGURES

Map of San Vicente Reservoir

Plan View of Existing and Expanded Reservoir and Inflow/Outflow Locations

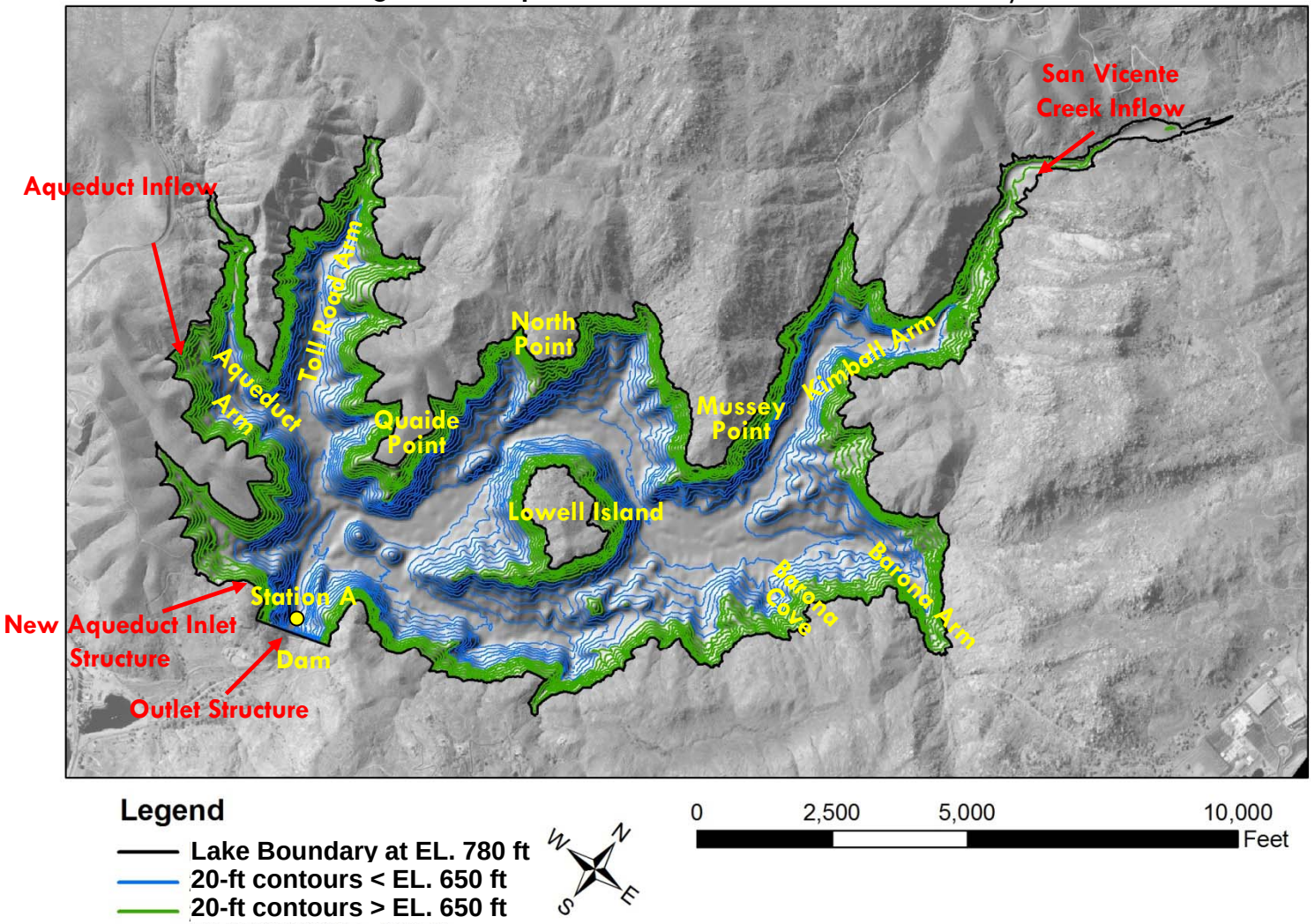

FSI V094005
May 01, 2012

Figure 1

FLOW SCIENCE®

ELCOM-CAEDYM

Schematic of Processes Modeled in ELCOM-CAEDYM

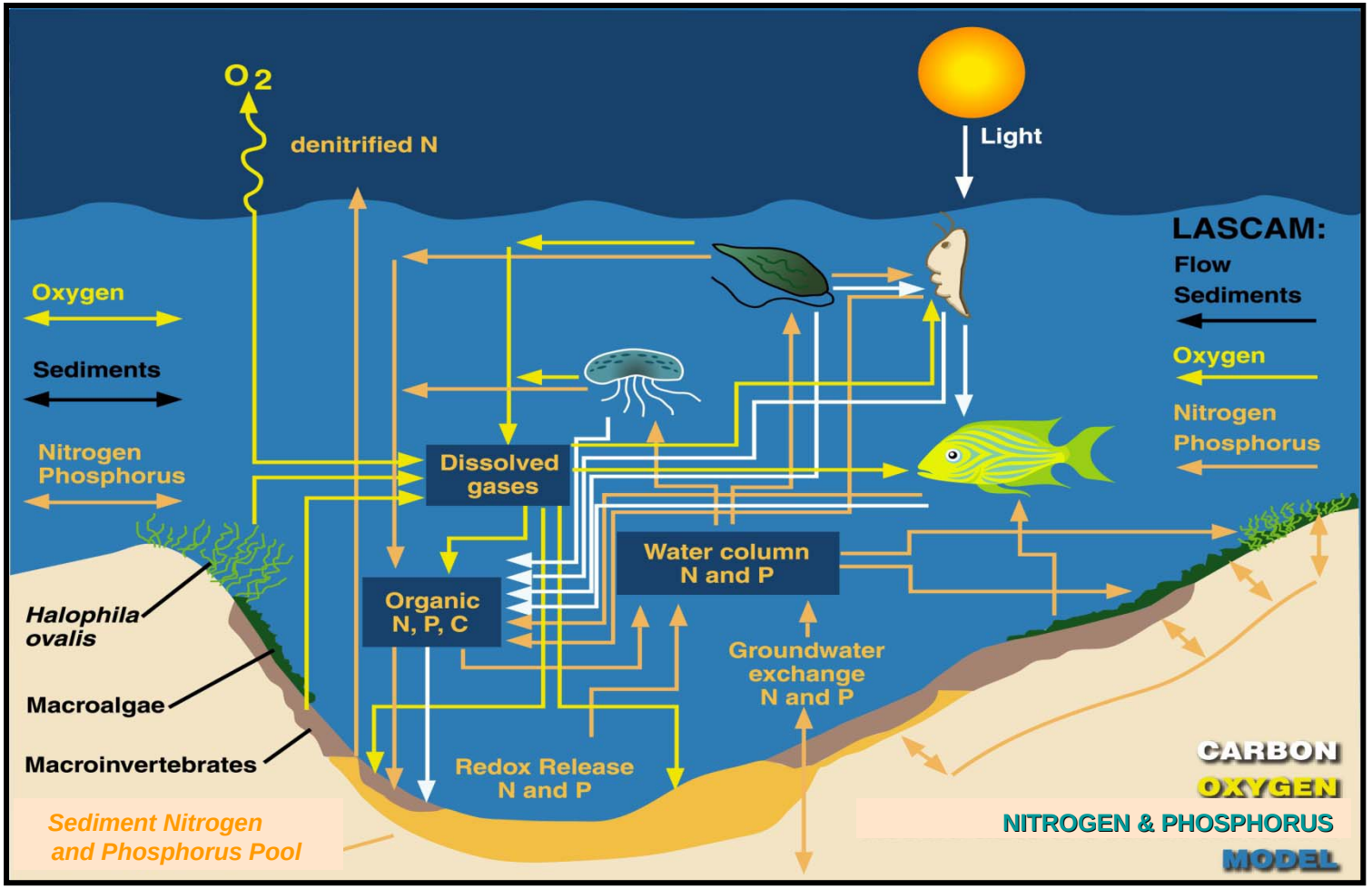

FSI V094005
May 01, 2012

Figure 2

FLOW SCIENCE®

SVR Water Quality Model Grid

(Grid Size = 100 m)

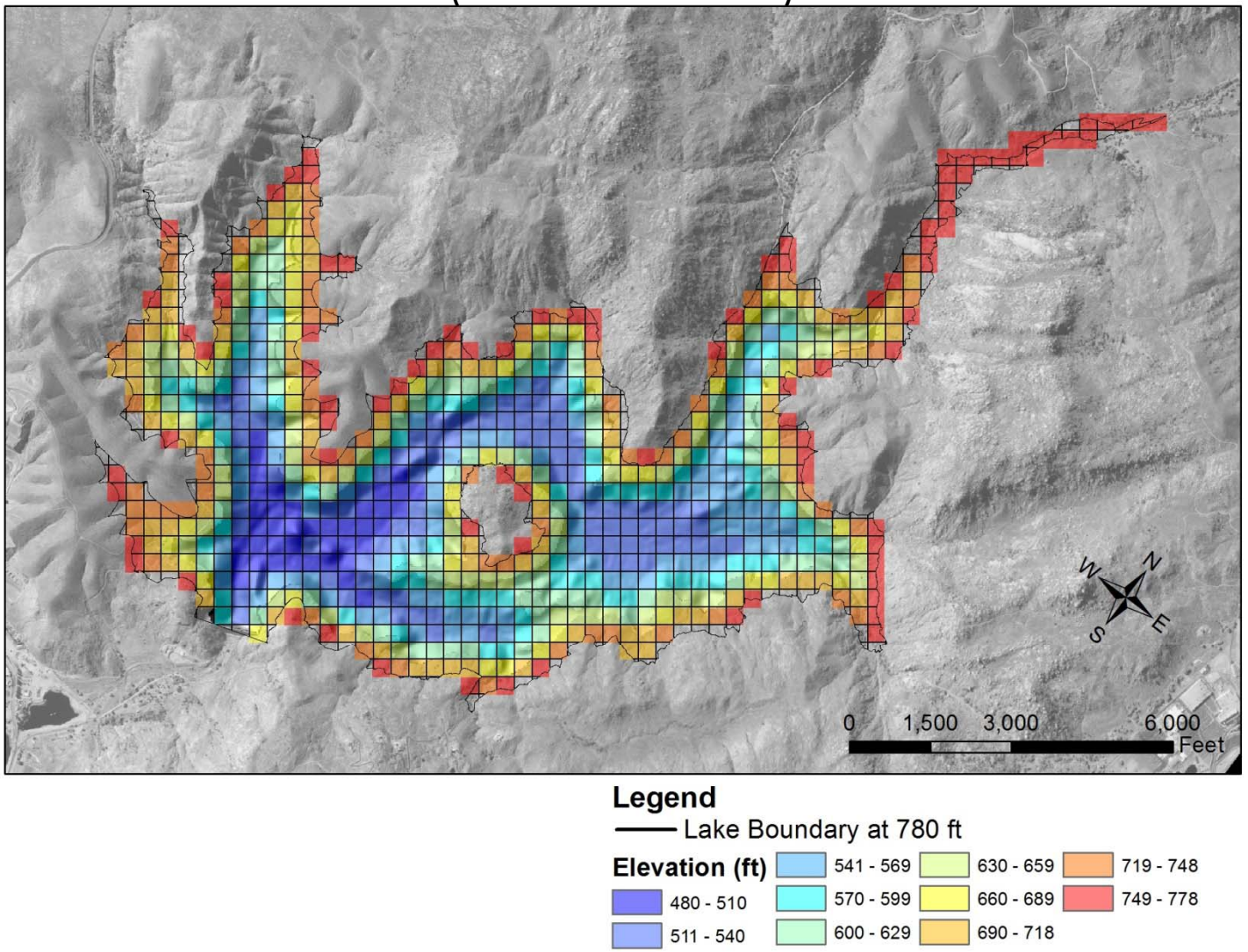

Figure 3

FSI V094005
May 01, 2012

FLOW SCIENCE®

SVR Water Quality Model Calibration Results

Station A – Water Temperature Comparison

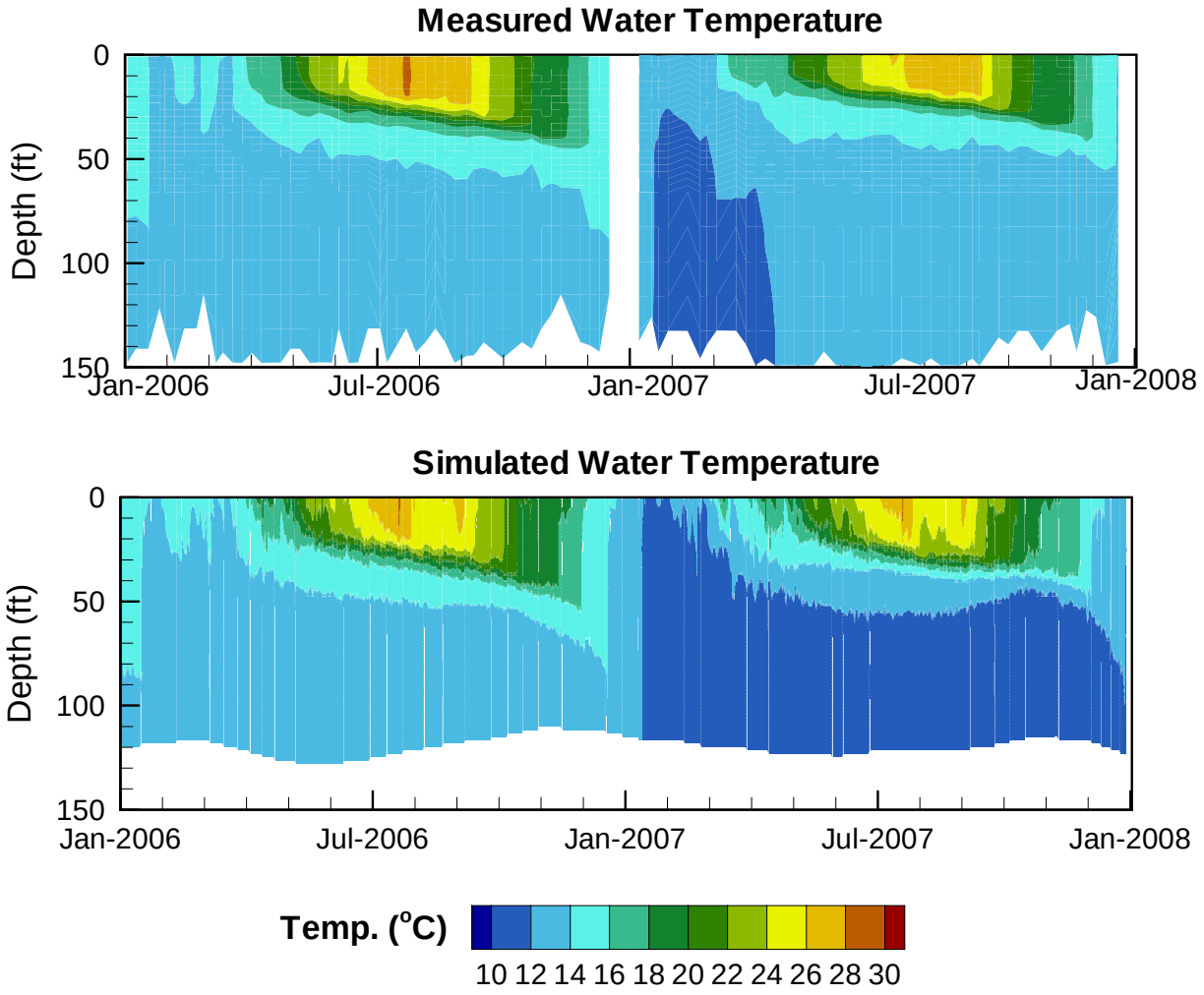

Figure 4

FSI V094005
May 01,, 2012

FLOW SCIENCE®

SVR Water Quality Model Calibration Results

Station A – Dissolved Oxygen Comparison

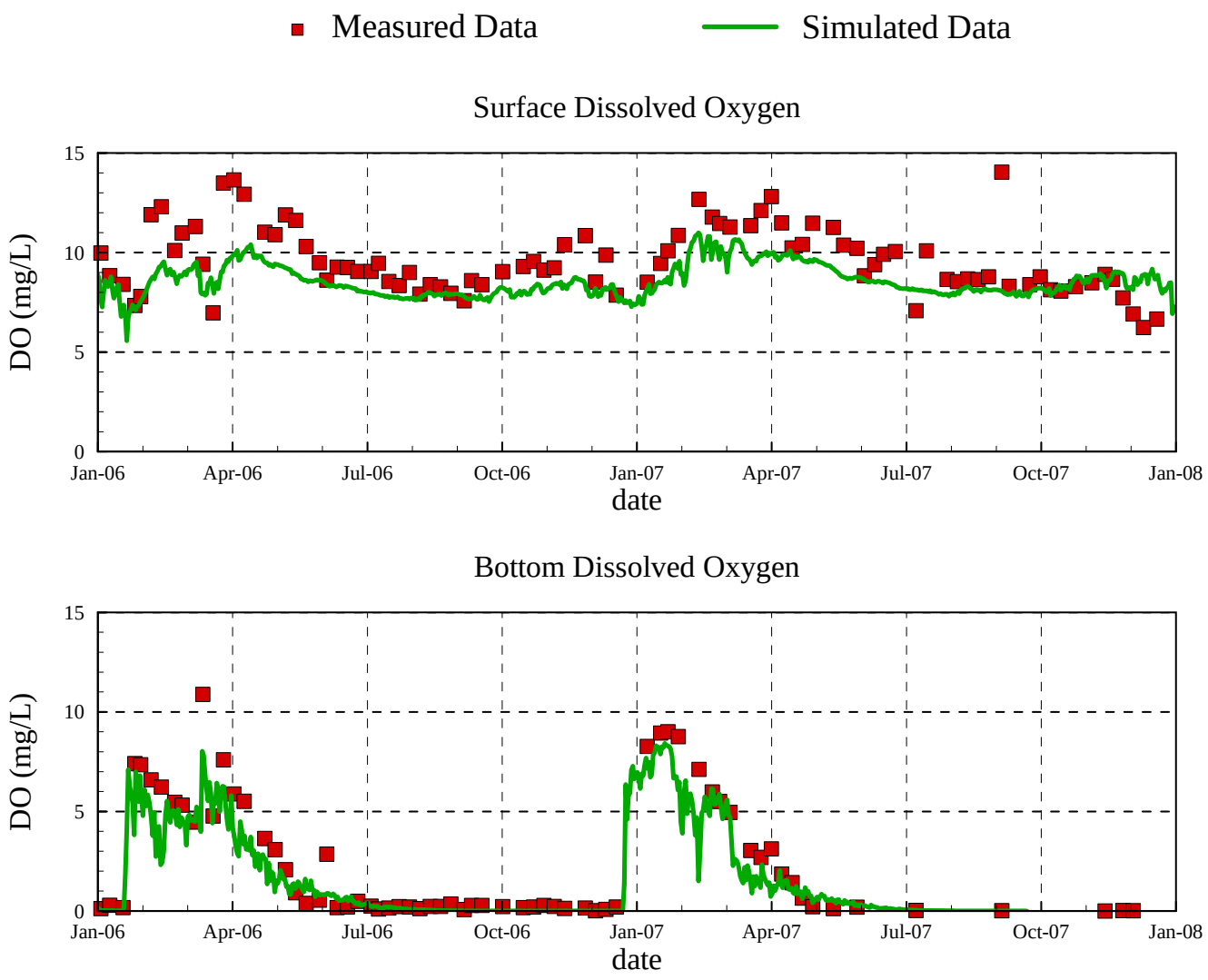

Figure 5

FSI V094005
May 01, 2012

FLOW SCIENCE®

SVR Water Quality Model Calibration Results

Station A – Secchi Depth Comparison

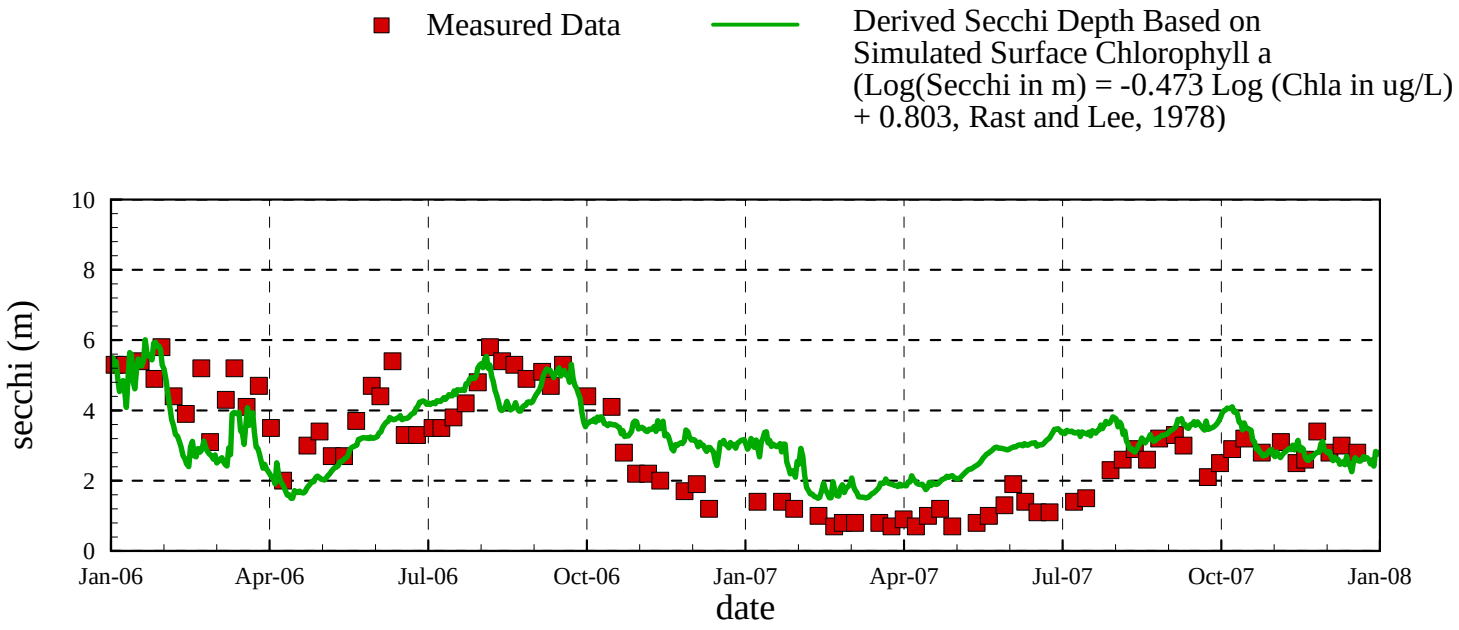

FSI V094005
May 01, 2012

Figure 6

FLOW SCIENCE®

Aqueduct Inflow Nutrient Concentrations

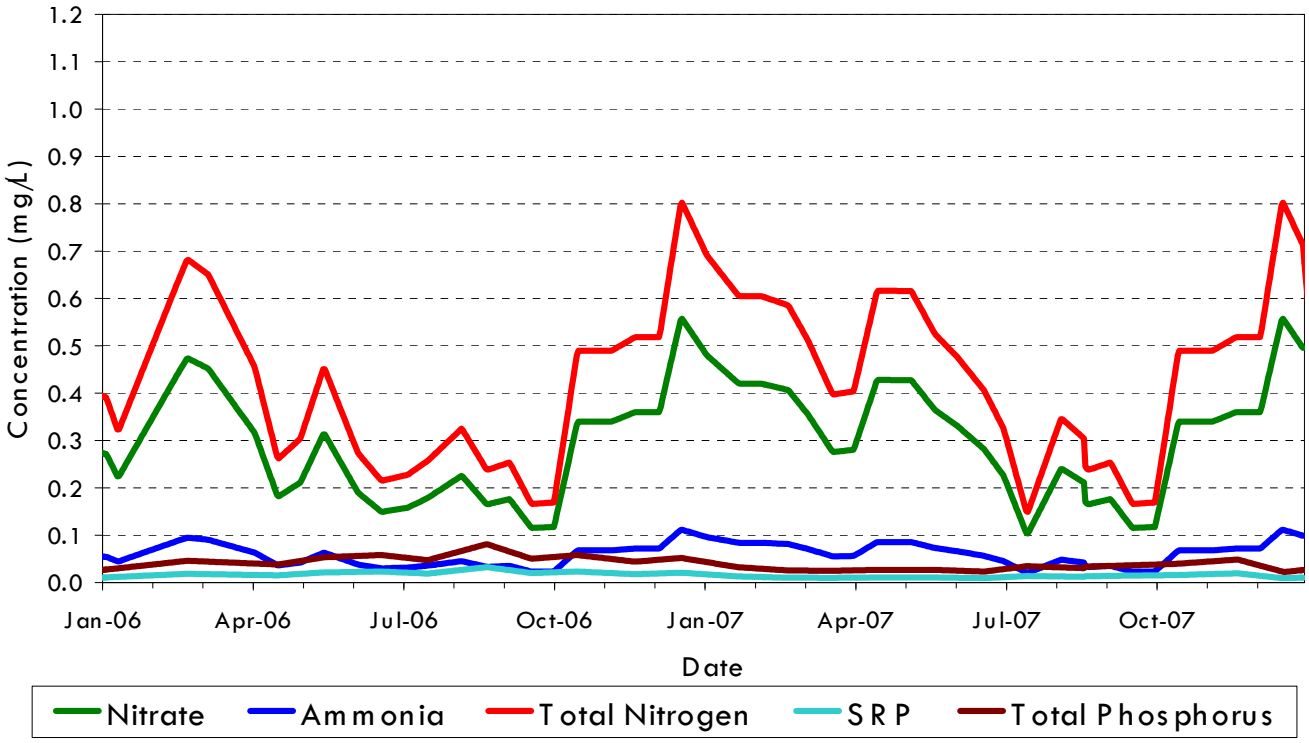

FSI V094005
May 01, 2012

Figure 7

FLOW SCIENCE®

Comparison of Existing Case and Expanded Reservoir Case

Simulated Temperature at Station A

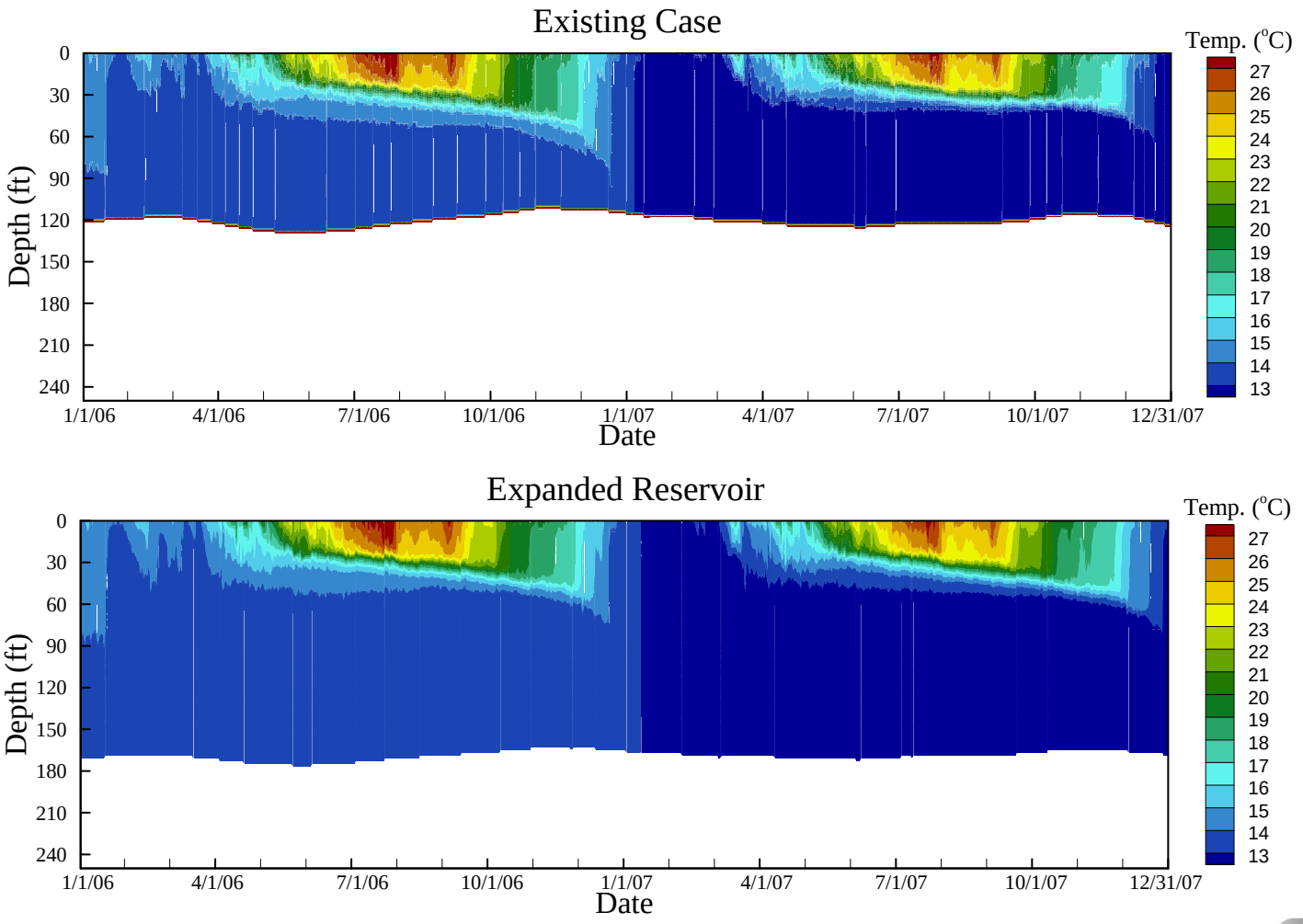

Figure 8

FSI V094005
May 01, 2012

FLOW SCIENCE®

Comparison of Existing Case and Expanded Reservoir Case

Simulated Dissolved Oxygen at Station A

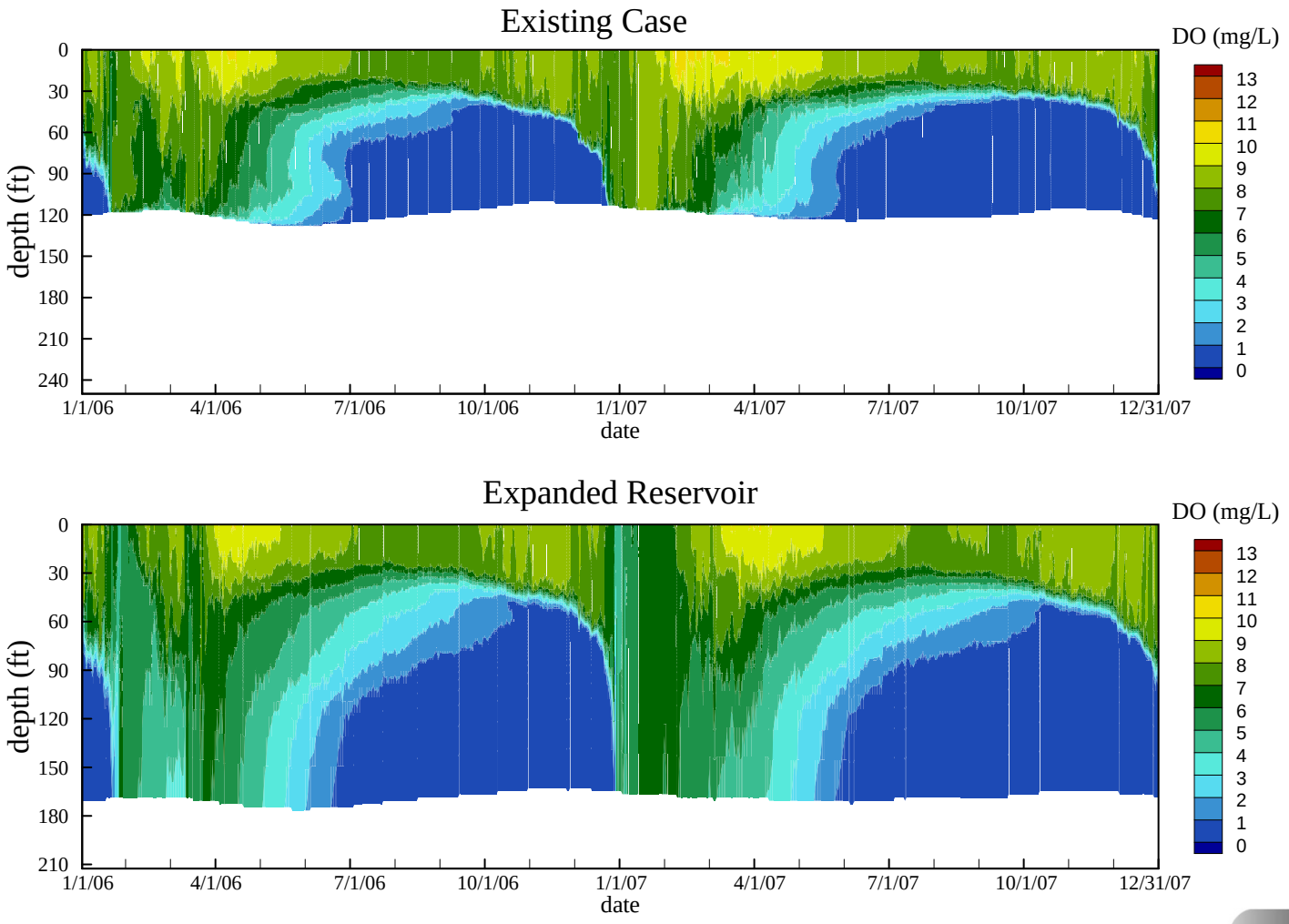

Figure 9

FSI V094005
May 01, 2012

FLOW SCIENCE®

Comparison of Existing Case and Expanded Reservoir Case

Simulated Surface and Bottom Dissolved Oxygen at Station A

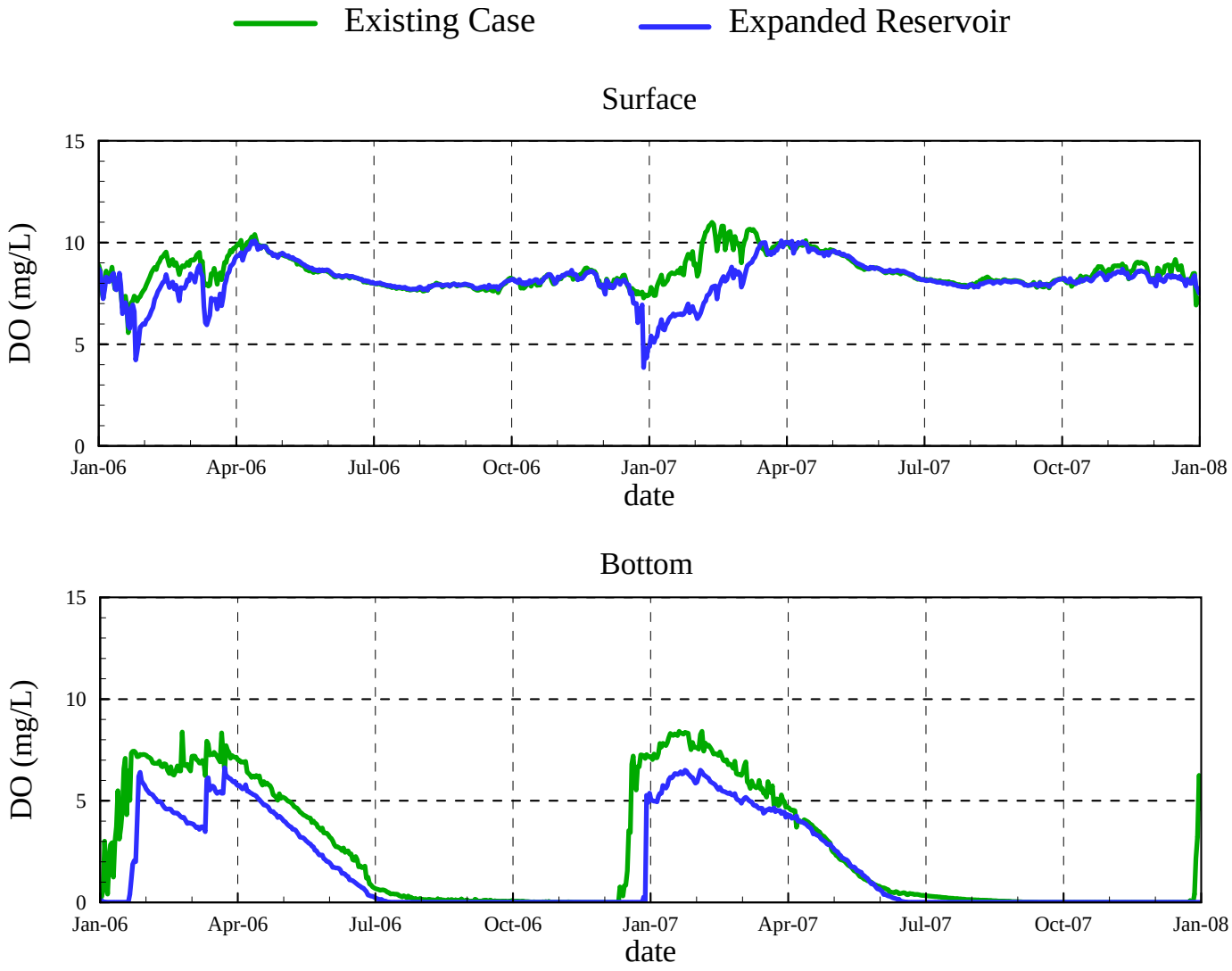

Figure 10

FSI V094005
May 01, 2012

FLOW SCIENCE®

Comparison of Existing Case and Expanded Reservoir Case

Simulated Surface and Bottom Ammonia (as N) at Station A

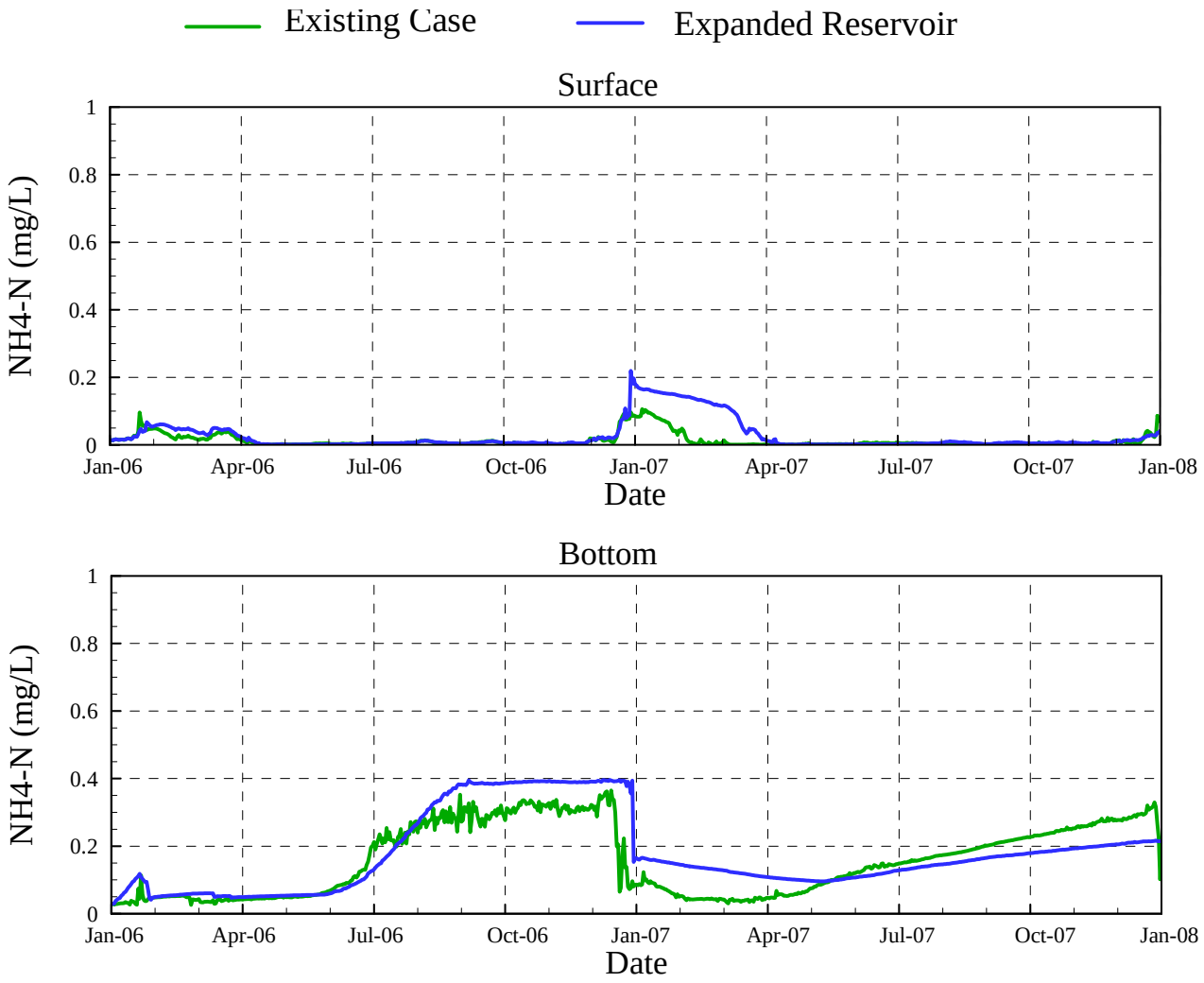

Figure 11

FSI V094005
May 01, 2012

FLOW SCIENCE®

Comparison of Existing Case and Expanded Reservoir Case

Simulated Surface and Bottom Nitrate (as N) at Station A

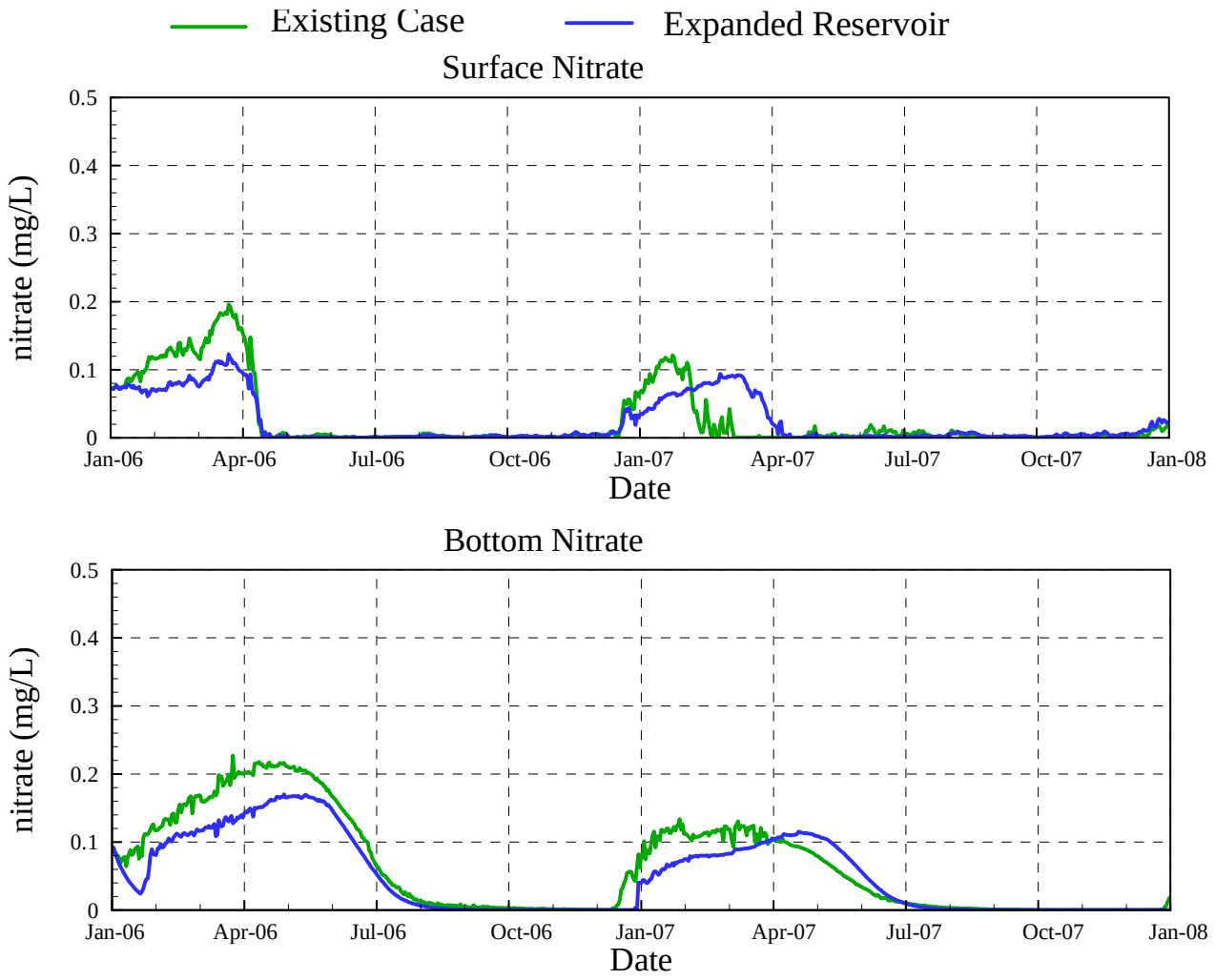

Figure 12

FSI V094005
May 01, 2012

FLOW SCIENCE®

Comparison of Existing Case and Expanded Reservoir Case

Simulated Surface and Bottom TN at Station A

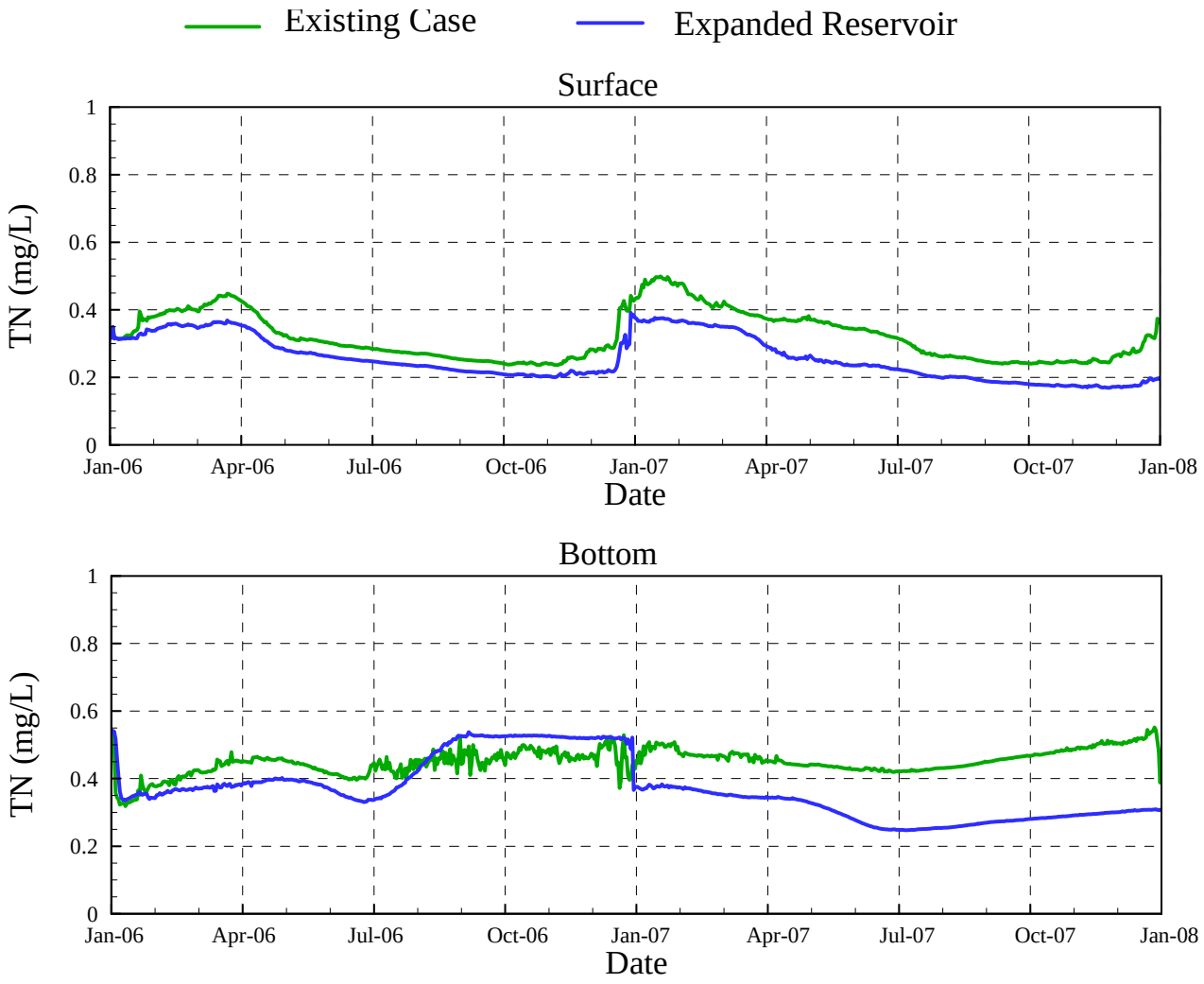

Figure 13

FSI V094005
May 01, 2012

FLOW SCIENCE®

Comparison of Existing Case and Expanded Reservoir Case

Simulated Surface and Bottom SRP at Station A

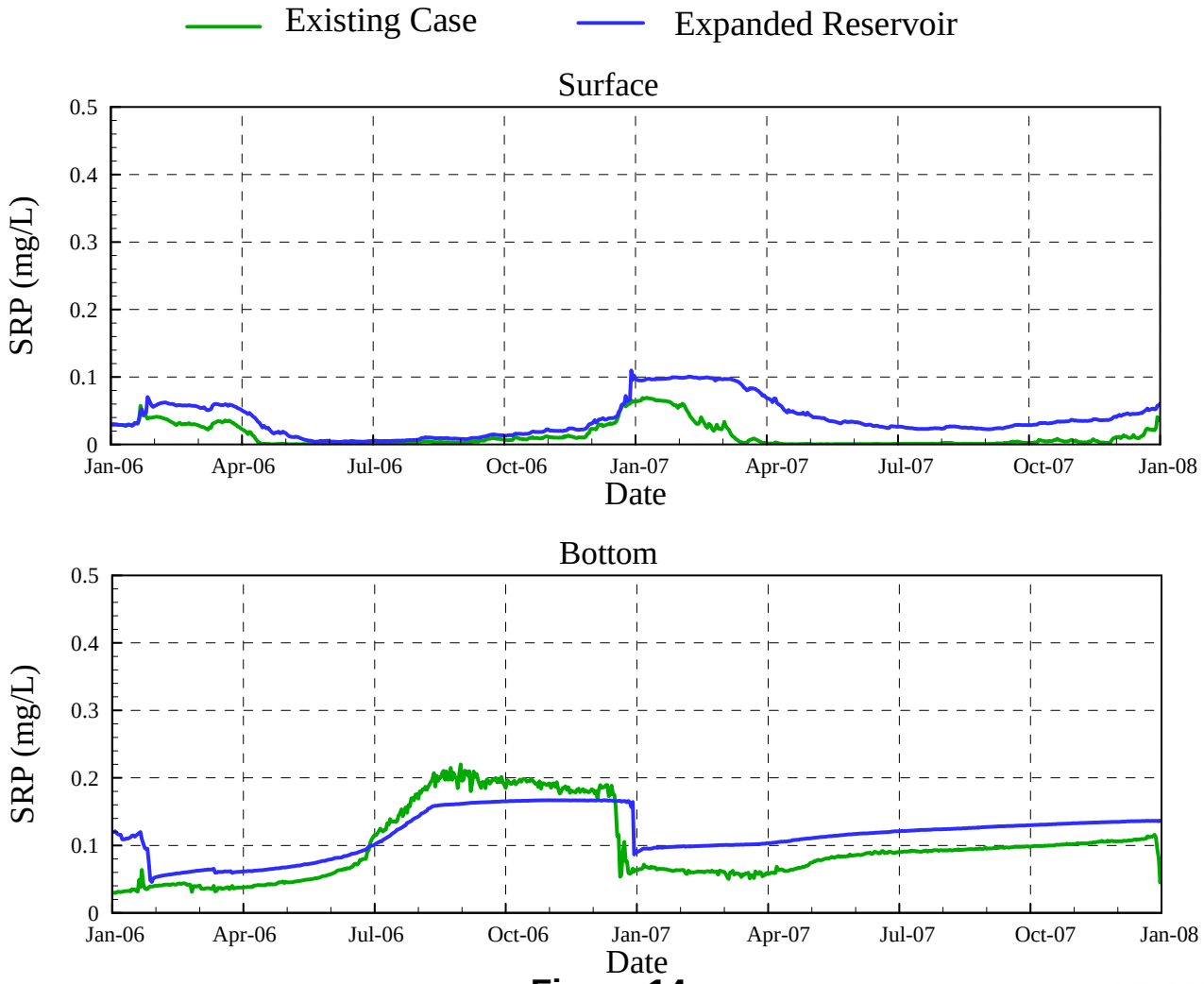

Figure 14

FLOW SCIENCE®

Comparison of Existing Case and Expanded Reservoir Case

Simulated Surface and Bottom TP at Station A

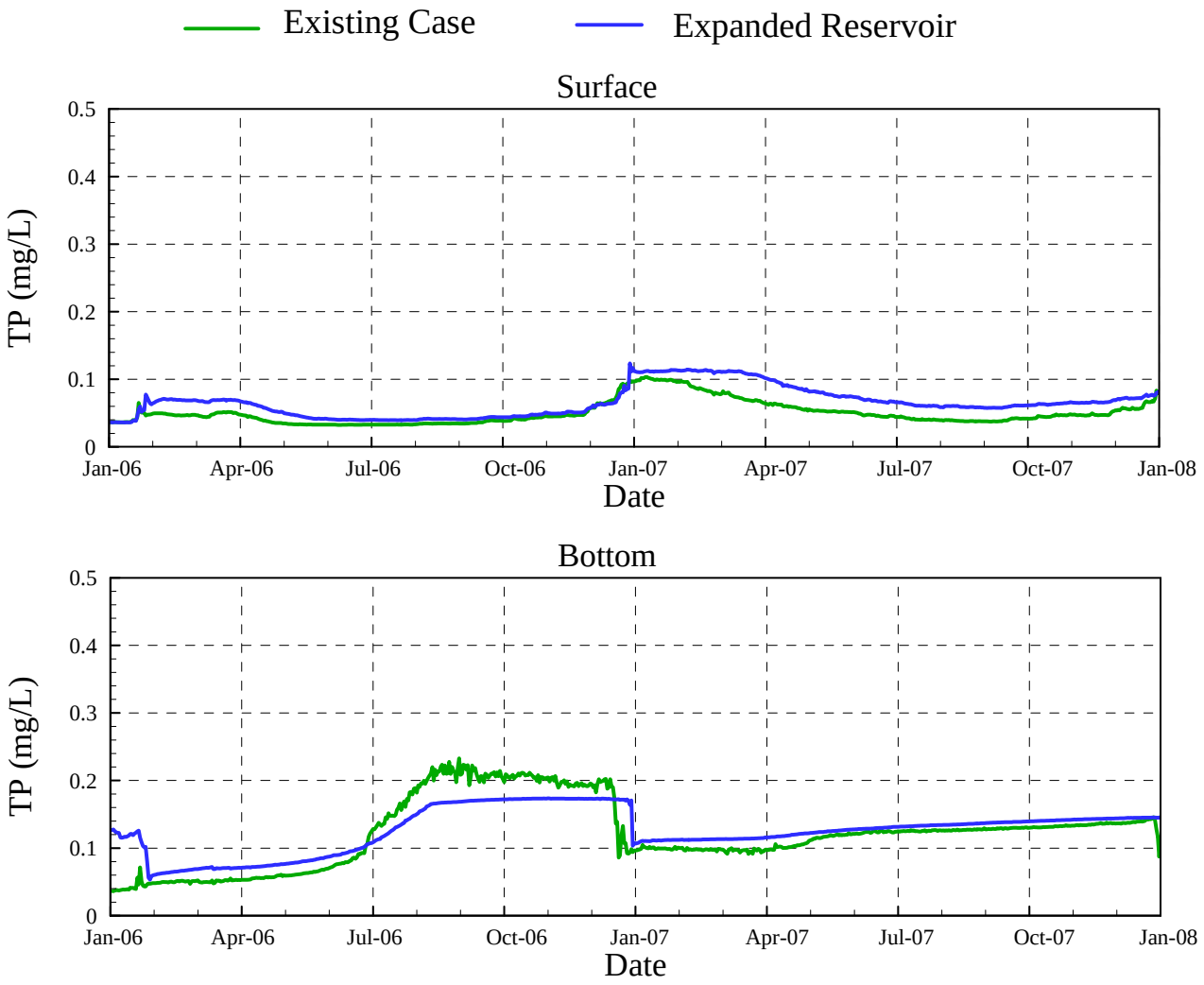

Figure 15

FSI V094005
May 01, 2012

FLOW SCIENCE®

Comparison of Existing Case and Expanded Reservoir Case

Simulated Surface Chlorophyll *a* at Station A

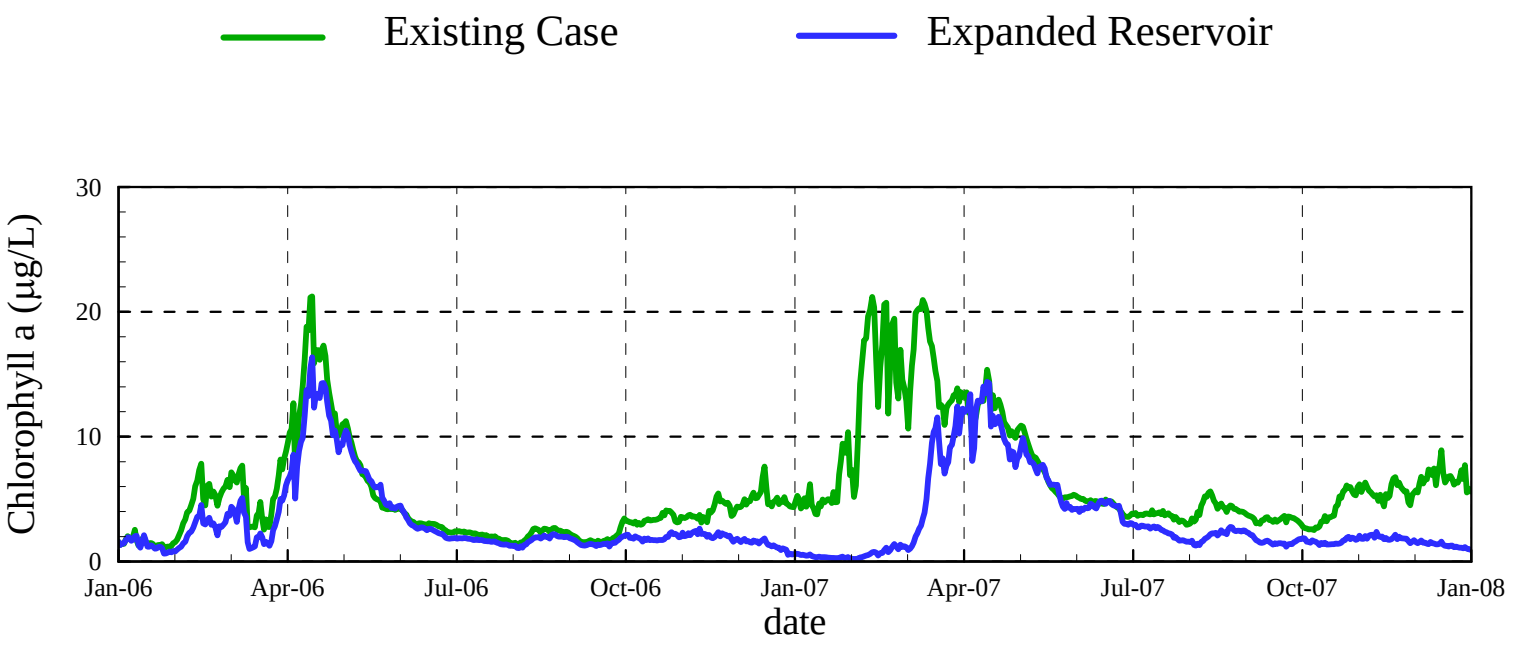

FSI V094005
May 01, 2012

Figure 16

FLOW SCIENCE®

Comparison of Existing Case and Expanded Reservoir Case

Simulated Secchi Depth at Station A

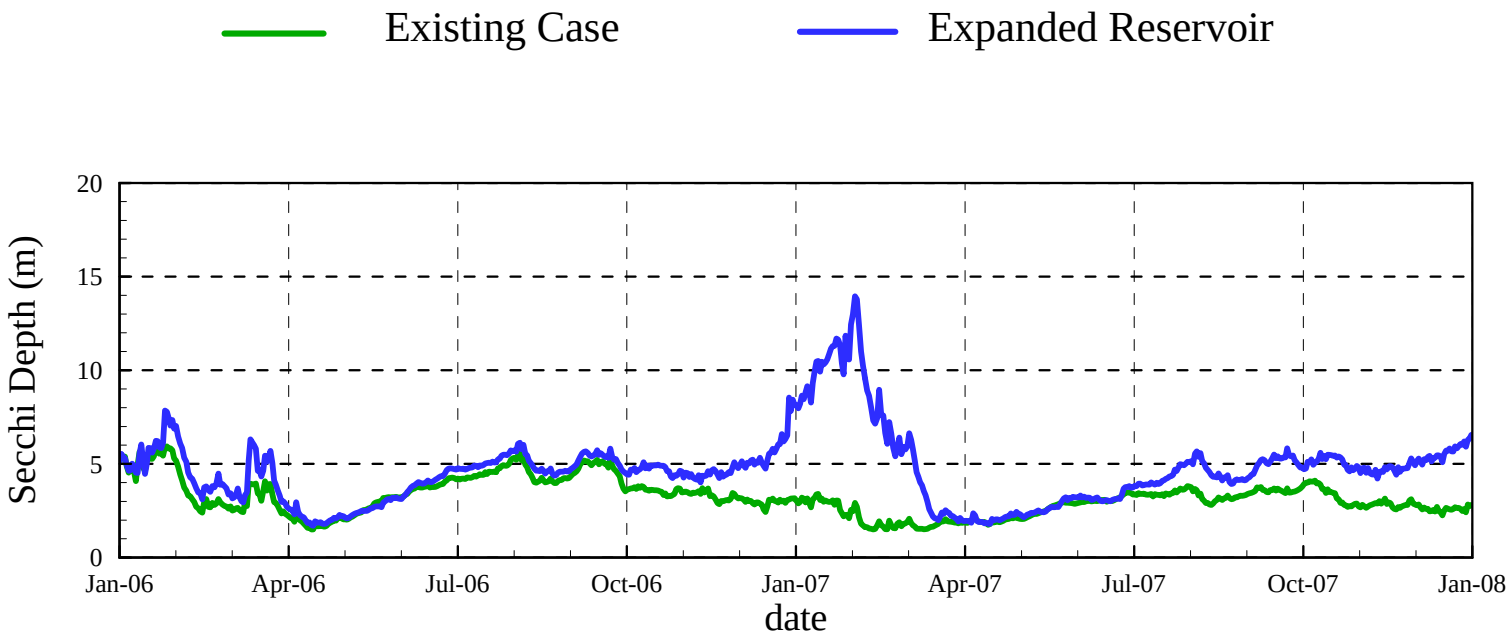

FSI V094005
May 01, 2012

Figure 17

FLOW SCIENCE®

Comparison of Existing Case and Expanded Reservoir Case

Simulated Surface and Bottom pH at Station A

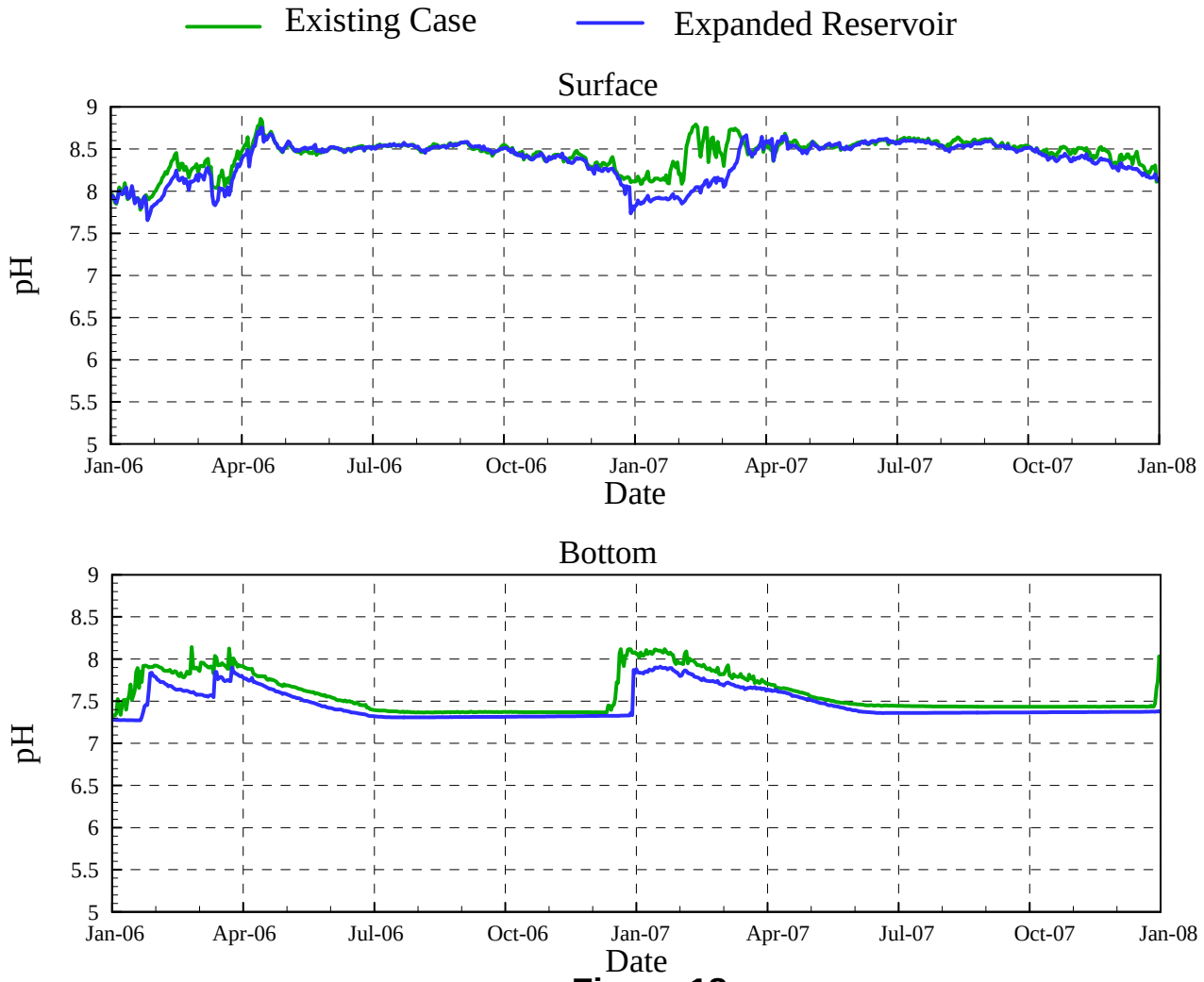

Figure 18

FSI V094005
May 01, 2012

FLOW SCIENCE®

Purified Water and Aqueduct Inflow Rates of Existing Case, No Purified Water and Base Case Scenarios

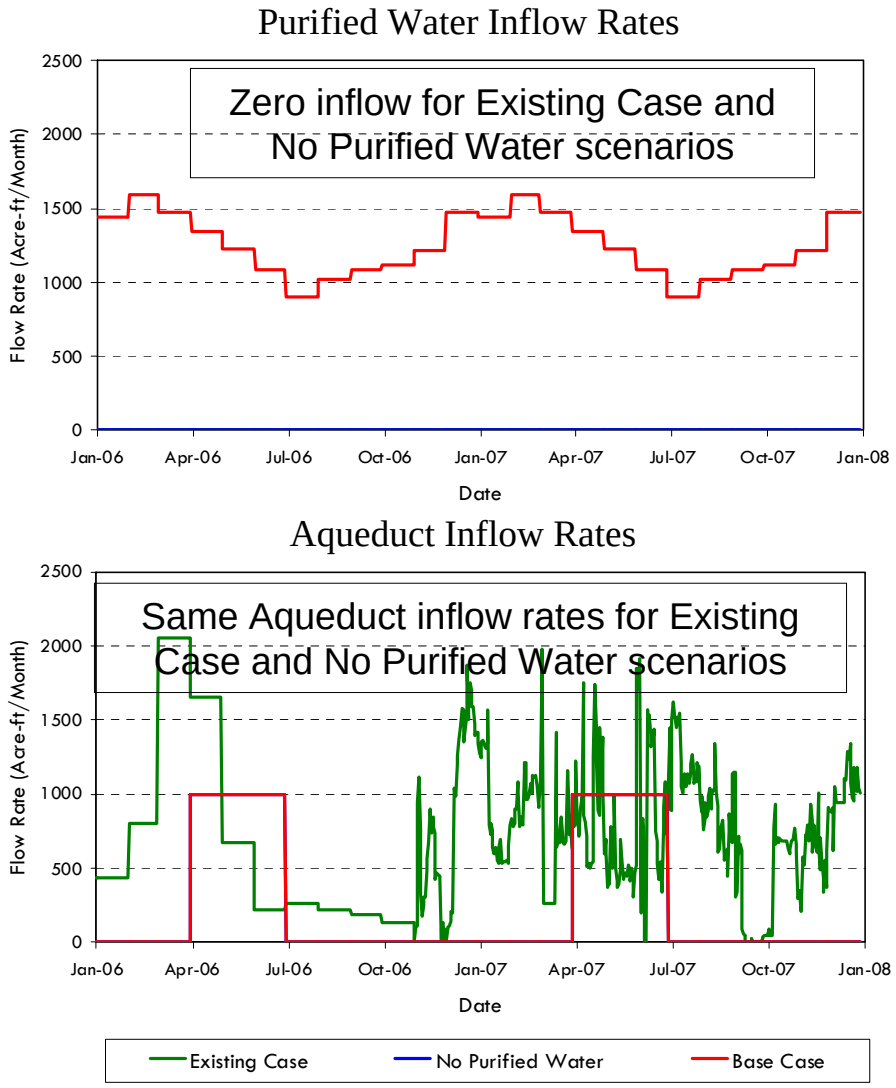

FSI V094005
May 01, 2012

Figure 19

FLOW SCIENCE®

Reservoir Water Volumes for Existing Case, No Purified Water and Base Case Scenarios

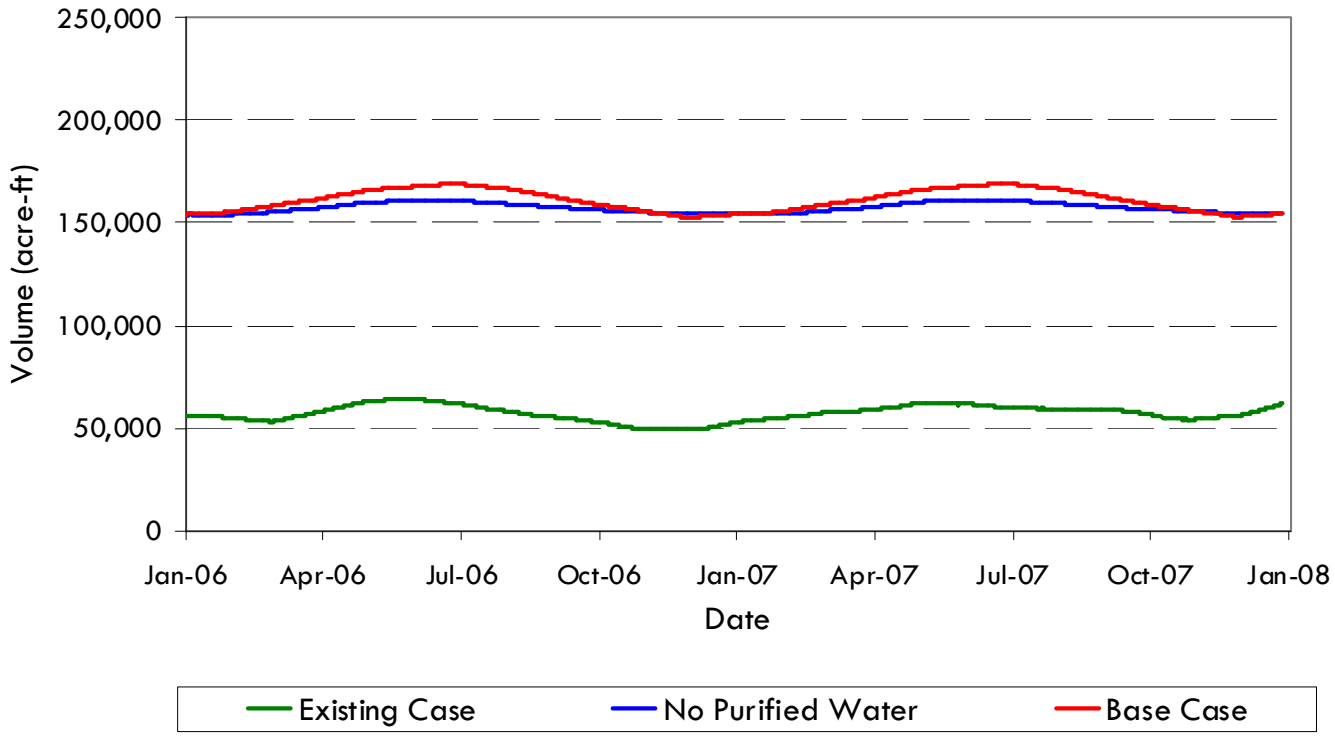

FSI V094005
May 01, 2012

Figure 20

FLOW SCIENCE®

Comparison of Existing Case, No Purified Water and Base Case Scenarios

Simulated Water Temperature at Station A

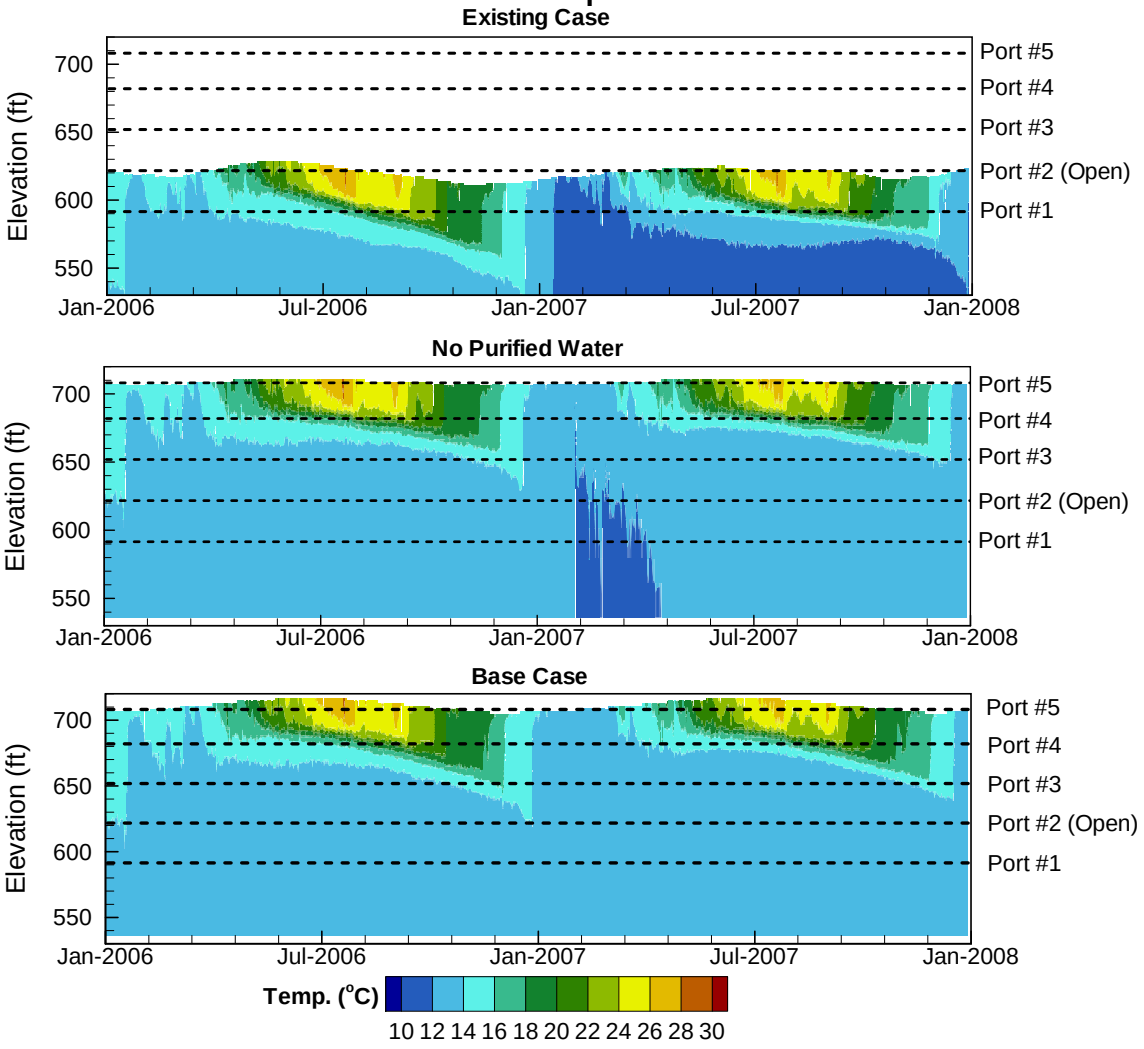

FSI V094005
May 01, 2012

Figure 21

FLOW SCIENCE®

Comparison of Existing Case, No Purified Water and Base Case Scenarios

Simulated Surface and Bottom Dissolved Oxygen at Station A

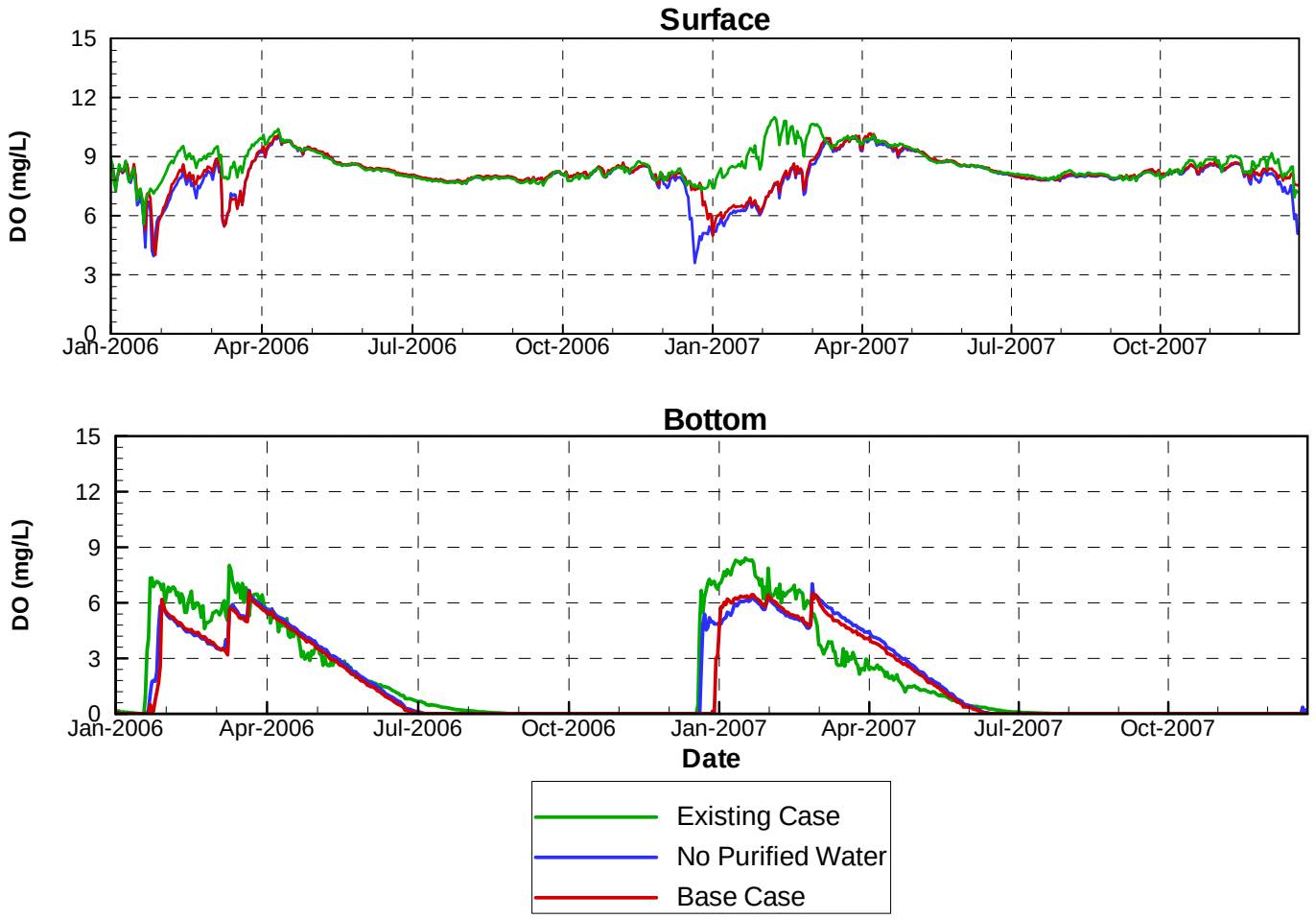

Figure 22

FSI V094005
May 01, 2012

FLOW SCIENCE®

Comparison of Existing Case, No Purified Water and Base Case Scenarios

Simulated Surface and Bottom Nitrate (as N) at Station A

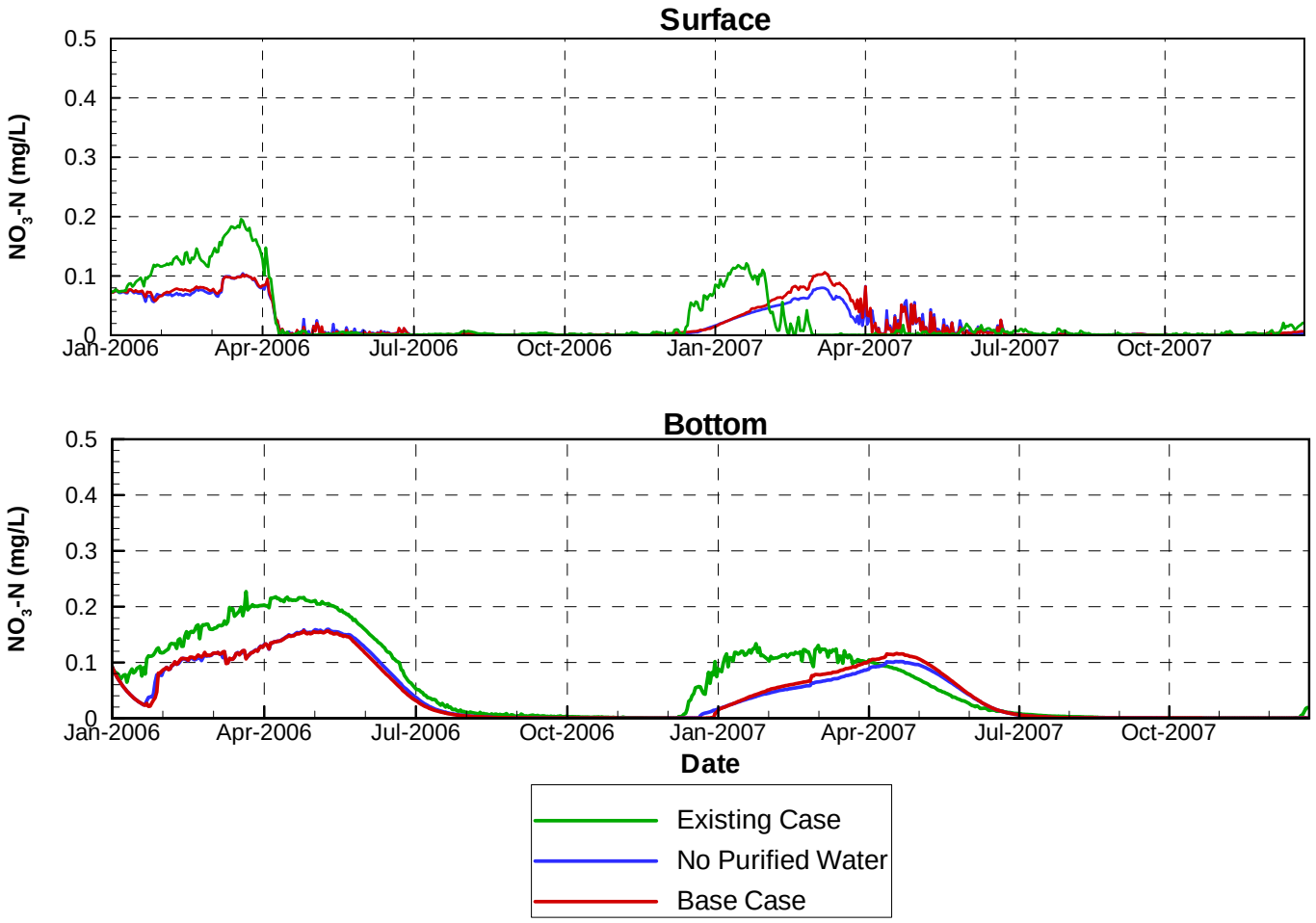

FSI V094005
May 01, 2012

Figure 23

FLOW SCIENCE®

Comparison of Existing Case, No Purified Water and Base Case Scenarios

Simulated Surface and Bottom Ammonia (as N) at Station A

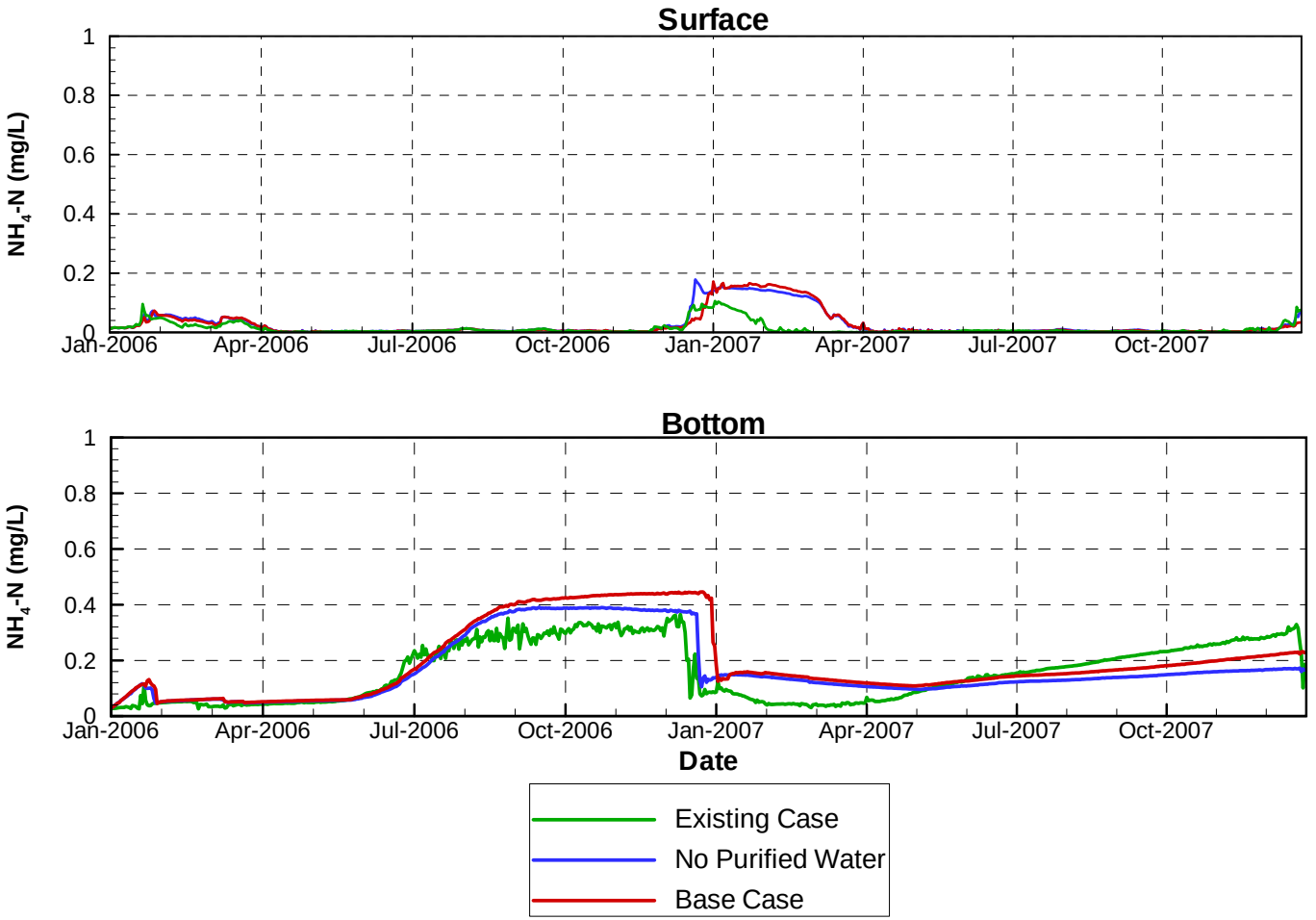

Figure 24

FSI V094005
May 01, 2012

FLOW SCIENCE®

Comparison of Existing Case, No Purified Water and Base Case Scenarios

Simulated Surface and Bottom Total Nitrogen at Station A

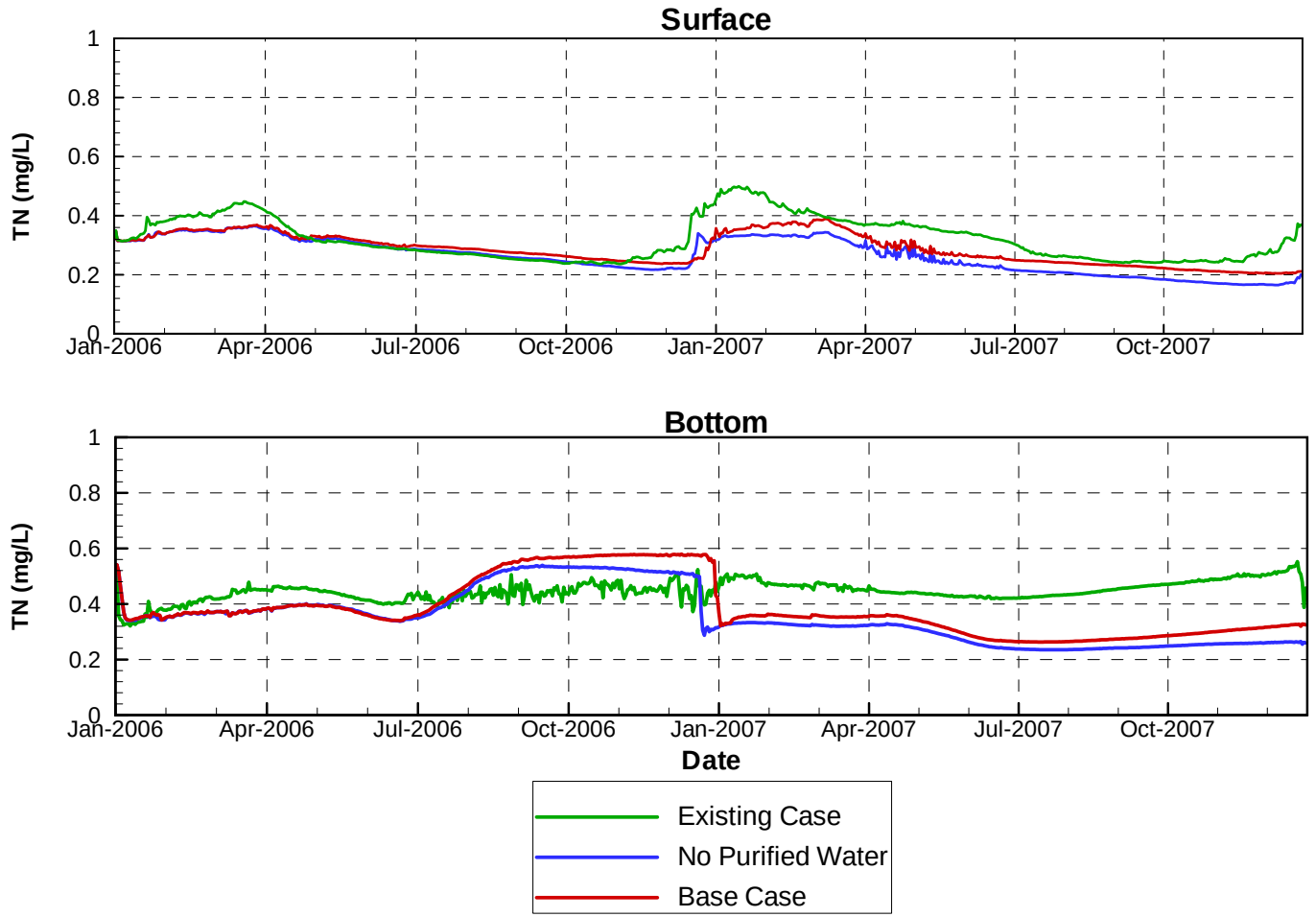

FSI V094005
May 01, 2012

Figure 25

FLOW SCIENCE®

Comparison of Existing Case, No Purified Water and Base Case Scenarios

Simulated Surface and Bottom SRP at Station A

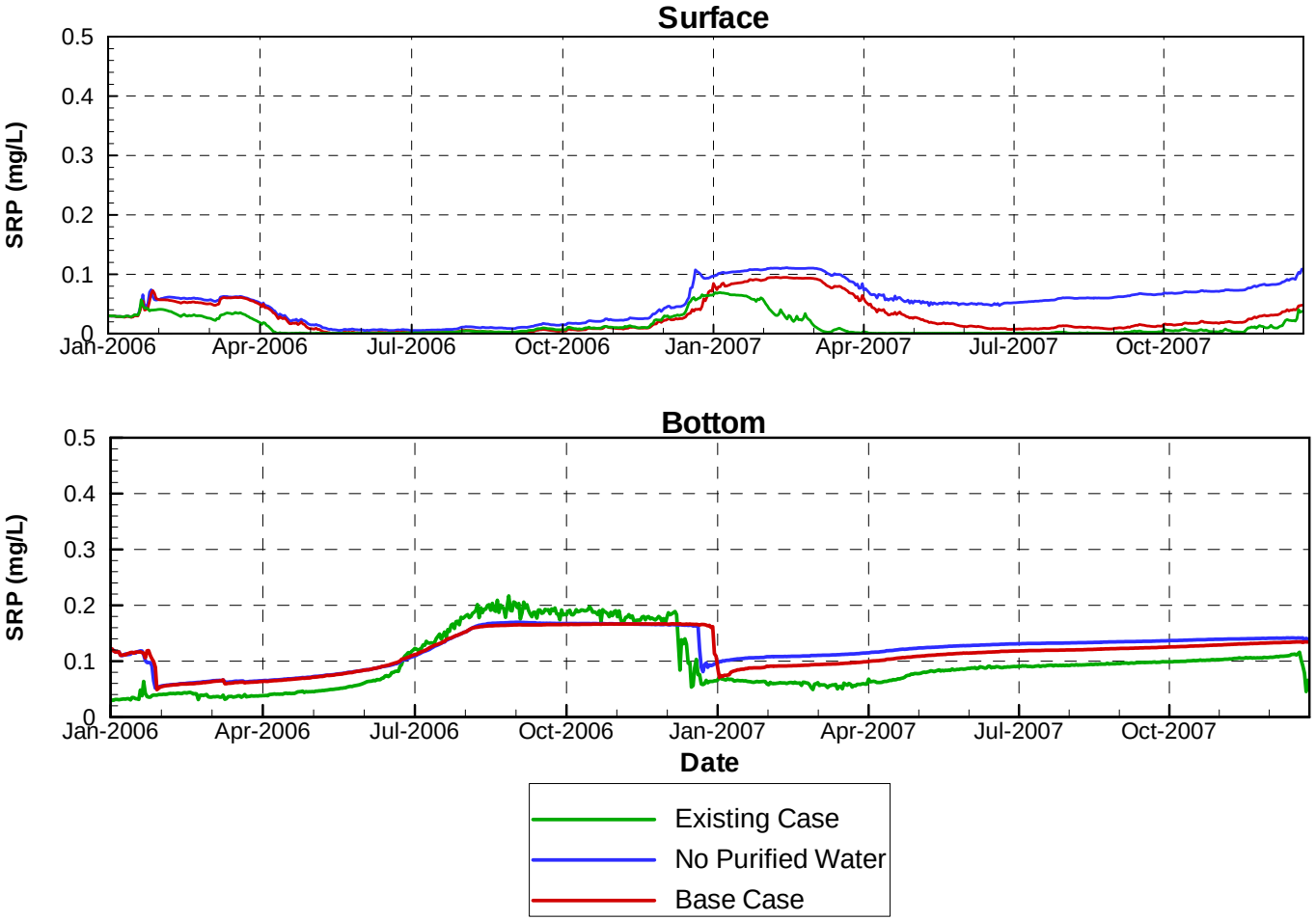

Figure 26

FSI V094005
May 01, 2012

FLOW SCIENCE®

Comparison of Existing Case, No Purified Water and Base Case Scenarios

Simulated Surface and Bottom TP at Station A

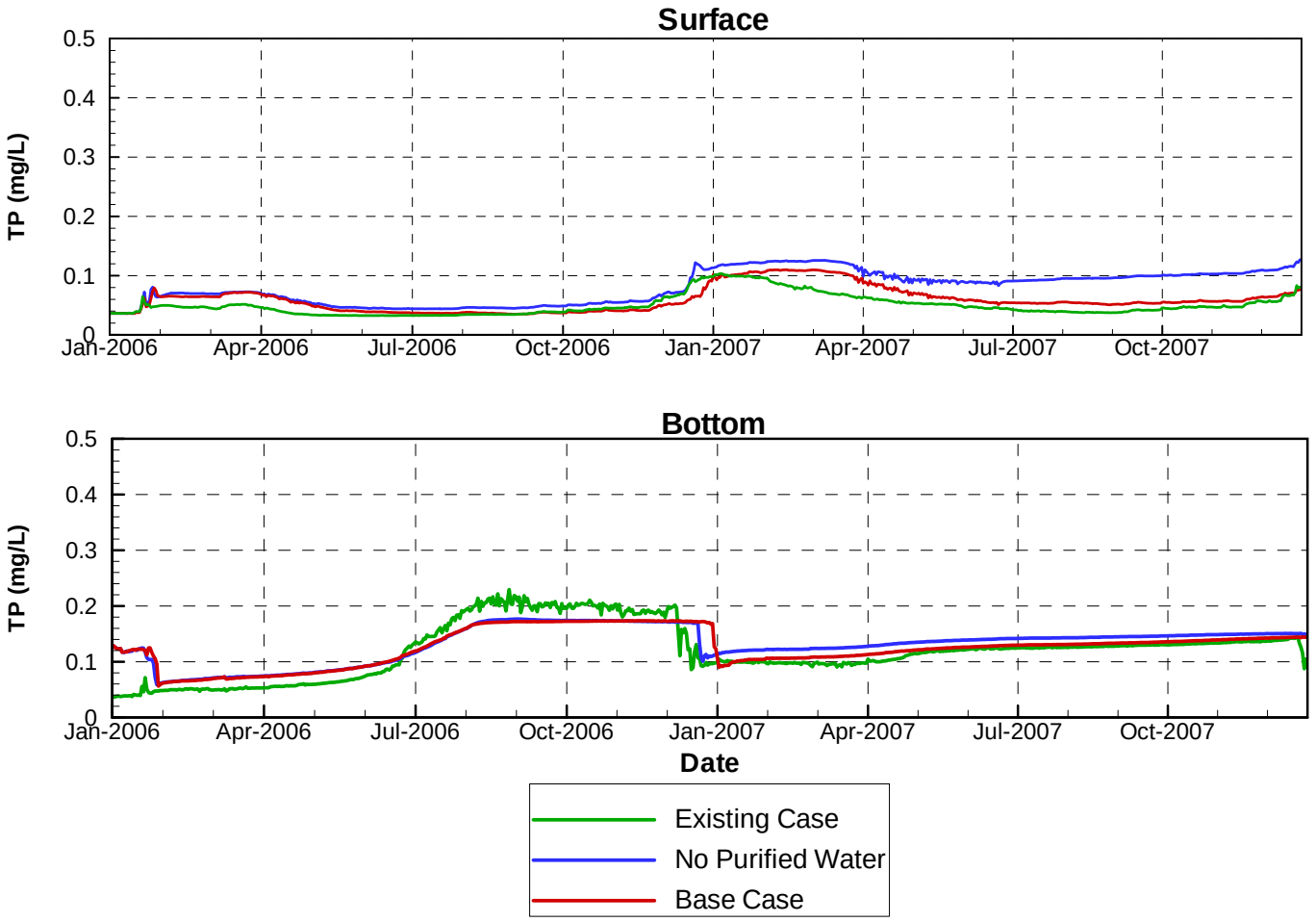

Figure 27

FLOW SCIENCE®

Comparison of Existing Case, No Purified Water and Base Case Scenarios

Simulated Surface Chlorophyll *a* at Station A

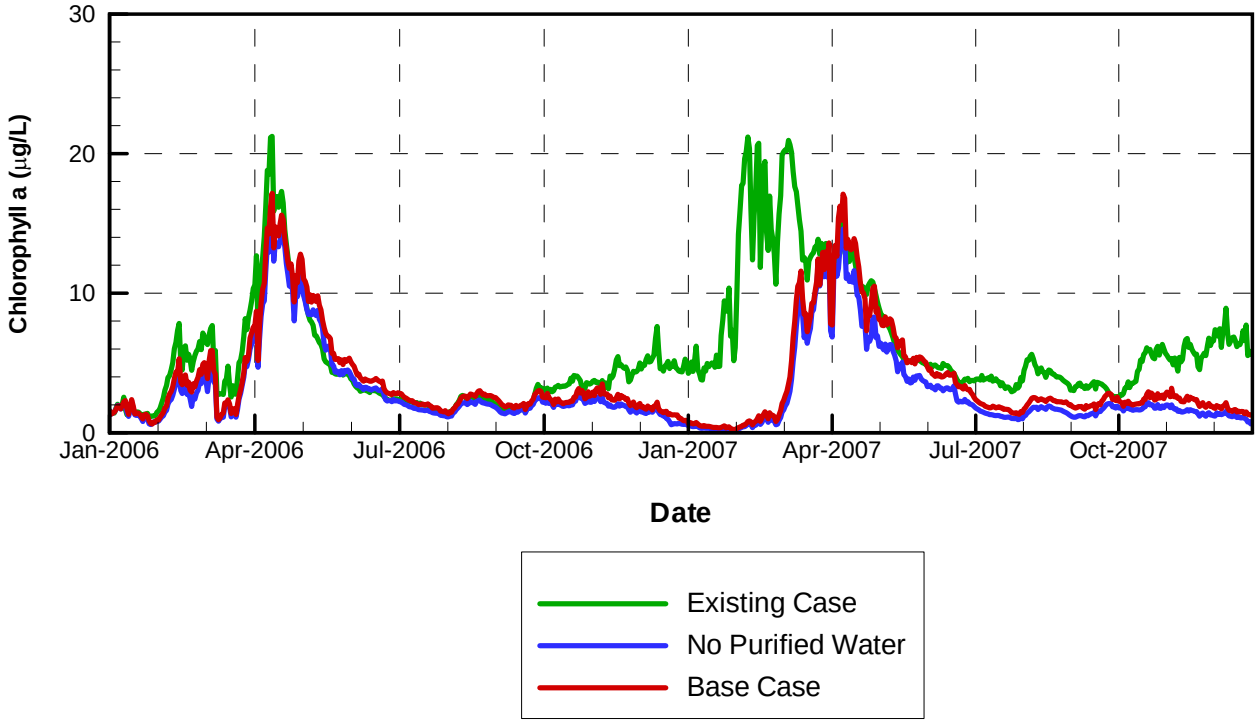

FSI V094005
May 01, 2012

Figure 28

FLOW SCIENCE®

Comparison of Existing Case, No Purified Water and Base Case Scenarios

Secchi Depth at Station A

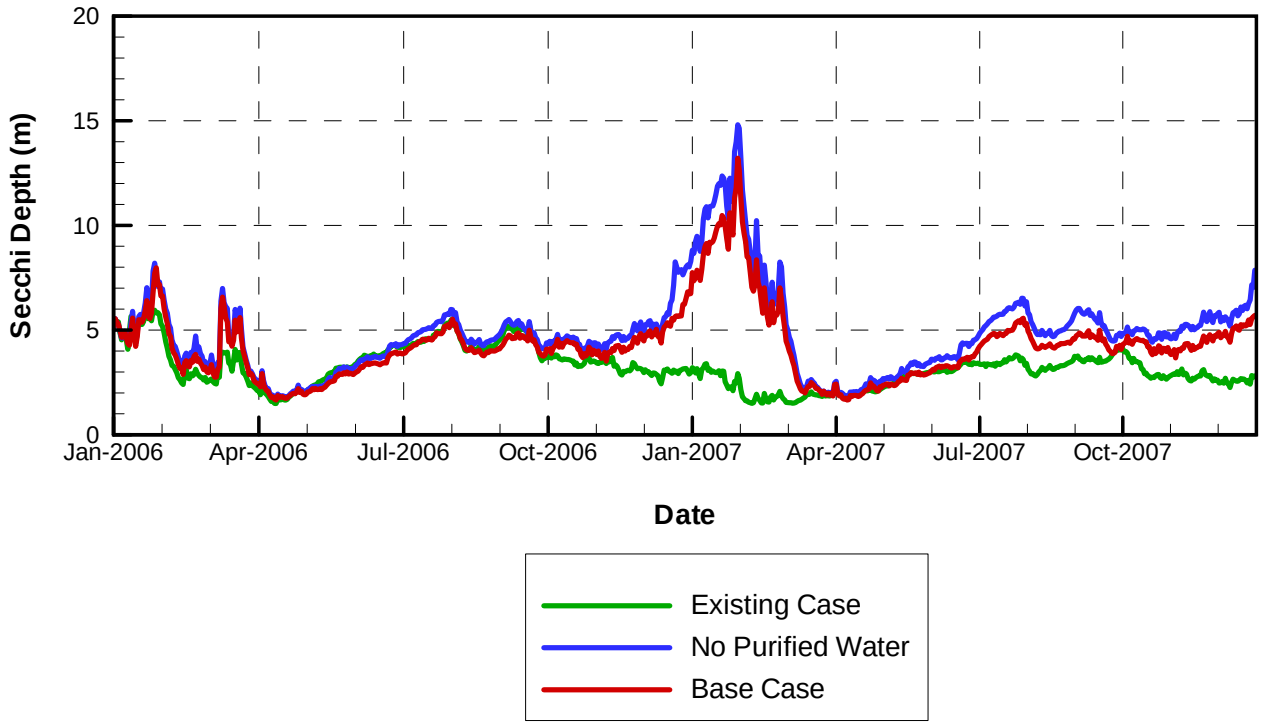

FSI V094005
May 01, 2012

Figure 29

FLOW SCIENCE®

Comparison of Existing Case, No Purified Water and Base Case Scenarios

Simulated Surface and Bottom pH at Station A

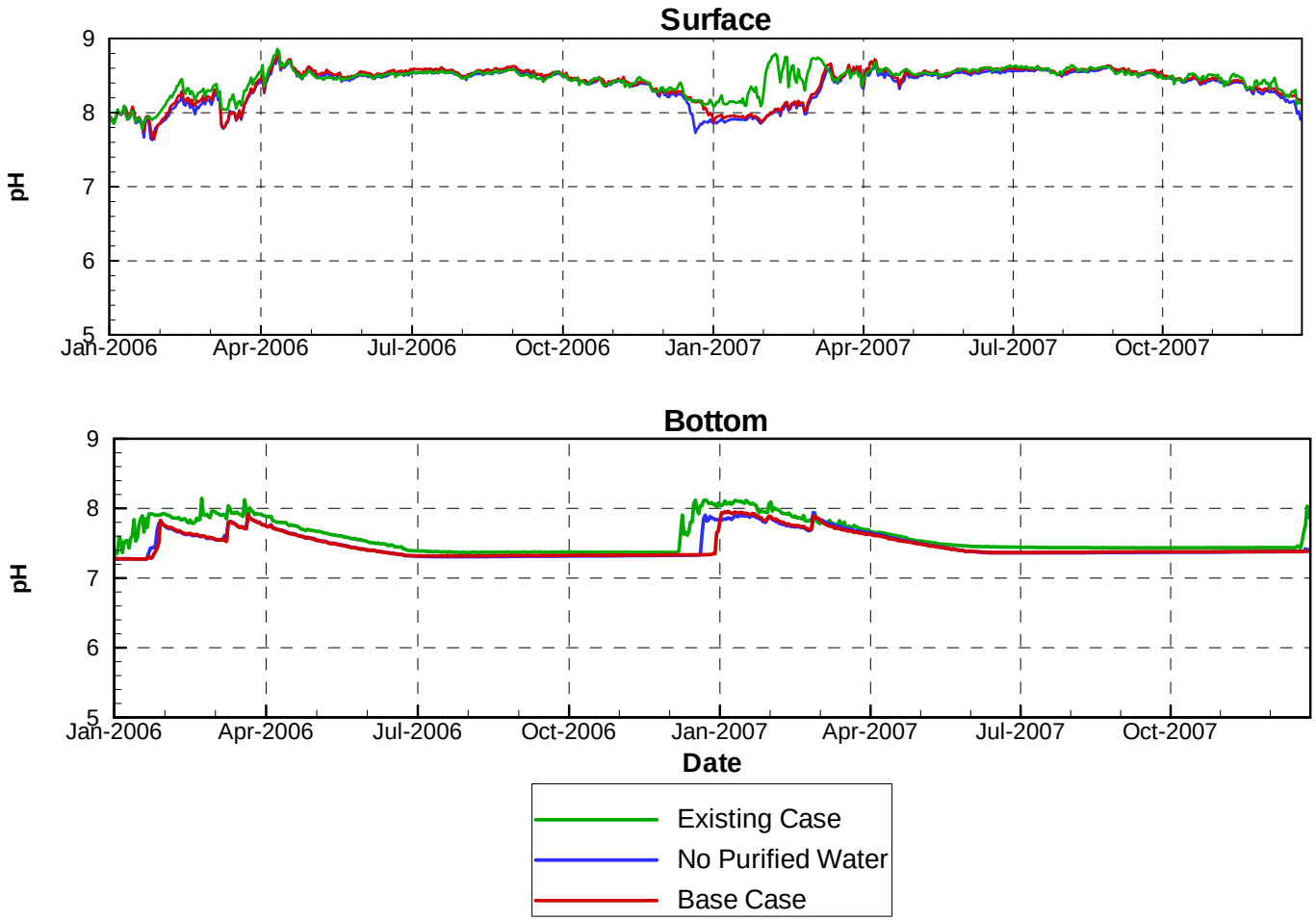

Figure 30

FSI V094005
May 01, 2012

FLOW SCIENCE®

APPENDIX A

Description of ELCOM/CAEDYM/Visual Plumes Models and Evidence of Validation

DESCRIPTION OF ELCOM/CAEDYM MODELS AND EVIDENCE OF VALIDATION

The coupling of biogeochemical and hydrodynamic processes in numerical simulations is a fundamental tool for research and engineering studies of water quality in coastal oceans, estuaries, lakes, and rivers. A modeling system for aquatic ecosystems has been developed that combines a three-dimensional hydrodynamic simulation method with a suite of water quality modules that compute interactions between biological organisms and the chemistry of their nutrient cycles. This integrated approach allows for the feedback and coupling between biogeochemical and hydrodynamic systems so that a complete representation of all appropriate processes can be included in an analysis. The hydrodynamic simulation code is the Estuary Lake and Coastal Ocean Model (ELCOM) and the biogeochemical model is the Computational Aquatic Ecosystem Dynamics Model (CAEDYM).

The purpose of this appendix is to demonstrate that ELCOM and CAEDYM are accepted models that have been systematically tested and debugged, and then successfully validated in numerous applications. A history of the models is provided, followed by an outline of the general model methodology and evolution that emphasizes the basis of the ELCOM/ CAEDYM codes in previously validated models and research. Then the process of code development, testing, and validation of ELCOM/CAEDYM is detailed. Specific model applications are described to illustrate how the ELCOM/CAEDYM models have been applied to coastal oceans, estuaries, lakes, and rivers throughout the world and the results successfully validated against field data. Finally, a general description of the governing equations, numerical models, and processes used in the models is provided along with an extensive bibliography of supporting material.

A comprehensive description of the equations and methods used in the models is provided in the "Estuary Lake and Coastal Ocean Model: ELCOM v2.2 Science Manual" by Hodges and Dallimore (2006), "Estuary Lake and Coastal Ocean Model: ELCOM v2.2 User Manual" by Hodges and Dallimore (2007), "Computational Aquatic Ecosystem Dynamics Model: CAEDYM: v2.2 Science Manual" by Hipsey, Romero, Antenucci and Hamilton (2005), and the "Computational Aquatic Ecosystem Dynamics Model: CAEDYM: v2.2 User Manual" by Hipsey, Romero, Antenucci and Hamilton (2005).

A.1.1 MODEL HISTORY

The ELCOM/CAEDYM models were originally developed at the Centre for Water Research (CWR) at the University of Western Australia, although the hydrodynamics

code ELCOM is an outgrowth of a hydrodynamic model developed earlier by Professor Vincenzo Casulli in Italy and now in use at Stanford University under the name TRIM-3D. The CAEDYM model was essentially developed at CWR as an outgrowth of earlier water quality modules used in the one-dimensional model, Dynamic Reservoir Simulation Model - Water Quality (DYRESM-WQ, Hamilton and Schladow, 1997).

The original ELCOM/CAEDYM models, as developed by CWR, were implemented in Fortran 90 (with F95 extensions) on a UNIX computer system platform. In 2001, the codes for both models were ported to a personal computer (PC) platform through an extensive recompiling and debugging effort by Flow Science Incorporated (Flow Science) in Pasadena, California. Since then, Flow Science has updated the PC version of the code several times when new versions of the code have been released by CWR.

A.1.2 MODEL METHODOLOGY

ELCOM is a three-dimensional numerical simulation code designed for practical numerical simulation of hydrodynamics and thermodynamics for inland and coastal waters. The code links seamlessly with the CAEDYM biogeochemical model undergoing continuous development at CWR, as shown graphically in **Figure A.1**. The

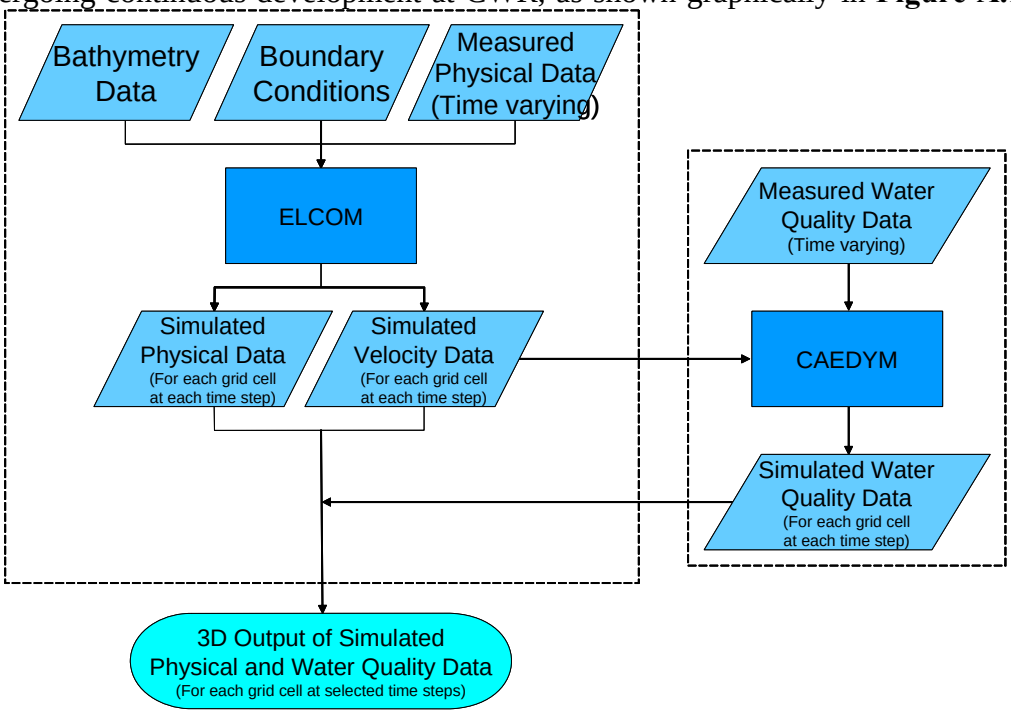

Figure A.1 Flow chart showing the integration of the linked ELCOM/CAEDYM models.

combination of the two codes provides three-dimensional simulation capability for examination of changes in water quality that arise from anthropogenic changes in either quality of inflows or reservoir operations.

The numerical method used in ELCOM is based on the TRIM-3D model scheme of Casulli and Cheng (1992) with adaptations made to improve accuracy, scalar conversion, numerical diffusion, and implementation of a mixed-layer model. The ELCOM model also extends the TRIM-3D scheme by including conservative advection of scalars. The unsteady Reynolds-averaged, Navier-Stokes equations, and the scalar transport equations serve as the basis of ELCOM. The pressure distribution is assumed hydrostatic and density changes do not impact the inertia of the fluid (the Boussinesq approximation), but are considered in the fluid body forces. There is an eddy-viscosity approximation for the horizontal turbulence correlations that represent the turbulent momentum transfer. Vertical momentum transfer is handled by a Richardson number-based diffusion coefficient. Since numerical diffusion generally dominates molecular processes, molecular diffusion in the vertical direction is neglected in ELCOM.

Both ELCOM and TRIM-3D are three-dimensional, computational fluid dynamics (CFD) models. CFD modeling is a validated and well-established approach to solving the equations of fluid motions in a variety of disciplines. Prior to the development of TRIM-3D, there were difficulties in modeling density-stratified flows and such flows required special numerical methods. With TRIM-3D, Casulli and Cheng (1992) developed the first such successful method to model density-stratified flows, such as occur in the natural environment. Since then, TRIM-3D has been validated by numerous publications. ELCOM is based on the same proven method, but incorporates additional improvements as described above. Furthermore, the ELCOM model is based on governing equations and numerical algorithms that have been used in the past (*e.g.*, in validated models such as TRIM-3D), and have been validated in refereed publications. For example:

- The hydrodynamic algorithms in ELCOM are based on the Euler-Lagrange method for advection of momentum with a conjugate gradient solution for the free-surface height (Casulli and Cheng, 1992).

- The free-surface evolution is governed by vertical integration of the continuity equation for incompressible flow applied to the kinematic boundary condition (*e.g.*, Kowalik and Murty, 1993).

- The numerical scheme is a semi-implicit solution of the hydrostatic Navier-Stokes equations with a quadratic Euler-Lagrange, or semi-Lagrangian (Staniforth and Côté, 1991).

- Passive and active scalars (*i.e.*, tracers, salinity, and temperature) are advected using a conservative ULTIMATE QUICKEST discretization (Leonard, 1991). The ULTIMATE QUICKEST approach has been implemented in two-dimensional format and demonstration of its effectiveness in estuarine flows has been documented by Lin and Falconer (1997).

- Heat exchange is governed by standard bulk transfer models found in the literature (*e.g.*, Smooch and DeVries, 1980; Imberger and Patterson, 1981; Jacquet, 1983).

- The vertical mixing model is based on an approach derived from the mixing energy budgets used in one-dimensional lake modeling as presented in Imberger and Patterson (1981), Spigel et al (1986), and Imberger and Patterson (1990). Furthermore, Hodges presents a summary of validation using laboratory experiments of Stevens and Imberger (1996). This validation exercise demonstrates the ability of the mixed-layer model to capture the correct momentum input to the mixed-layer and reproduce the correct basin-scale dynamics, even while boundary-induced mixing is not directly modeled.

- The wind momentum model is based on a mixed-layer model combined with a model for the distribution of momentum over depth (Imberger and Patterson, 1990).

The numerical approach and momentum and free surface discretization used in ELCOM are defined in more detail in Hodges, Imberger, Saggio, and Winters (1999). Similarly, the water quality processes and methodology used in CAEDYM are described in more detail in Hamilton and Schladow (1997). Further technical details on ELCOM and CAEDYM are provided in Sections **Error! Reference source not found.** and **Error! Reference source not found.** below.

A.1.3 VALIDATION AND APPLICATION OF ELCOM/CAEDYM

Since initial model development, testing and validation of ELCOM and/or CAEDYM have been performed and numerous papers on model applications have been presented, written, and/or published as described in more detail below. In summary:

- ELCOM solves the full three-dimensional flow equations with small approximations.

- ELCOM/CAEDYM was developed, tested, and validated over a variety of test cases and systems by CWR.

- Papers on ELCOM/CAEDYM algorithms, methodology, and applications have been published in peer reviewed journals such as the *Journal of Geophysical Research*, the *Journal of Fluid Mechanics*, the *Journal of Hydraulic Engineering*, the *International Journal for Numerical Methods in Fluids*, and *Limnology and Oceanography*.

- ELCOM/CAEDYM was applied by Flow Science to Lake Mead, Nevada. As part of this application, mass balances were verified and results were presented to a model review panel over a two-year period. The model review panel, the National Park Service, the United States Bureau of Reclamation, the Southern Nevada Water Authority, and the Clean Water Coalition (a consortium of water and wastewater operators in the Las Vegas, Nevada, region) all accepted the ELCOM/CAEDYM model use and validity.

- There are numerous applications of ELCOM/CAEDYM in the literature that compare the results to data, as summarized in Section **Error! Reference source not found.**.

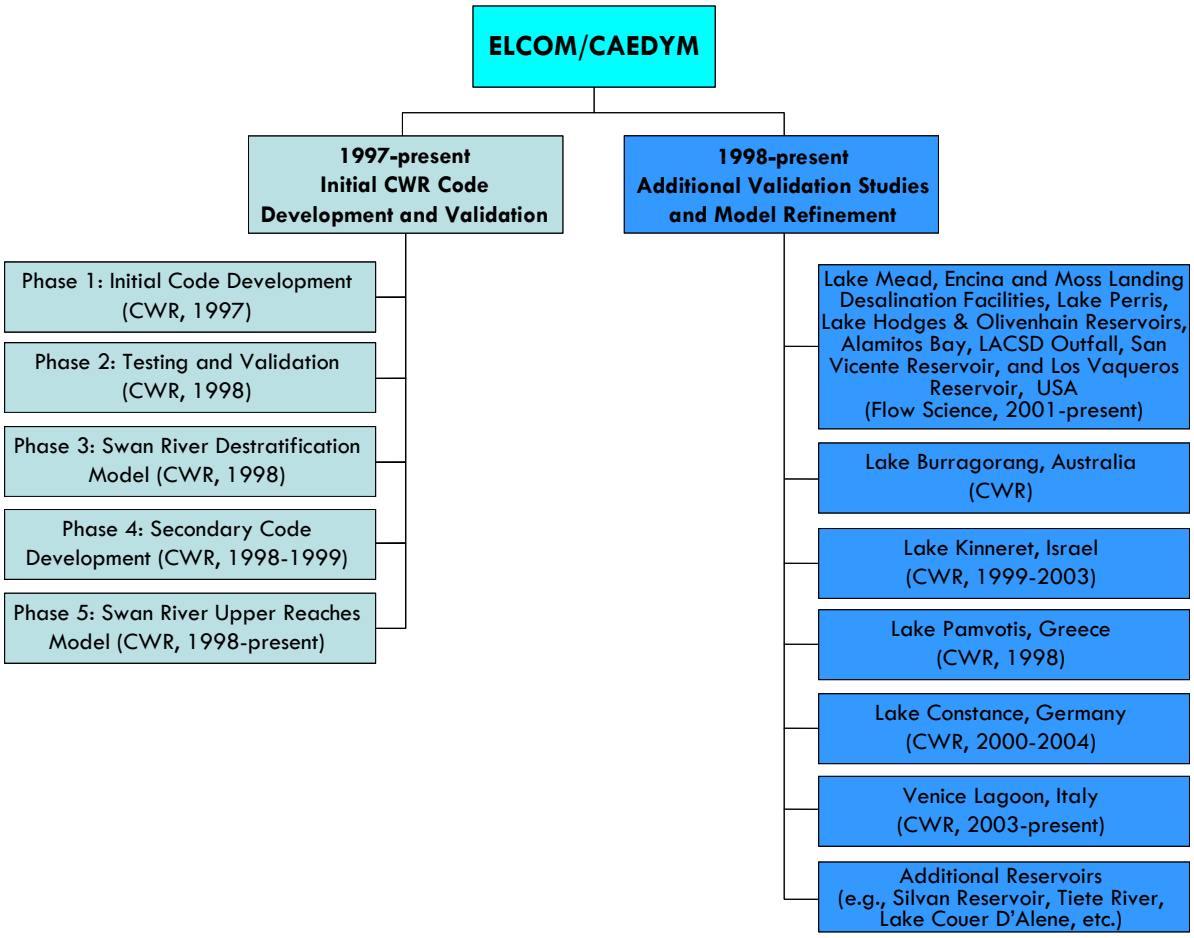

Figure A.2 ELCOM/CAEDYM code development, testing, validation, and applications by CWR and Flow Science Incorporated.

The process of code development, testing, and validation of ELCOM/CAEDYM by CWR, and the ongoing validation and refinement of the codes through further application of the models are detailed in the following subsections. The major components of the development, testing, and validation process are summarized in **Figure A.2**.

A.1.3.1 CWR Code Development, Testing, and Validation

Initial development of the code by CWR occurred from March through December 1997 (Phase 1), followed by a period of testing and validation from January through April 1998 (Phases 2 and 3). Secondary code development by CWR occurred from September 1998 through February 1999 (Phase 4). Testing and validation were

performed over a variety of test cases and systems to ensure that all facets of the code were tested. In addition, Phase 5 modeling of the Swan River since 1998 has been used to gain a better understanding of the requirements and limitations of the model (Hodges et al, 1999).

A.1.3.1.1 *Phase 1: Initial Code Development*

The ELCOM code was initially conceived by CWR as a Fortran 90/95 adaptation of the TRIM-3D model of Casulli and Cheng (1992) in order to: 1) link directly to the CAEDYM water quality module developed concurrently at CWR and 2) provide a basis for future development in a modern programming language. Although written in Fortran 77, TRIM-3D is considered a state-of-the-art numerical model for estuarine applications using a semi-implicit discretization of the Reynolds-averaged hydrostatic Navier-Stokes equations and an Euler-Lagrange method for momentum and scalar transport.

During development of ELCOM, it became clear that additional improvements to the TRIM-3D algorithm were required for accurate solution of density-stratified flows in estuaries. After the basic numerical algorithms were written in Fortran 90, subroutine-by-subroutine debugging was performed to ensure that each subroutine produced the expected results. Debugging and testing of the entire model used a series of test cases that exercised the individual processes in simplified geometries. This included test cases for the functioning of the open boundary condition (tidal forcing), surface wave propagation, internal wave propagation, scalar transport, surface thermodynamics, density underflows, wind-driven circulations, and flooding/drying of shoreline grid cells. Shortcomings identified in the base numerical algorithms were addressed during secondary code development (Phase 4).

Towards the end of the initial code development, ELCOM/CAEDYM were coupled and test simulations were run to calibrate the ability of the models to work together on some simplified problems. Results showing the density-driven currents induced by phytoplankton shading were presented at the Second International Symposium on Ecology and Engineering (Hodges and Herzfeld, 1997). Further details of modeling of density-driven currents due to combinations of topographic effects and phytoplankton shading were presented at a joint meeting of the American Geophysical Union (AGU) and the American Society of Limnology and Oceanography (ASLO) by Hodges et al. (1998), and at a special seminar at Stanford University (Hodges 1998). Additionally, presentations by Hamilton (1997), Herzfeld et al. (1997), and Herzfeld and Hamilton (1998) documented the concurrent development of the CAEDYM ecological model.

A.1.3.1.2*Phase 2: Testing and Validation*

The simplified geometry tests of Phase I revealed deficiencies in the TRIM-3D algorithm including the inability of the TRIM-3D Euler-Lagrange method (ELM) to provide conservative transport of scalar concentrations (e.g., salinity and temperature). Thus, a variety of alternate scalar transport methods were tested, with the best performance being a flux-conservative implementation of the ULTIMATE filter applied to third-order QUICKEST discretization based on the work of Leonard (1991).

Model testing and validation against simple test cases was again undertaken. In addition, a simulation of a winter underflow event in Lake Burragorang in New South Wales, Australia, was performed to examine the ability of the model to capture a density underflow in complex topography in comparison to field data taken during the inflow event. These tests showed that the ability to model underflows is severely constrained by the cross-channel grid resolution.

A.1.3.1.3*Phase 3: Swan River Destratification Model*

Phase 3 involved examining a linked ELCOM/CAEDYM destratification model of the Swan River system during a period of destratification in 1997 when intensive field monitoring had been conducted. The preliminary results of this work were presented at the Swan-Canning Estuary Conference (Hertzfeld *et al*, 1998). More comprehensive results were presented at the Western Australian Estuarine Research Foundation (WAERF) Community Forum (Imberger, 1998).

A.1.3.1.4*Phase 4: Secondary Code Development*

In conducting the Phase 3 Swan River destratification modeling, it became clear to CWR that long-term modeling of the salt-wedge propagation would require a better model for mixing dynamics than presently existed. Thus, the availability of an extensive field data set for Lake Kinneret, Israel, led to its use as a test case for development of an improved mixing algorithm for stratified flows (Hodges *et al*, 1999).

A further problem appeared in the poor resolution of momentum terms using the linear ELM discretization (*i.e.*, as used in the original TRIM-3D method). Since the conservative ULTIMATE QUICKEST method (used for scalar transport, see Phase 1 above) does not lend itself to efficient use for discretization of momentum terms in a semi-implicit method, a quadratic ELM approach was developed for more accurate discretization of the velocities.

A.1.3.1.5 *Phase 5: Swan River Upper Reaches Model*

Phases 1-4 developed and refined the ELCOM code for accurate modeling of three-dimensional hydrodynamics where the physical domain is well resolved. Phase 5 is an ongoing process of model refinement that concentrates on developing a viable approach to modeling longer-term evolution hydrodynamics and water quality in the Swan River where fine-scale resolution of the domain is not practical. The Swan River application is also used for ongoing testing and calibration of the CAEDYM water quality module.

The Swan River estuary is located on the Swan Coastal Plain, Western Australia. It is subject to moderate to high nutrient loads associated with urban and agricultural runoff and suffered from *Microcystis aeruginosa* blooms in January 2000. In an effort to find a viable means of conducting seasonal to annual simulations of the Swan River that retain the fundamental along-river physics and the cross-channel variability in water quality parameters, CWR has developed and tested ELCOM/CAEDYM extensively. A progress report by Hodges et al (1999) indicates that ELCOM is capable of accurately reproducing the hydrodynamics of the Swan River over long time scales with a reasonable computational time.

Furthermore, studies conducted by Robson and Hamilton (2002) proved that ELCOM/CAEDYM accurately reproduced the unusual hydrodynamic circumstances that occurred in January 2000 after a record maximum rainfall, and predicted the magnitude and timing of the *Microcystis* bloom. These studies show that better identification and monitoring procedures for potentially harmful phytoplankton species could be established with ELCOM/CAEDYM and will assist in surveillance and warnings for the future.

A.1.3.2 Model Applications

In addition to the initial code development, testing, and validation by CWR, numerous other applications of ELCOM/CAEDYM have been developed by CWR and validated against field data. Additionally, Flow Science has applied ELCOM/CAEDYM extensively at Lake Mead (USA) and validated the results against measured data. The results of numerous ELCOM/CAEDYM model applications are presented below.

A.1.3.2.1 *Lake Mead (Nevada, USA)*

An ELCOM/CAEDYM model of Boulder Basin, Lake Mead near Las Vegas, Nevada, was used to evaluate alternative discharge scenarios for inclusion in an Environmental Impact Statement (EIS) for the Clean Water Coalition (CWC), a

consortium of water and wastewater operators in the Las Vegas region. **Figure A.3** is a cut-away of the three-dimensional model grid used for Boulder Basin, showing the varying grid spacing in the vertical direction.

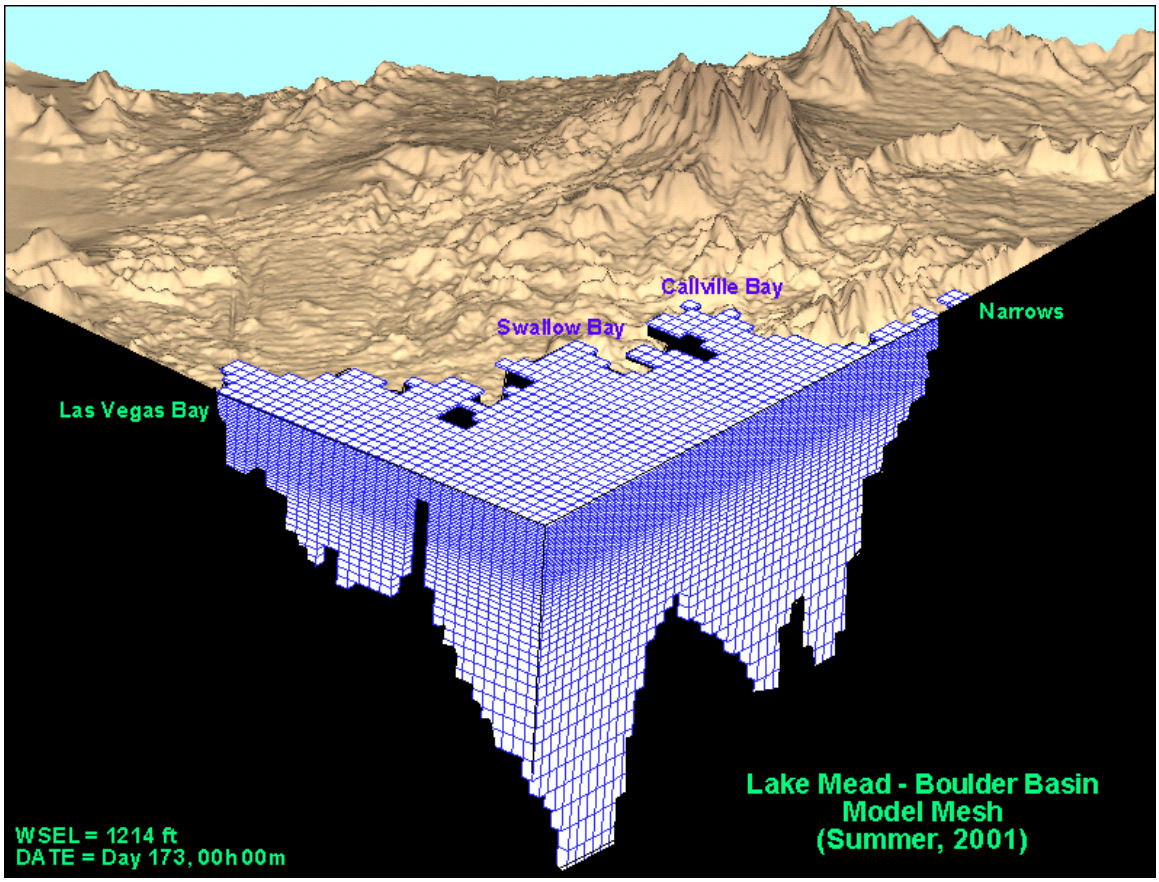

Figure A.3 Model grid for Lake Mead Boulder Basin model.

As part of the EIS process, a model review panel met monthly for two years to review the validation of the ELCOM/CAEDYM model, its calibration against field data, and its application. The modeling committee approved the use of the model. Subsequently, a scientific Water Quality Advisory Panel concluded that the ELCOM/CAEDYM model was applicable and acceptable. The members of the Water Quality Advisory Panel were diverse and included Jean Marie Boyer, Ph.D., P.E. (Water Quality Specialist/Modeler, Hydrosphere), Chris Holdren, Ph.D., CLM (Limnologist, United States Bureau of Reclamation), Alex Horne, Ph.D. (Ecological Engineer, University of California Berkeley), and Dale Robertson, Ph.D. (Research Hydrologist, United States Geological

Survey). More specifically, the Water Quality Advisory Panel agreed on the following findings:

- The ELCOM/CAEDYM model is appropriate for the project.
- There are few three-dimensional models available for reservoirs. ELCOM is one of the best hydrodynamic models and has had good success in the Boulder Basin of Lake Mead and other systems.
- The ELCOM model accurately simulates most physical processes.
- The algorithms used in CAEDYM are widely accepted (a biological consultant, Professor David Hamilton of The University of Waikato, New Zealand, was retained to review the CAEDYM coefficients and algorithms).

The Boulder Basin ELCOM/CAEDYM model was calibrated against four years of measured data for numerous physical and water quality parameters including temperature, salinity, conductivity, dissolved oxygen, pH, nutrients (nitrogen and phosphorus), chlorophyll *a*, perchlorate, chloride, sulfate, bromide, and total organic carbon. Detailed results of this calibration and the subsequent evaluation of alternative discharge scenarios were made available in late 2005 in the CWC EIS that was being prepared for this project. An example of the calibration results for chlorophyll *a* for 2002 is presented in **Figure A.4** below. In this figure, simulated concentrations are compared against field data measured in the lake by the United States Bureau of Reclamation (USBR) and the City of Las Vegas (COLV).

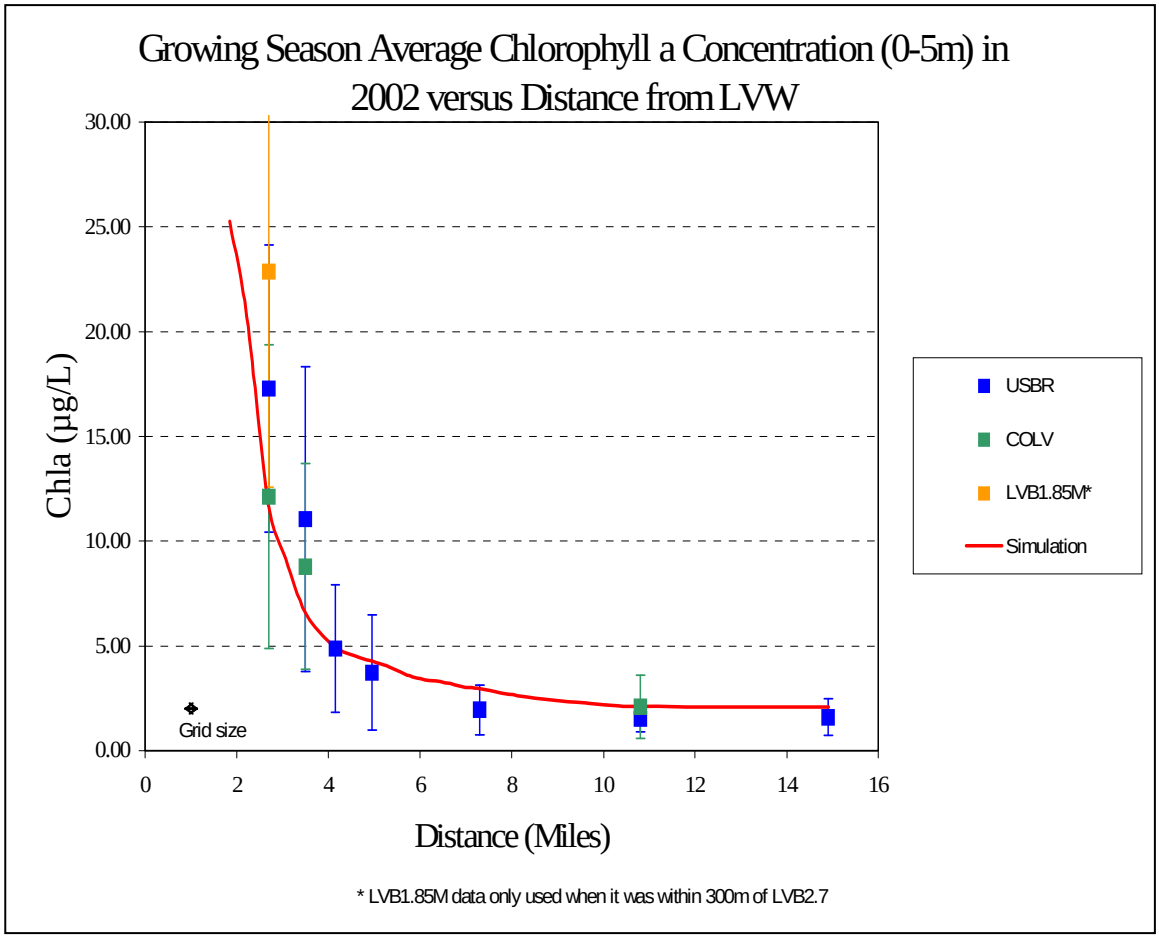

Figure A.4 ELCOM/CAEDYM calibration results for chlorophyll a in Boulder Basin for 2002 as a function of distance from the inflow at Las Vegas Wash.

Most recently, the original Boulder Basin model was extended to include all of Lake Mead, including the Overton Arm and Gregg Basin. The extended whole lake ELCOM/CAEDYM model has been calibrated against nine (9) years of data for use in informing design and operations management decisions. Specifically, the model has been used to simulate temperature (including stratification patterns), salinity, conductivity, dissolved oxygen, nutrients, chlorophyll *a* (as a surrogate for algae), perchlorate, total organic carbon, bromide, and suspended solids. **Figure A.5** below shows the extent of the expanded whole lake domain and the calibration results for conductivity for February 2005.

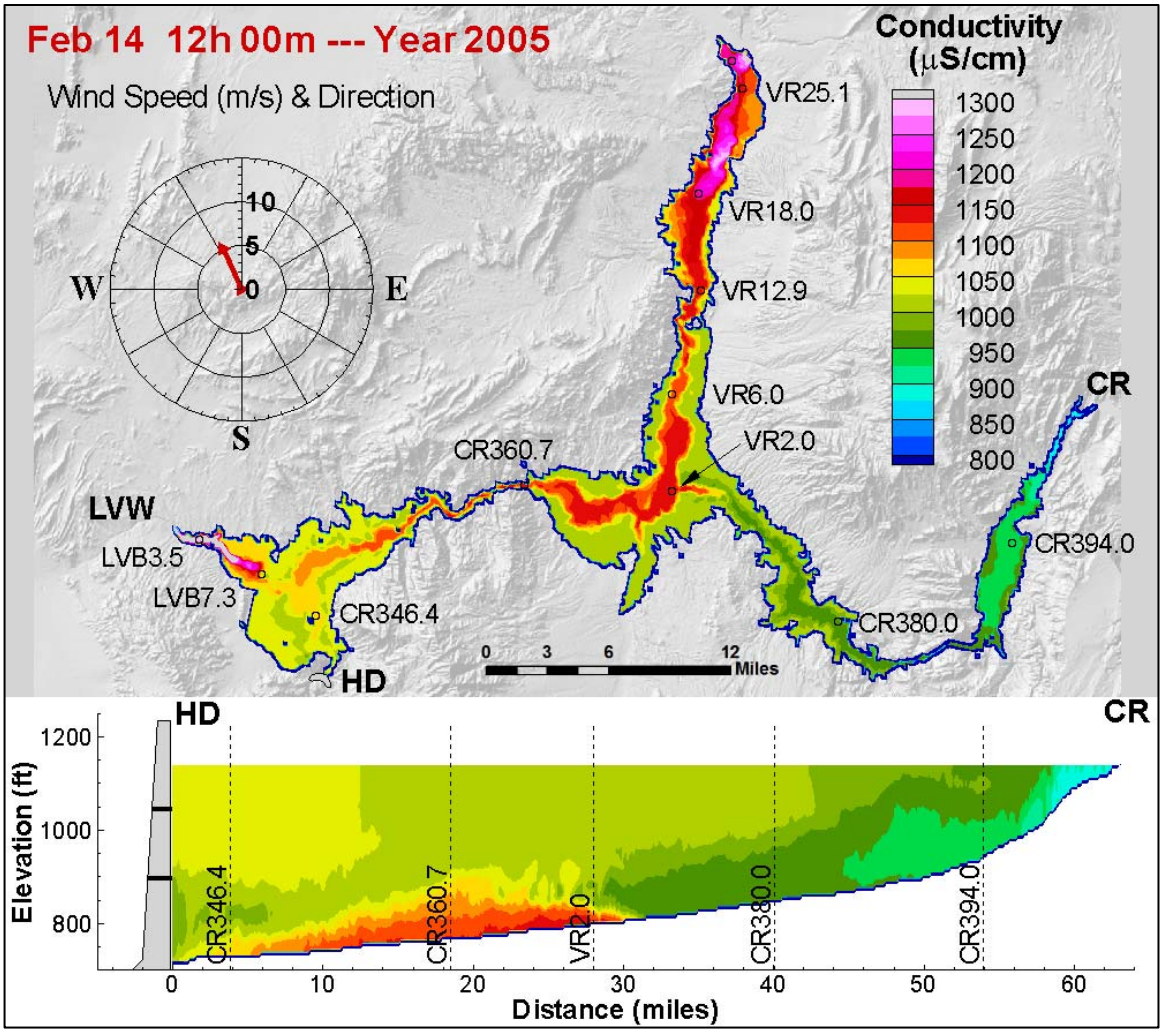

Figure A.5 ELCOM/CAEDYM calibration results for conductivity in the Lake Mead Whole Lake Model (including plan view of entire lake and cross-section from Hoover Dam to the mouth of the Colorado River).

ELCOM/CAEDYM model of the entire Lake Mead is being continually updated and calibrated on approximately a yearly basis, with funding having been provided by the CWC, the Southern Nevada Water Authority, and the National Park Service. These various stakeholders have demonstrated a long term commitment to maintaining the model because it has proven to be a worthy and successful tool. Additional funding for

ELCOM/CAEDYM modeling of the impacts of climate change on Lake Mead is being provided by the USBR under the WaterSMART grant program.

A.1.3.2.2*Lake Burragorang (New South Wales, Australia)*

ELCOM was applied and validated for Lake Burragorang in order to rapidly assess the potential impacts on water quality during an underflow event (CWR). Underflows usually occur during the winter when inflow water temperature is low compared to the reservoir. This causes the upheaval of hypolimnetic water at the dam wall, and as a result it transports nutrient rich waters into the euphotic zone.

The thermal dynamics during the underflow event were reproduced accurately by ELCOM for the case with idealized bathymetry data with coarse resolutions (straightened curves and rotating the lake in order to bypass the resolution problem), but not for the simulation with the complex, actual bathymetry. This is because the model tests showed that the ability to model underflows is severely constrained by the cross-channel grid resolution. When the cross-channel direction is poorly resolved at bends and curves, an underflow is unable to propagate downstream without a significant loss of momentum. Nevertheless, the simulations with the coarse idealized domain certainly can be used as aids and tools to visualize the behavior of reservoirs. Particularly, ELCOM was able to capture the traversal of the underflow down the length of Lake Burragorang and then had sufficient momentum to break against the wall causing the injection of underflow waters into the epilimnion near the dam. This simulated dynamic was in agreement with what was measured in the field.

A.1.3.2.3*Lake Kinneret (Israel)*

ELCOM was applied to model basin-scale internal waves that are seen in Lake Kinneret, Israel, since understanding of basin-scale internal waves behaviors provide valuable information on mixing and transport of nutrients below the wind-mixed layer in stratified lakes. In studies done by Hodges et al. (1999) and Laval et al (2003), the ELCOM simulation results were compared with field data under summer stratification conditions to identify and illustrate the spatial structure of the lowest-mode basin-scale Kelvin and Poincare waves that provide the largest two peaks in the internal wave energy spectra. The results demonstrated that while ELCOM showed quantitative differences in the amplitude and steepness of the waves as well as in the wave phases, the basin-scale waves were resolved very well by ELCOM. In particular, the model captures the qualitative nature of the peaks and troughs in the thermocline and the depth of the wind-mixed layer at relatively coarse vertical grid resolutions (Hodges et al, 1999).

A.1.3.2.4 *Lake Pamvotis (Greece)*

ELCOM/CAEDYM was applied to Lake Pamvotis, a moderately sized (22 km^2), shallow (4 m average depth) lake located in northwest Greece. Since the lake has undergone eutrophication over the past 40 years, many efforts are directed at understanding the characteristics of the lake and developing watershed management and restoration plans.

Romero and Imberger (1999) simulated Lake Pamvotis over a one month period during May to June, 1998, and compared the simulated thermal and advective dynamics of the lake with data obtained from a series of field experiments. The simulation results over-predicted heating; however, diurnal fluctuations in thermal structures were similar to those measured. Since the meteorological site was sheltered from the winds, the wind data used in the simulation was believed to be too low, causing insufficient evaporative heat-loss and subsequent over-heating by ELCOM. An increase in the wind speed by a factor of three gave temperature profiles in agreement with the field data. Moreover, the study demonstrated that the model is capable of predicting the substantial diurnal variations in the intensity and direction of both vertical and horizontal velocities. Romero and Imberger were also able to illustrate the functionality of ELCOM when coupled to the water quality model, CAEDYM, and confirmed that the model could be used to evaluate the effect of various strategies to improve poor water quality in localized areas in the lake.

A.1.3.2.5 *Lake Constance (Germany, Austria, Switzerland)*

Appt (2000) and Appt et al. (2004) applied ELCOM to characterize the internal wave structures and motions in Lake Constance [Bodensee] since internal waves are a key factor in understanding the transport mechanisms for chemical and biological processes in a stratified lake such as Lake Constance. Lake Constance is an important source of drinking water and a major tourism destination for its three surrounding countries of Germany, Austria, and Switzerland. Due to anthropogenic activities and climatic changes, Lake Constance water quality has deteriorated and its ecosystem has changed.

It was shown that ELCOM was able to reproduce the dominant internal wave and major hydrodynamic processes occurring in Lake Constance. For instance, three types of basin-scale waves were found to dominate the wave motion: the vertical mode-one Kelvin wave, the vertical mode-one Poincare waves, and a vertical mode-two Poincare wave. Moreover, an upwelling event was also reproduced by ELCOM suggesting that the width and length ratio of the basin, spatial variations in the wind, and Coriolis effects play critical roles in the details of the upwelling event. This on-going research has shown

that ELCOM can be used as a tool to predict and understand hydrodynamics and water quality in lakes.

A.1.3.2.6 *Venice Lagoon (Italy)*

ELCOM/CAEDYM is being used to develop a hydrodynamic and sediment transport model of Venice Lagoon, Italy, since future gate closures at the mouth of the lagoon are likely to impact flushing patterns. This project is an integral part of the Venice Gate Projects in Italy that was launched in May 2003 to prevent flooding.

ELCOM was validated for the tidal amplitude and phase using the data obtained from 12 tidal stations located throughout the lagoon (Yeates, 2004). Remaining tasks include model validation of temperature, salinity, and velocity against measurements made in the major channels of the lagoon.

A.1.3.2.7 *Silvan Reservoir (Australia)*

ELCOM is currently being applied to reproduce the circulation patterns observed in Silvan Reservoir, Australia, during a field experiment that was conducted in March 2004 to determine the transport pathways in the lake. This experiment confirmed the upwelling behavior of the lake and the strong role of the inflows in creating hydraulic flows in the reservoir (Antenucci, 2004).

A.1.3.2.8 *Billings and Barra Bonita Reservoirs (Brazil)*

ELCOM/CAEDYM is being applied to Billings and Barra Bonita Reservoirs in Brazil. Billings Reservoir is an upstream reservoir that feeds Barra Bonita via the Tiete River. The objective of the project is to develop an integrated management tool for these reservoirs and river reaches for use in the future planning of water resource utilization in Sao Paulo, Brazil (Romero and Antenucci, 2004).

A.1.3.2.9 *Lake Coeur D'Alene (Idaho, USA)*

ELCOM/CAEDYM is being applied to investigate the trade-off between reducing heavy metal concentrations and a potential increase in eutrophication due to remediation procedures in Lake Coeur D'Alene, Idaho. In order to investigate heavy metal fate and transport, CAEDYM is being improved further to include heavy metals and a feedback loop to phytoplankton based on metal toxicity (Antenucci, 2004).

A.1.3.2.10 *Seawater Desalination at Encina (California, USA)*

Flow Science conducted ELCOM modeling in 2004-2006 for a proposed desalination facility to be sited adjacent to the Encina Power Plant in Carlsbad, California. The proposed Encina facility involved source water taken from inside Agua Hedionda Lagoon and discharge of brines with the power plant cooling water via a surface channel across the beach south of the lagoon mouth. Flow Science used both a fine grid model to simulate water quality and dilution local to the intake and outfall and a larger grid model to simulate the effect of treated wastewater discharges and ocean currents and tides in the ocean near the lagoon. For the Encina study, Flow Science also used ELCOM to predict mixing in the vicinity of the plant discharge. The study area encompassed about 100 square miles of the ocean and also included some inland lagoons. The model resolved various tidal conditions and plant operating scenarios. The model compared favorably to existing oceanic data in the vicinity of the discharge.

A.1.3.2.11 *Moss Landing Desalination Project (California, USA)*

Flow Science applied ELCOM to simulate the flow and mixing in the entire Monterey Bay, including Elkhorn Slough. The purpose of the modeling was to evaluate the impacts of the proposed Moss Landing Desalination facility on receiving waters. The desalination facility was proposed to utilize a nearby existing power plant intake in Moss Landing Harbor and discharge to the ocean via the power plant's existing outfall, which is a submerged outfall located in Monterey Bay offshore of the harbor entrance. The ELCOM model resolved the details of the mixing in the vicinity of the power plant/desalination facility combined discharge. The model results compared favorably to existing measured water quality parameters. The results were used to determine compliance with water quality regulations for the combined outfall. The study was performed in 2004-2006.

A.1.3.2.12 *Lake Perris (California, USA)*

In 2005, ELCOM was applied to Lake Perris in order to compare the impacts of several recreational use strategies on measured fecal coliform concentrations at the reservoir outlet tower. The physical results of the simulation were validated against measured temperature and salinity data over a one-year period. The comparison of fecal coliform concentrations against measured data was fair due to a lack of data describing the timing and magnitude of loading and the settling and re-suspension of fecal matter.

The ELCOM model was expanded in 2006 - 2007 to include CAEDYM in order to evaluate the performance of a proposed hypolimnetic oxygenation system and observed

water quality benefits. The model was calibrated against two years of historical data and used to assess the magnitude and extent of oxygenation in the hypolimnion as a result of system operation. Impacts on dissolved oxygen concentrations and nutrient dynamics and algal production potential (as represented by chlorophyll *a*) were also evaluated, and recommendations were provided for final design of the system. The project has not yet been constructed due to seismic safety risks with the dam that must first be addressed.

A.1.3.2.13 *Lake Hodges and Olivenhain Reservoir (California, USA)*

The San Diego County Water Authority (SDCWA) is planning a tunnel connection between Lake Hodges and Olivenhain Reservoir. The tunnel and an associated hydroelectric turbine will allow for operation of the two reservoirs as part of a pumped storage project. Due to the difference in water quality between the two reservoirs, the SDCWA was concerned that the planned pumped storage project could adversely impact water quality in Olivenhain Reservoir. In order to evaluate the water quality impacts of the planned pumped storage operations on Olivenhain Reservoir, Flow Science developed a coupled ELCOM model of the two reservoirs in 2007-2008 to simulate temperature and salinity and several tracers in order to characterize the extent of mixing of the pumped storage inflow water from Lake Hodges within Olivenhain Reservoir and the percentages of Lake Hodges and Olivenhain Reservoir water throughout each reservoir due to the pumped storage operations and subsequent mixing.

A.1.3.2.14 *Lower San Gabriel River, Intake Channel, and Alamitos Bay (California, USA)*

The Los Angeles Department of Water and Power (LADWP) Haynes Generating Station (HnGS) and AES Generating Station (AES) each utilize three outfalls located on the east and west bank of the Lower San Gabriel River, respectively, and discharge cooling water to the Lower San Gabriel River Flood Control Channel (LSGR). Flow Science conducted ELCOM modeling from 2003-2010 to evaluate the mixing of flows within the river channel and found that, under typical operating conditions, the cooling water discharges form a “barrier” between freshwater from the upstream river channel and ocean water downstream of the LSGR. Both modeling and field work (conducted by others) confirmed that the net direction of flow downstream of HnGS and AES is downstream, even during flood tide conditions. Flow Science’s modeling also evaluated temperature, salinity, and mixing in the LSGR for a wide range of potential future conditions and for hypothetical conditions in which both HnGS and AES cooling water flows are removed from the LSGR. Water quality in the adjacent Alamitos Bay, which is strongly influenced by flushing induced by cooling water flows from HnGS and AES, was also evaluated using ELCOM. In addition, Flow Science used CAEDYM to evaluate

nutrient concentrations, algae, and dissolved oxygen within the Bay for a range of actual and potential future operating conditions. The HnGS Intake Channel (which connects Alamitos Bay to HnGS) was also evaluated with ELCOM/CAEDYM.

Results of the Flow Science analyses have been used by LADWP in NPDES permit discussions with the Regional Water Board, in CEQA evaluations supporting the potential future repowering of HnGS Units 5 and 6, and in comments on the State's draft Once-Through Cooling (OTC) policy.

A.1.3.2.15 *Joint Water Pollution Control Plant Outfall Evaluation (California, USA)*

The Sanitation Districts of Los Angeles County (LACSD) are conducting a detailed study to evaluate the feasibility of a proposed new ocean outfall to carry treated wastewater from the Joint Water Pollution Control Plant (JWPCP) in Carson, California, to an ocean discharge location off the southern California coast near the Palos Verdes and San Pedro Shelves. As part of the Feasibility Study, Flow Science developed an ELCOM model in 2007 to evaluate the impact of this proposed ocean outfall. The near-field effluent discharge model, NRFIELD2, coupled with the far field hydrodynamic model, ELCOM, was used to simulate the mixing and determine the concentrations of a conservative effluent tracer and various indicator bacteria (assuming no chlorination). The coupled model was validated using measured current and temperature data in the vicinity of the potential discharge sites. The water quality impacts of five proposed diffuser discharge sites were evaluated, and the modeling results will be used by LACSD to estimate concentrations of indicator bacteria at selected locations at the shore and inshore regions that would result from a discharge without chlorination. Ongoing ELCOM modeling will be performed to assist LACSD in selecting a preferred diffuser location. An example of the simulated effluent tracer concentrations during summer for one of the potential diffuser sites is presented in **Figure A.6** below.

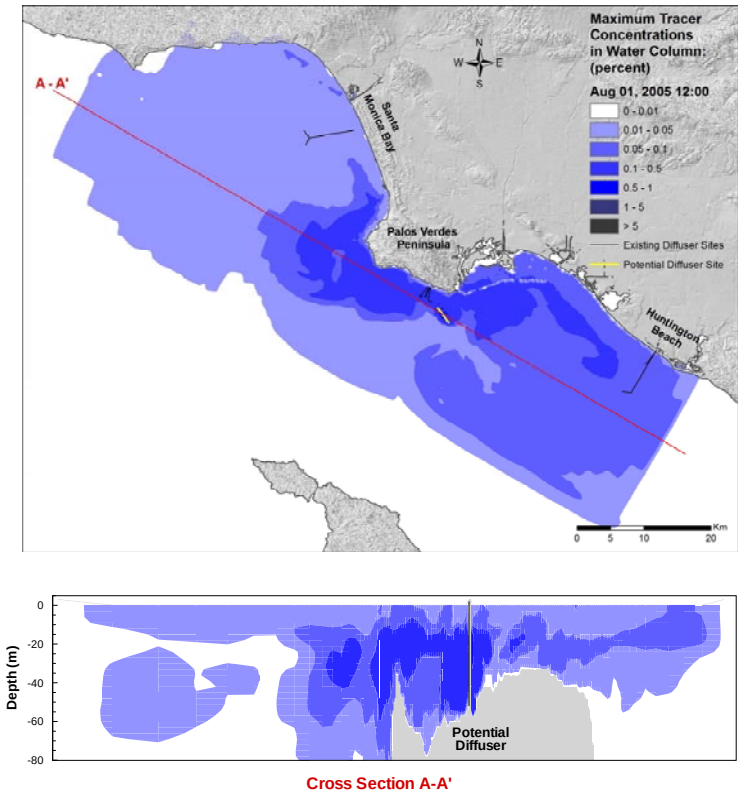

Figure A.6 Plan and section views of ELCOM simulated effluent tracer concentrations from proposed diffuser Site 1 in summer (August 1, 2005).

A.1.3.2.16 *San Vicente Reservoir (California, USA)*

Flow Science is assisting the City of San Diego in assessing the mixing and dilution potential resulting from the potential injection of highly treated effluent into San Vicente Reservoir. In 2010, Flow Science developed an ELCOM/CAEDYM model to assess the mixing and dispersion properties in San Vicente Reservoir as well as a field program to validate the modeling. The ELCOM/CAEDYM model includes temperature, salinity, conductivity, dissolved oxygen, nutrients, chlorophyll *a* (as a surrogate for algae), and multiple tracers. The model provides an accurate three-dimensional representation of water quality within the reservoir. The model was calibrated for the reservoir at its

current capacity against two years of historical data. The calibrated model has since been applied to the expanded reservoir to evaluate the impacts of the advanced water treatment (AWT) water. The model is being used to predict water quality conditions in the future enlarged reservoir and will also be used to help manage water quality in the enlarged reservoir once it is filled. The work is being reviewed by an expert panel being overseen by the National Water Research Institute. The panel is expected to complete its review and accept the use of the modeling.

A.1.3.2.17 *Los Vaqueros Reservoir (California, USA)*

In conjunction with the Contra Costa Water District (CCWD), Flow Science developed a three-dimensional ELCOM/CAEDYM model of Los Vaqueros Reservoir beginning in 2006 that is capable of providing an accurate, three-dimensional representation of water quality including temperature, salinity/TDS, nutrients and algae. The ELCOM model was calibrated against two years of historical data and validated against four years of data, while the CAEDYM model was calibrated for four years of historical data. **Figure A.7** shows a comparison of the measured versus simulated annual and growing season average chlorophyll *a* concentrations which show very good agreement. In ongoing work, Flow Science is using the ELCOM/CAEDYM model to evaluate the water quality of the reservoir under future conditions where the impounding dam is raised. This will expand the capacity of the reservoir from 100,000 acre-ft to 160,000 acre ft. The water quality model is being used to determine the changes in outflow water quality resulting from the expansion and to provide preliminary design recommendations for the inlet/outlet facilities with respect to improving water quality.

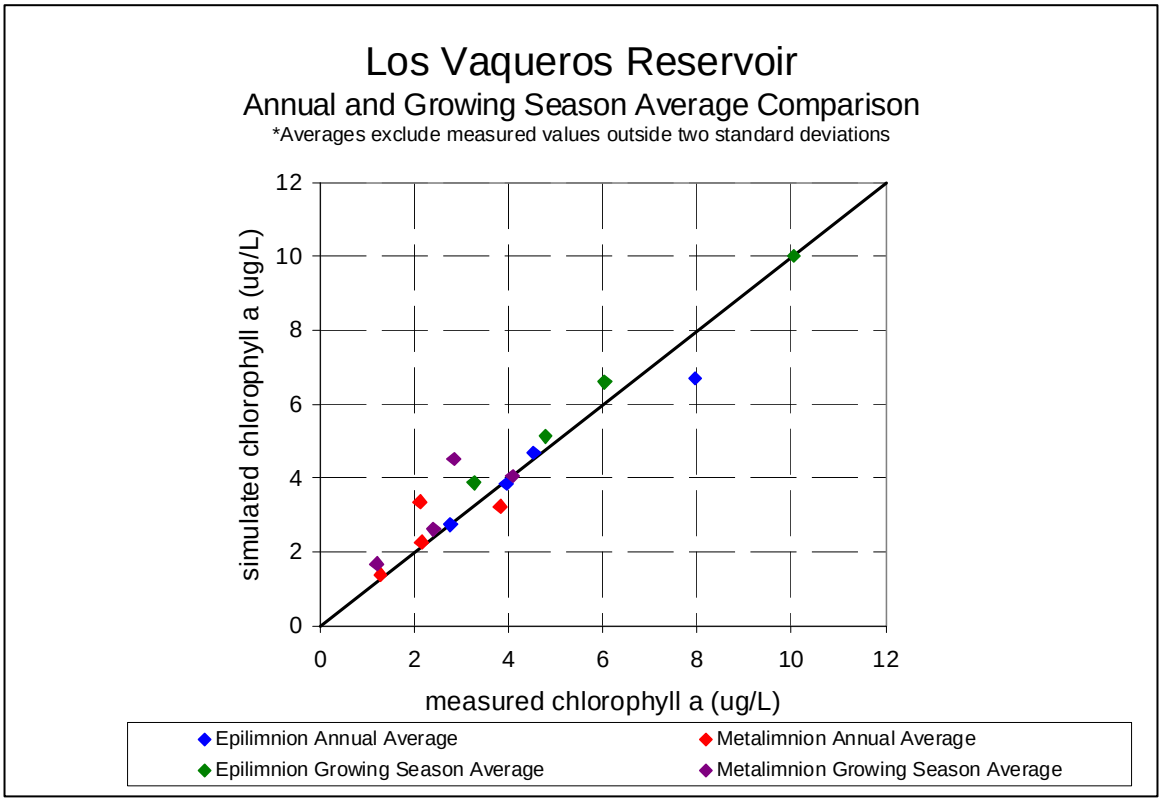

Figure A.7 Comparison of simulated ELCOM/CAEDYM results and measured chlorophyll *a* data for 2006-2009.

A.1.3.2.18 *Other Applications*

Other ELCOM/CAEDYM applications and development in on-going research at CWR include:

- Plume dynamics and horizontal dispersion (Marmion Marine Park, Australia).
- Inflow and pathogen dynamics (Helena, Myponga and Sugarloaf Reservoirs, Australia).
- Mixing and dissipation in stratified environments (Tone River, Japan, and Brownlee Reservoir, USA).

- Tidally forced estuaries and coastal lagoons (Marmion Marine Park and Barbamarco Lagoon, Italy).

- Three-dimensional circulation induced by wind and convective exchange (San Roque Reservoir, Argentina, and Prospect Reservoir, Australia).

- Sea-surface temperature fluctuation and horizontal circulation (Adriatic Sea).

- Response of bivalve mollusks to tidal forcing (Barbamarco Lagoon, Italy).

A.1.4 TECHNICAL DESCRIPTION OF ELCOM

As outlined above, ELCOM solves the unsteady, viscous Navier-Stokes equations for incompressible flow using the hydrostatic assumption for pressure. ELCOM can simulate the hydrodynamics and thermodynamics of a stratified system, including baroclinic effects, tidal forcing, wind stresses, heat budget, inflows, outflows, and transport of salt, heat and passive scalars. Through coupling with the CAEDYM water quality module, ELCOM can be used to simulate three-dimensional transport and interactions of flow physics, biology, and chemistry. The hydrodynamic algorithms in ELCOM are based upon the proven semi-Lagrangian method for advection of momentum with a conjugate-gradient solution for the free-surface height (Casulli and Cheng, 1992) and a conservative ULTIMATE QUICKEST transport of scalars (Leonard, 1991). This approach is advantageous for geophysical-scale simulations since the time step can be allowed to exceed the Courant-Friedrichs-Lewy (CFL) condition for the velocity without producing instability or requiring a fully-implicit discretization of the Navier-Stokes equations.

A.1.4.1 Governing Equations

Significant governing equations and approaches used in ELCOM include:

- Three-dimensional simulation of hydrodynamics (unsteady Reynolds-averaged Navier-Stokes equations).

- Advection and diffusion of momentum, salinity, temperature, tracers, and water quality variables.

- Hydrostatic approximation for pressure.

- Boussinesq approximation for density effects.

- Surface thermodynamics module accounts for heat transfer across free surface.
- Wind stress applied at the free surface.
- Dirichlet boundary conditions on the bottom and sides.

A.1.4.2 Numerical Method

Significant numerical methods used in ELCOM include:

- Finite-difference solution on staggered-mesh Cartesian grid.
- Implicit volume-conservative solution for free-surface position.
- Semi-Lagrangian advection of momentum allows time steps with CFL > 1.0.
- Conservative ULTIMATE QUICKEST advection of temperature, salinity, and tracers.
- User-selectable advection methods for water quality scalars using upwind, QUICKEST, or semi-Lagrangian to allow trade-offs between accuracy and computational speed.
- Solution mesh is Cartesian and allows non-uniformity (*i.e.* stretching) in horizontal and vertical directions.

The implementation of the semi-Lagrangian method in Fortran 90 includes sparse-grid mapping of three-dimensional space into a single vector for fast operation using array-processing techniques. Only the computational cells that contain water are represented in the single vector so that memory usage is minimized. This allows Fortran 90 compiler parallelization and vectorization without platform-specific modification of the code. A future extension of ELCOM will include dynamic pressure effects to account for nonlinear dynamics of internal waves that may be lost due to the hydrostatic approximation.

Because the spatial scales in a turbulent geophysical flow may range from the order of millimeters to kilometers, it is presently impossible to conduct a Direct Navier-Stokes (DNS) solution of the equations of motion (*i.e.* an exact solution of the equations). Application of a numerical grid and a discrete time step to a simulation of a geophysical domain is implicitly a filtering operation that limits the resolution of the equations.

Numerical models (or closure schemes) are required to account for effects that cannot be resolved for a particular grid or time step. There are four areas of modeling in the flow physics: (l) turbulence and mixing, (2) heat budgets, (3) hydrodynamic boundary conditions, and (4) sediment transport.

A.1.4.3 Turbulence Modeling and Mixing

ELCOM presently uses uniform fixed eddy viscosity as the turbulence closure scheme in the horizontal plane (in future versions a Smagorinsky 1963 closure scheme will be implemented to represent subgrid-scale turbulence effects as a function of the resolves large-scale strain-rates). These methods are the classic "eddy viscosity" turbulence closure. With the implementation of the Smagorinsky closure, future extensions will allow the eddy-viscosity to be computed on a local basis to allow improvements in modeling local turbulent events and flow effects of biological organisms (e.g., drag induced by macroalgae or seagrass).

In the present code, the user has the option to extend the eddy-viscosity approach to the vertical direction by setting different vertical eddy-viscosity coefficients for each grid layer. However, in a stratified system, this does not adequately account for vertical turbulent mixing that may be suppressed or enhanced by the stratification (depending on the stability of the density field and the magnitude of the shear stress). To model the effect of density stratification on turbulent mixing the CWR has developed a closure model based on computation of a local Richardson number to scale. The latter is generally smaller than the time step used in geophysical simulations, so the mixing is computed in a series of partial time steps. When the mixing time-scale is larger than the simulation time step, the mixing ratio is reduced to account for the inability to obtain mixing on very short time scales. This model has the advantage of computing consistent mixing effects without regard to the size of the simulation time-step (*i.e.* the model produces mixing between cells that is purely a function of the physics and not the numerical step size).

A.1.4.4 Heat Budget

The heat balance at the surface is divided into short-wave (penetrative) radiation and a heat budget for surface heat transfer effects. The surface heat budget requires user input of the net loss or gain through conduction, convection, and long wave radiation in the first grid layer beneath the free surface. The short wave range is modeled using a user-prescribed input of solar radiation and an exponential decay with depth that is a function of a bulk extinction coefficient (a Beer's law formulation for radiation absorption). This coefficient is the sum of individual coefficients for the dissolved

organics ("gilvin"), phytoplankton biomass concentration, suspended solids, and the water itself. The extinction coefficients can either be computed in the water quality module (CAEDYM) or provided as separate user input.

A.1.4.5 Hydrodynamic Boundary Conditions

The hydrodynamic solution requires that boundary conditions on the velocity must be specified at each boundary. There are six types of boundary conditions: (1) free surface, (2) open edge, (3) inflow-outflow, (4) no-slip, (5) free-slip, and (6) a Chezy-Manning boundary stress model (the latter is presently not fully implemented). For the free surface, the stress due to wind and waves is required. The user can either input the wind/wave stress directly, or use a model that relates the surface stress to the local wind speed and direction *via* a bulk aerodynamic drag coefficient. Open boundaries (e.g. tidal inflow boundaries for estuaries) require the user to supply the tidal signature to drive the surface elevation. Transport across open boundaries is modeled by enforcing a Dirichlet condition on the free-surface height and allowing the inflow to be computed from the barotropic gradient at the boundary. Inflow-outflow boundary conditions (e.g. river inflows) are Dirichlet conditions that specify the flow either at a particular boundary location *or inside the domain*. Allowing an inflow-outflow boundary condition to be specified for an interior position (*i.e.* as a source or sink) allows the model to be used for sewage outfalls or water outlets that may not be located on a land boundary. Land boundaries can be considered zero velocity (no-slip), zero-flux (free-slip) or, using a Chezy-Manning model, assigned a computed stress.

A.1.4.6 Sediment Transport

While sediment transport is fundamentally an issue of flow physics, the algorithms for the sediment transport are more conveniently grouped with the water quality algorithms in CAEDYM. Settling of suspended particulate matter is computed using Stokes law to obtain settling velocities for the top and bottom of each affected grid cell. This allows the net settling flux in each cell to be computed. A two-layer sediment model has been developed that computes resuspension, deposition, flocculation, and consolidation of sediment based on (1) the shear stress at the water/sediment interface, (2) the type of sediment (cohesive/non-cohesive), and (3) the thickness of the sediment layer. Determination of the shear stress at the water/sediment interface requires the computation of bottom shear due to current, wind, and waves. A model has been developed to account for the effects of small-scale surface waves that cannot be resolved on a geophysical-scale grid. This model computes the theoretical wave height and period for small-scale surface waves from the wind velocity, water depth, and domain fetch. From these, the wavelength and orbital velocities are calculated. The wave-induced shear

stress at the bottom boundary resulting from the wave orbital velocities is combined with a model for the current-induced shear stress to obtain the total bottom shear that effects sediment resuspension. The cohesiveness of the sediment determines the critical shear stresses that are necessary to resuspend or deposit the sediments. A model of consolidation of the sediments is used to remove lower sediment layers from the maximum mass that may be resuspended.

A.1.5 TECHNICAL DESCRIPTION OF CAEDYM

CAEDYM is an outgrowth of previous CWR water quality modules in DYRESM-WQ and the Estuary Lake Model - Water Quality (ELMO-WQ) codes. CAEDYM is designed as a set of subroutine modules that can be directly coupled with one, two, or three-dimensional hydrodynamic "drivers", catchment surface hydrological models, or groundwater models. Additionally, it can be used in an uncoupled capacity with specification of velocity, temperature, and salinity distributions provided as input files rather than as part of a coupled computation. The user can specify the level of complexity in biogeochemical process representation so both simple and complex interactions can be studied. Direct coupling to a hydrodynamic driver (e.g. ELCOM) allows CAEDYM to operate on the same spatial and temporal scales as the hydrodynamics. This permits feedbacks from CAEDYM into ELCOM for water quality effects such as changes in light attenuation or effects of macroalgae accumulation on bottom currents. **Figure A.8** shows an illustration of the interactions of modeled parameters in CAEDYM. Being an “N-P-Z” (nutrient-phytoplankton-zooplankton) model, CAEDYM can be used to assess eutrophication. Unlike the traditional general ecosystem model, CAEDYM serves as a species- or group-specific model (*i.e.* resolves various phytoplankton species). Furthermore, oxygen dynamics and several other state variables are included in CAEDYM.

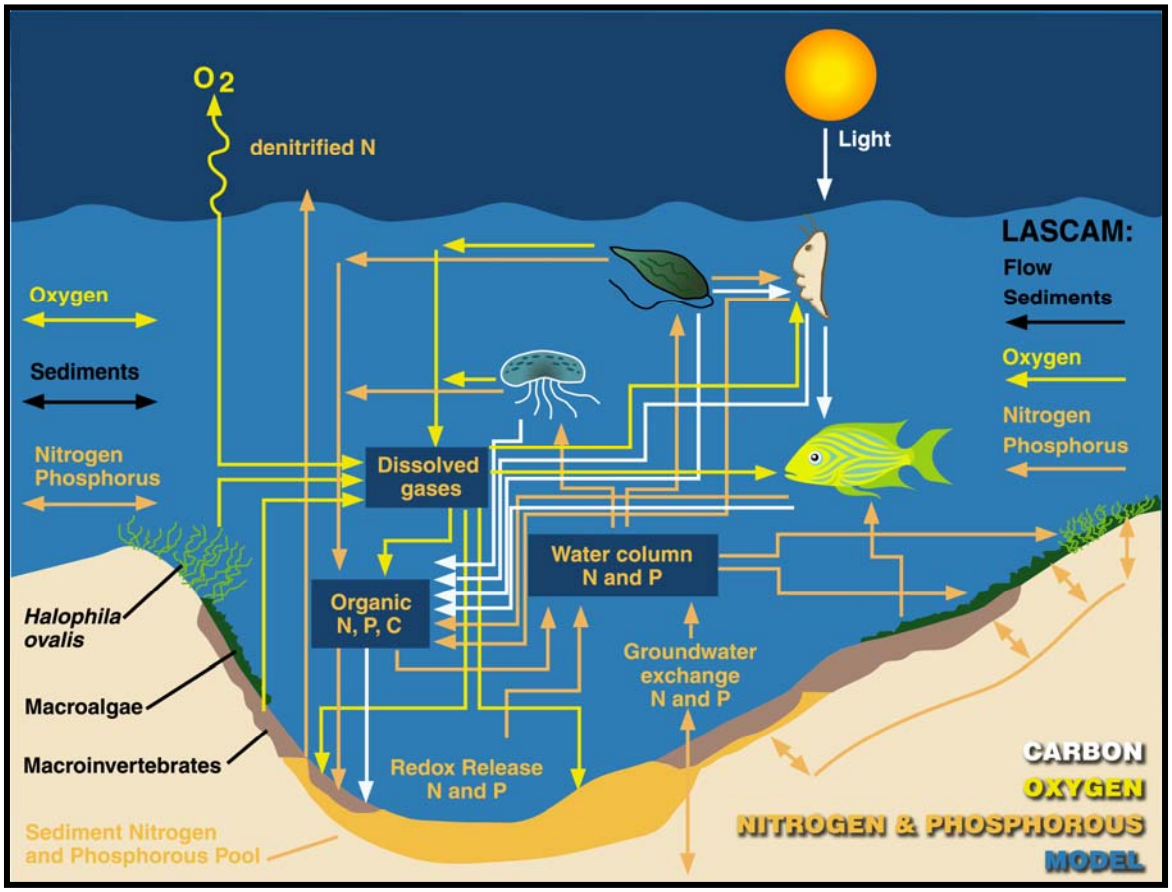

Figure A.8 Illustration of interactions of modeled parameters in CAEDYM.

The representation of biogeochemical processes in ecological models has, historically, been treated in a simple manner. In fact, the pioneering work on modeling marine ecosystems (Riley et al, 1949; Steel, 1962) is still used as a template for many of the models that are currently used (Hamilton and Schladow, 1997). The level of sophistication and process representation included in CAEDYM is of a level hitherto unseen in any previous aquatic ecosystem model. This enables many different components of the system to be examined, as well as providing a better representation of the dynamic response of the ecology to major perturbations to the system (e.g. the response to various management strategies). **Figure A.9** shows the major state variables included in the CAEDYM model. Using CAEDYM to aid in management decisions and system understanding requires (1) a high level of process representation, (2) process

interactions and species differentiation of several state variables, and (3) applicability over a spectrum of spatial and temporal scales. The spectrum of scales relates to the need for managers to assess the effects of temporary events, such as anoxia at specific

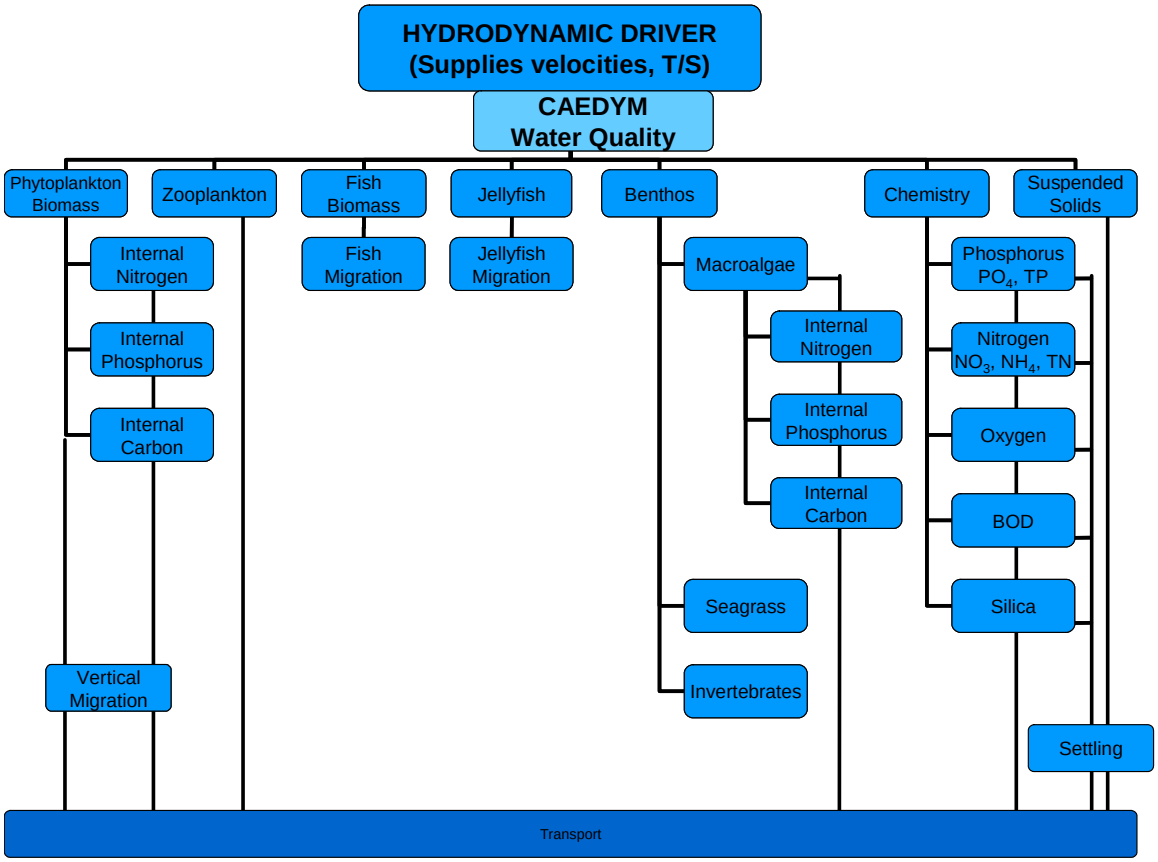

Figure A.9 Major state variables included in the CAEDYM model.

locations, through to understanding long-term changes that may occur over seasons or years. There is considerable flexibility in the time step used for the ecological component. Long time steps (relative to the hydrodynamic advective scale) may be used to reduce the frequency of links to ELCOM when long-term (*i.e.* seasonal or annual) simulations are run.

A.1.5.1 Biological Model

The biological model used in CAEDYM consists of seven phytoplankton groups, five zooplankton groups, six fish groups, four macroalgae groups and three invertebrate groups, as well as models of seagrass and jellyfish. This set will be expanded as biological models are developed, tested, and calibrated to field data. There is flexibility for the user in choosing which species to include in a simulation. Vertical migration is simulated for motile and non-motile phytoplankton, and fish are migrated throughout the model domain according to a migration function based on their mortality. A weighted grazing function is included for zooplankton feeding on phytoplankton and fish feeding on zooplankton. The biomass grazed is related to both food availability and preference of the consumer for its food supply. Improved temperature, respiration and light limitation functions have been developed to represent the environmental response of the organisms. The benthic processes included a self-shading component and beach wrack function for macroalgae, sediment bioturbation and nutrient cycling by polychaetes, and effects of seagrass on sediment oxygen status.

In particular, the seven phytoplankton groups modeled are dinoflagellates, freshwater diatoms, marine/estuarine diatoms, freshwater cyanobacteria, marine estuarine cyanobacteria, chlorophytes, and cryptophytes. Phytoplankton biomass is represented in terms of chlorophyll *a*. Phytoplankton concentrations are affected by the following processes:

- Temperature growth function
- Light limitation
- Nutrient limitation by phosphorus and nitrogen (and when diatoms are considered, silica)
- Loss due to respiration, natural mortality, excretion, and grazing
- Salinity response
- Vertical migration and settling

A.1.5.2 Nutrients, Metals, and Oxygen Dynamics

The transport and chemical cycling of nutrients is an important part of simulating the interaction of biological organisms in an ecosystem. CAEDYM includes as state variables the following:

- Nutrients (dissolved inorganic phosphorus, total phosphorus, total nitrogen, ammonium nitrate, and silica).
- Dissolved oxygen and biochemical oxygen demand.
- Metals (dissolved and particulate forms of iron and manganese).
- Suspended sediment (the particulate and colloidal fractions).
- pH

The model incorporates oxygen dynamics and nutrient cycling in both the sediments and water column. A sediment pool of organic detritus and inorganic sediments, both of which may be resuspended into the water column, is included. Redox-mediated release of dissolved nutrients is simulated from the sediments to the water column.

Processes included in the water and sediment oxygen dynamics include:

- Atmospheric exchange (Wanninkhof, 1992).
- Oxygen production and consumption through phytoplankton, macroalgae, and seagrass/macrophyte photosynthesis and respiration, respectively.
- Utilization of dissolved oxygen due to respiration of higher organisms such as zooplankton and fish and due to photosynthesis and respiration in jellyfish
- Water column consumption of oxygen during nitrification.
- Biochemical oxygen demand due to mineralization of organic matter in the water column and in the sediments.

Oxygen flux from the water column to the sediments, sediment oxygen demand (SOD), as developed from Fick's law of diffusion.

The last two processes are used together with a sediment porosity and diffusion coefficient (Ullman and Aller, 1982) in order to define the depth of the toxic layer in the sediments.

Nutrient processes included in the sediment and water column dynamics include:

- Phytoplankton nutrient uptake, with provision for luxury storage of nutrients.
- Release of dissolved inorganic nutrients from phytoplankton excretion.
- Excretion of nutrients as fecal material by zooplankton.
- Nitrification and denitrification by bacterial mediated action.
- Generation of inorganic nutrients from organic detritus.
- Transfer of nutrients through the food chain (e.g. phytoplankton--zooplankton--fish).
- Uptake of nutrients by macroalgae and seagrasses.
- Adsorption/desorption of nutrients from inorganic suspended sediments.
- Sediment/water transfer of nutrients (*via* such processes as sediment resuspension, sedimentation, redox-mediated nutrient release, and bioturbation).

In essence, CAEDYM represents the type of interactive processes that occur amongst the ecological and chemical components in the aquatic ecosystem. As a broad generalization, one component of the system cannot be manipulated or changed within the model without affecting other components of the system. Similarly in nature, changing an integral component in the aquatic system will have wide-ranging and follow-on effects on many of the other system components. CAEDYM is designed to have the complexity and flexibility to be able to handle the continuum of responses that will be elicited as components of a system that are manipulated. Thus, the model represents a valuable tool to examine responses under changed conditions, as for example, when new approaches to managing an ecosystem are adopted.

A.2 DESCRIPTION OF ELCOM/CAEDYM/VISUAL PLUMES (ECP)

A.2.1 INTRODUCTION

Outfalls are commonly used to discharge treated effluent into open waters. The hydrodynamics of an effluent discharged through an outfall can be conceptualized as a mixing process occurring in two separate regions: a near-field region and a far-field region. In the near-field region the effluent generally experiences a significant amount of mixing, and dilution occurs very rapidly. In this region, the initial jet characteristics of momentum flux, buoyancy flux, flow rate, as well as outfall geometry greatly influence the effluent trajectory and degree of mixing (Fischer et al, 1979). As the effluent plume travels further away from the source, the source characteristics become less important and the far-field region is attained. Mixing of the effluent plume in this region is caused by spatial and temporal variations of ambient velocity fields and dilution generally occurs slowly over a long distance, but may be rapid if there is a high degree of turbulence in the environment.

Due to different dominant temporal and spatial scales of flow velocity and effluent concentration in the near and far field region, a complete model that accounts for all important spatial and temporal scales in both the near-field and far-field regions is not feasible. Instead, these two regions are usually treated by separate models termed the near-field model and the far-field model respectively.

The near-field model has been under intensive study from the 1950s through the early 1990s. Thorough reviews of these studies are provided by Fischer et al. (1979), Baumgartner et al. (1994), and Roberts et al. (1989 a, b, c). These studies have produced a number of near-field models that were verified by both field and laboratory data. Among them, Visual Plumes (VP or PLUMES), endorsed by the U.S. Environmental Protection Agency (USEPA), is the most popular model and has been widely used by regulatory agencies and outfall designers to estimate the near-field dilution.

A variety of models can be used to model far-field mixing processes. These include ELCOM/ CAEDYM, Princeton Ocean Model (POM), and MIT General Circulation Model (MITGCM). All of these models obtain a velocity field from the numerical calculation of the equations of motion and account for influences by tide, wind stress, and pressure gradient due to free surface gradients (barotropic) or density gradients (baroclinic). Given the velocity field, the pollutant concentration field is

typically obtained by solving the Eulerian advective diffusion equation in three dimensions or by using the Lagrangian particle-tracking method.

In simple water bodies with well-defined uni-directional current regimes, the use of near-field models alone may suffice to evaluate a design of an outfall discharge that meets regulations. However, in regions with multiple current regimes (inertial, tide, wind, and buoyancy driven) and with large pollutant loadings, especially where several sources may interact, near-field models must be supplemented by far-field transport and water quality models. The latter are capable of prediction, over a greater distance in the water body, of the concentration distributions for different pollutants, nutrients, and other bio-chemical parameters. They do not, however, have the high spatial resolution that is required to predict near-field mixing processes. Thus, a coupled approach is necessary. In the following sections, a method of coupling the near-field model PLUMES and the far-field model ELCOM/CAEDYM is discussed. The coupled code is referred to as ELCOM/CAEDYM/PLUMES (ECP). Note that there is no standard procedure for the coupling of near and far field models and the coupling procedure varies from code to code mainly because of the different code structures among all of the near-field and far-field models.

A.2.2 NEAR-FIELD MODEL – PLUMES

PLUMES is an interface program that contains the near-field models such as the Roberts, Snyder, and Baumgartner model (RSB) and UM and CORnell MIXing Zone Expert System (CORMIX) (Baumgartner et al., 1994). In ECP, the UM model is chosen to simulate near-field dilution. The UM model is an integral near-field model that uses one-dimensional conservation equations for mass, momentum, salinity and temperature, to model the growth of the plume once the effluent has left the port. Assumptions are made about the shape of the plume and the distribution of pollutant concentration within the plume. Several mechanisms of entrainment such as aspirated, forced, and turbulent diffusion are considered. Both positively and negatively buoyant plumes, single source and multi-port diffuser configurations can be modeled. Model outputs include average dilution, centerline dilution, and horizontal distance of the effluent plume. The major limitation of UM lies in the assumption of an infinite receiving water body, similar to all other available integral-type models (e.g. RSB model). Thus, UM should only be used for deep-water outfalls without boundary interactions. More details on UM and PLUMES can be found in Baumgartner et al. (1994).

A.2.3 FAR-FIELD MODEL – ELCOM/CAEDYM

ELCOM is a three-dimensional hydrodynamic model for lakes and reservoirs and is used to predict the velocity, temperature, and salinity distribution in natural water bodies subjected to external environmental forcing, such as wind stress, surface heating, or cooling. Through coupling with the CAEDYM water quality module, ELCOM can be used to simulate three dimensional transport and interactions of flow physics, biology, and chemistry. ELCOM/CAEDYM is the chosen far-field model in ECP.

A.2.4 COUPLING PLUMES AND ELCOM/CAEDYM

The adopted coupling procedure is based on four steps: ambient conditions modeling, near-field modeling, coupling of near-field and far-field models, and far-field modeling.

1. Ambient conditions modeling

   The near-field model, UM, needs the input of ambient conditions such as the prevailing velocity, temperature, and salinity profiles in the vicinity of the outfall. These profiles are extracted from the ELCOM/CAEDYM simulation at the beginning of a time step at a vertical column of grid cells containing or overlapping the diffuser (the "Diffuser Cell Column" in **Figure A.10**). The depth of the diffuser is also updated based on the surface elevation at that time step.

2. Near-field modeling

   The UM model is applied at each time step using the ambient conditions extracted from ELCOM/CAEDYM. Furthermore, effluent data is obtained from input files for ELCOM/CAEDYM, and the diffuser geometry is specified in the input file called "diffuser_config.dat." The UM model is modified to consider the trapping or surfacing of the plume as the end of the near-field region. The computed average dilution along the trajectory of the plume is then stored for the following coupling step.

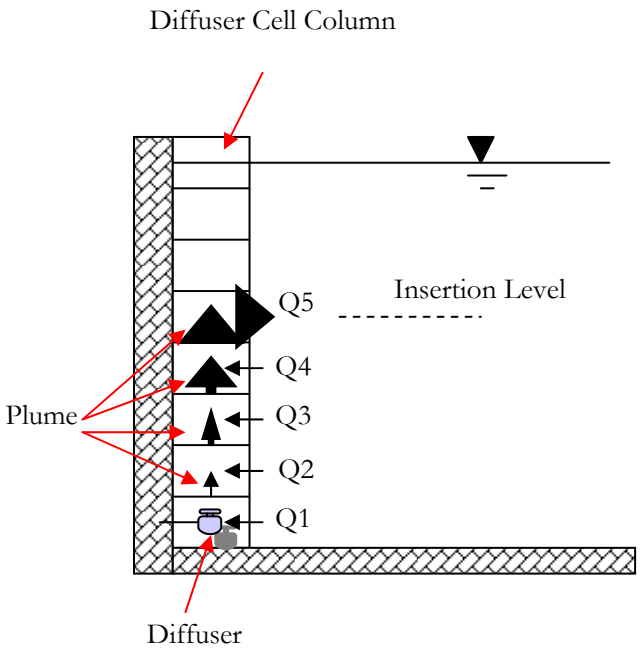

Figure A.10 Schematic of coupling procedure for near-field and far-field models.

3. Coupling of near-field and far-field models

After identifying the "Diffuser Cell Column" (**Figure A.10**), the dilution in each of the cells along this column can be calculated from the linear interpolation of results from UM. Water is then withdrawn from each of these cells based on the dilution occurring in the cell. This withdrawn water is then mixed with the effluent to form the effluent plume and passed to the cell above. Finally, the diluted effluent is then inserted into the cell where the UM model indicates the occurrence of trapping or surfacing (**Figure A.10**). Flow rate, temperature, salinity, and tracer concentrations within this inserted inflow are determined by mass conservation.

4. Far-field modeling

ELCOM/CAEDYM treats the previous coupling process as a series of outflows and inflows along the "Diffuser Cell Column" and proceeds with its time-marching far-field simulation for the time step. Steps 1 - 4 are then repeated for the next time step until the simulation ends.

A.2.5 VERIFICATION OF ECP

The UM model was originally written in TURBO PASCAL and was converted into FORTRAN and included in ECP. The comparison between the results from UM of PLUMES and UM of ECP shows an exact match (**Figure A.11**) and the conversion of the UM model is verified.

Output from UM Model of PLUMES

depth (m)	dilution (m)	horiz dis	
50.000	1.000	0.000	
49.761	1.971	0.005	
49.311	3.913	0.035	
48.585	7.797	0.127	
47.525	15.566	0.327	
46.035	31.104	0.696	
45.928	32.424	0.725	merging
43.228	62.180	1.529	
37.335	124.335	3.385	
25.609	248.651	7.517	
22.323	285.625	8.893	trap level
15.436	395.624	12.750	begin overlap, dilution
	overestimated		
14.308	442.027	13.760	surface hit

Output from UM Model of ECP

depth (m)	dilution (m)	horiz dis	
50.000	1.000	0.000	
49.761	1.971	0.005	
49.311	3.913	0.035	
48.585	7.797	0.127	
47.525	15.566	0.327	
46.035	31.104	0.696	
45.928	32.424	0.725	merging
43.228	62.180	1.529	
37.335	124.335	3.385	
25.609	248.651	7.517	
22.323	285.625	8.893	trap level
15.436	395.624	12.750	begin overlap, dilution
	overestimated		
14.308	442.027	13.760	surface hit

Figure A.11 Comparison of outputs from UM of PLUMES and ECP

Mass conservation within ECP was tested by simulating an idealized lake with a single outfall (inflow) and no outflow. Total mass of both a conservative tracer and total phosphorus (TP) in the lake was calculated at each time step and compared with a similar simulation using ELCOM/CAEDYM (where the outfall was treated as a single inflow). Less than 0.1% difference was found for the conservative tracer and less than 1% difference was found for TP at the end of a one-year simulation. These small differences indicate that mass conservation within the ECP code is comparable to that of ELCOM/CAEDYM.

The accuracy of ECP can also be qualitatively evaluated by simulating the behavior of a plume under stratified and unstratified ambient conditions. **Figure A.12** shows that ECP correctly predicts surfacing of the plume under unstratified conditions and the level of insertion of the plume under stratified conditions.

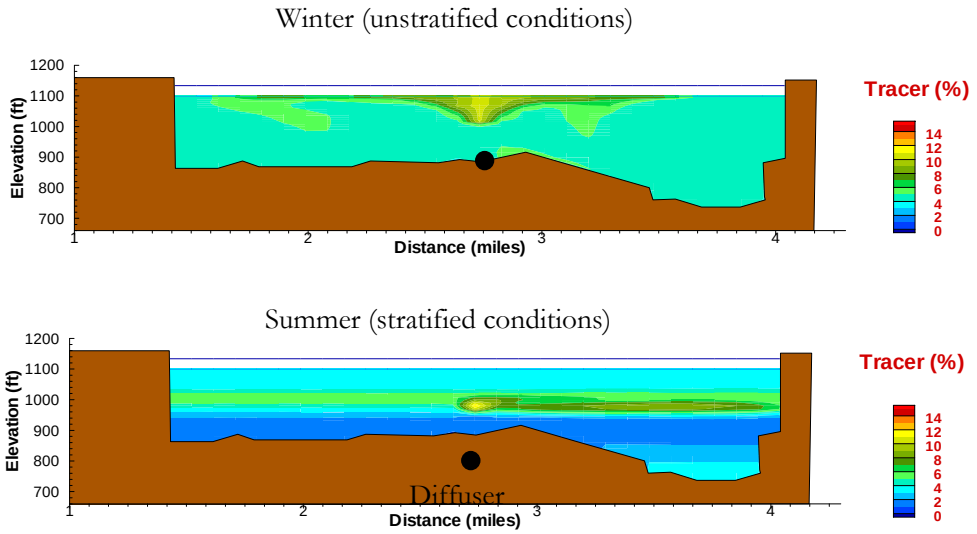

Figure A.12 Comparison of tracer concentrations released from an outfall under stratified and unstratified conditions using ECP.

A.3 BIBLIOGRAPHY

A.3.1 REFERENCED IN TEXT

Amorocho, J. and DeVries, J.J. (1980). "A new evaluation of the wind stress coefficient over water surfaces," Journal of Geophysical Research, 85:433-442.

Antenucci, Jason (2004). "Tracing Short-Circuiting Potential," from CWR Models: Bytes and Nybbles, Autumn 2004, Issue 10, page 2.

Antenucci, Jason (2004). "New Metals Model for CAEDYM," from CWR Services: Bytes and Nybbles, December 2004, Issue 11, page 1.

Appt, Jochen (January 2000), "Review on the modeling of short period internal waves in lakes with focus on Lake Constance," Pfaffenwaldring 61, D-70550 Stuttgart, Universität Stuttgart, Institut für Hydraulik und Grandmaster, Stuttgart.

Appt, J., Imberger, J., Kobus, H. (2004), "Basin-scale motion in stratified Upper Lake Constance," Limnology and Oceanography, 49(4), 919-933

Baumgartner, D. J., Frick, W. E. & Roberts, P. J. W. (1994), Dilution Models for Effluent Discharges (3rd ed.), *United States Environmental Protection Agency (EPA/600/R-94/086).*

Casulli, Vincenzo and Cheng, Ralph T. (1992), "Semi-implicit finite difference methods for three-dimensional shallow water flow," *International Journal for Numerical Methods in Fluids*, **15**, 629-48.

CWR, "Limnological Study of Lake Burragorang," Centre For Water Research, The University of Western Australia, Chapter 4 excerpt from report, pp. 104-126.

Fischer, H.B., List, E.J., Koh, R.C.Y., Imberger, J. & Brooks, N.H. (1979), Mixing in Inland and Coastal Waters, *Academic Press, New York*

Hamilton, D. (1997). "An integrated ecological model for catchment hydrology and water quality for the Swan and Canning Rivers," presented at the 2nd International Symposium on Ecology and Engineering, 10-12 November 1997, Freemantle, Australia. IAHR Eco-Hydraulics section.

Hamilton, D.P. and S.G. Schladow (1997), "Prediction of water quality in lakes and reservoirs: Part I: Model description," *Ecological Modelling, 96*, 91-110.

Herzfeld, M. and Hamilton, D. (1998), "A computational aquatic ecosystem dynamics model for the Swan River," *EOS Trans. AGU*, **79**(1), Ocean Sciences Meet. Suppl. OS11P-02.

Herzfeld, M.; Hodges, B.R.; and Hamilton, D. (1998), "Modelling the Swan River on small temporal and spatial scales," The Swan Canning Estuary conference, York, Australia, Apr., 1998.

Herzfeld, M.; Hamilton, D.; and Hodges, B.R. (1997), "Reality vs. management: The role of ecological numerical models," *2nd International Symposium on Ecology and Engineering*, 10-12 November 1997, Fremantle, Australia, IAHR Eco-Hydraulics section.

Hipsey, M.R., Romero, J.R., Antenucci, J.P. and Hamilton, D. (2005) "Computational Aquatic Ecosystem Dynamics Model: CAEDYM: v2.2 Science Manual", Centre for Water Research, The University of Western Australia.

Hipsey, M.R., Romero, J.R., Antenucci, J.P. and Hamilton, D. (2005) "Computational Aquatic Ecosystem Dynamics Model: CAEDYM: v2.2 User Manual", Centre for Water Research, The University of Western Australia.

Hodges, B.R. (1998), "Hydrodynamics of differential heat absorption," *Environmental Mechanics Laboratory Seminar*, Dept. of Civil Eng., Stanford University, Feb. 1998.

Hodges, B.R. and Dallimore C (2006), "Estuary Lake and Coastal Ocean Model: ELCOM v2.2 Science Manual", Centre for Water Research, The University of Western Australia.

Hodges, B.R. and Dallimore C (2007), "Estuary Lake and Coastal Ocean Model: ELCOM v2.2 User Manual", Centre for Water Research, The University of Western Australia.

Hodges, B.R. and Herzfeld, M. (1997), "Coupling of hydrodynamics and water quality for numerical simulations of Swan River," *2nd International Symposium on Ecology and Engineering*, 10-12 November, Fremantle, Australia, IAHR Eco-Hydraulics section.

Hodges, B.R.; Herzfeld, M.; Winters, K.; and Hamilton, D. (1998), "Coupling of hydrodynamics and water quality in numerical simulations," *EOS Trans. AGU*, **79**(1), Ocean Sciences Meet. Suppl. OS11P-01.

Hodges, B.R., Imberger, J., Saggio, A., and K. Winters (1999), "Modeling basin-scale internal waves in a stratified lake," *Limnology and Oceanography*), **45**(7), 1603-20.

Hodges, B.R., Yue, N., and Bruce, L. (May 27, 1999), "Swan River hydrodynamic model progress report," Centre For Water Research, The University of Western Australia, 14pp.

Jacquet, J. (1983). "Simulation of the thermal regime of rivers," In Orlob, G.T., editor, Mathematical Modeling of Water Quality: Streams, Lakes and Reservoirs, pages 150-176. Wiley-Interscience.

Kowalik, Z. and Murty, T.S. (1993). "Numerical Modeling of Ocean Dynamics," World Scientific.

Laval, B., Imberger, J., Hodges, B.R., and Stocker, R. (2003), "Modeling circulation in lakes: spatial and temporal variations," Limnology and Oceanography 48(3), 983-994.

Leonard, B.P. (1991), "The ULTIMATE conservative difference scheme applied to unsteady one-dimensional advection," *Computational Methods in Applied Mechanics and Engineering*, **88**, 17-74.

Lin, B. and Falconer, R.A. (1997). "Tidal flow and transport modeling using ULTIMATE QUICKEST," Journal of Hydraulic Engineering, 123:303-314.

Roberts, P.J.W., Snyder, W.H. & Baumgartner, D.J. (1989a), Ocean Outfalls I, Submerged wastefield formation, *J. Hydraulic Engineering*, **115**, 1-25

Roberts, P.J.W., Snyder, W.H. & Baumgartner, D.J. (1989b), Ocean Outfalls II, Spatial evolution of submerged wastefield, *J. Hydraulic Engineering*, **115**, 26-48

Roberts, P.J.W., Snyder, W.H. & Baumgartner, D.J. (1989c), Ocean Outfalls III, Effect of diffuser design on submerged wastefield, *J. Hydraulic Engineering*, **115**, 49-70

Robson, B.J. and Hamilton, D. P. (2002). "Three-Dimensional Modeling of a Microcystis bloom event in a Western Australian Estuary." Centre For Water Research, The University of Western Australia, 491- 496 pp.

Romero, J.R. and Antenucci, J. (2004). "The Tiete River: Supply for Sao Paolo, Brazil," from CWR Models: Bytes and Nybbles, Autumn 2004, Issue 10, page 4.

Romero, J.R. and Imberger, J. (1999). "Lake Pamvotis Project-Final report", ED report WP 1364 JR, Centre for Water Research, Crawley, Western Australia, Australia.

Spigel, R.H.; Imberger, J.; and Rayner, K.N. (1986), "Modeling the diurnal mixed layer," *Limnology and Oceanography*, **31**, 533-56.

Staniforth, A. and Côté, J. (1991). "Semi-Lagrangian integration schemes for atmospheric models – a review," Monthly Weather Review, 119:2206-2223.

Stevens, C. and Imberger, J. (1996). "The initial response of a stratified lake to a surface shear stress," Journal of Fluid Mechanics, 312:39-66.

Ullman, W.J. and R.C. Aller (1982), "Diffusion coefficients in nearshore marine sediments," *Limnol. Oceanogr., 27,* 552-556.

Wanninkhof, R. (1992), "Relationship between wind speed and gas exchange over the ocean," *J. Geophys. Res., 97(C5),* 7373-7382.

Yeates, Peter (2004). "ELCOM in the Venice Lagoon," from CWR Models: Bytes and Nybbles, Autumn 2004, Issue 10, page 2.

A.3.2 SUPPLEMENTAL REFERENCES

(November 1999), "Course notes, Computational aquatic ecosystem dynamics model, CAEDYM, Special introduction work session," TTF/3/Nov99, Centre for Water Research, University of Western Australia, 51pp.

(January 2000), "Course notes, Estuary & lake computer model, ELCOM, Special introduction training session," TTF/3/JAN2000, Centre for Water Research, University of Western Australia, 21pp+app.

(January 21, 2000) "Instructions for the use of the graphical user interface *modeler* in the configuration & visualization of DYRESM-CAEDYM," Draft version 2, 42pp.

Antenucci, J. and Imberger, J. (1999), "Seasonal development of long internal waves in a strongly stratified lake: Lake Kinneret," *Journal of Geophysical Research* (in preparation).

Antenucci, J. and Imberger, J. (2000), "Observation of high frequency internal waves in a large stratified lake," *5th International Symposium on Stratified Flows, (ISSF5)*, Vancouver, July 2000, **1**, 271-6.

Bailey, M.B. and Hamilton, D.H. (1997), "Wind induced sediment re-suspension: a lake wide model," *Ecological Modeling*, **99**, 217-28.

Burling, M.; Pattiaratchi, C.; and Ivey, G. (1996), "Seasonal dynamics of Shark Bay, Western Australia," *3rd National AMOS Conference*, 5-7 February 1996, University of Tasmania, Hobart, 128.

Chan, C.U.; Hamilton, D.P.; and Robson, B.J. (2001), "Modeling phytoplankton succession and biomass in a seasonal West Australian estuary," *Proceedings, SIL Congress XXVIII* (in press).

Chan, T. and Hamilton, D.P. (2001), "The effect of freshwater flow on the succession and biomass of phytoplankton in a seasonal estuary," *Marine and Freshwater Research* (in press).

De Silva, I.P.D.; Imberger, J.; and Ivey, G.N. (1997), "Localized mixing due to a breaking internal wave ray at a sloping bed," *Journal of Fluid Mechanics*, **350**, 1-27.

Eckert, W.; Imberger, J.; and Saggio, A. (1999), "Biogeochemical evolution in response to physical forcing in the water column of a warm monomictic lake," *Limnology and Oceanography* (submitted).

Gersbach, G.; Pattiaratchi, C.; Pearce, A.; and Ivey, G. (1996), "The summer dynamics of the oceanography of the south-west coast of Australia – The Capes current" *3rd National AMOS Conference*, 5-7 February 1996, University of Tasmania, Hobart, 132.

Hamilton, D.P. (1996), "An ecological model of the Swan River estuary: An integrating tool for diverse ecological and physico-chemical studies," *INTECOL's V International Wetlands Conference 1996 "Wetlands for the Future,"* September 1996, Perth, Australia.

Hamilton, D.P.; Chan, T.; Hodges, B.R.; Robson, B.J.; Bath, A.J.; and Imberger, J. (1999), "Animating the interactions of physical, chemical and biological processes to understand the dynamics of the Swan River Estuary," Combined Australian-New Zealand Limnology Conference, Lake Taupo.

Hamilton, D.P. (2000), "Record summer rainfall induces first recorded major cyanobacterial bloom in the Swan River," *The Environmental Engineer*, **1**(1), 25.

Hamilton, D.; Hodges, B.; Robson, B.; and Kelsey, P. (2000), "Why a freshwater blue-green algal bloom occurred in an estuary: the Microcystis bloom in the Swan River Estuary in 2000," Western Australian Marine Science Conference 2000, Path, Western Australia.

Hamilton, D.P.; Chan, T.; Robb, M.S.; Pattiaratchi, C.B.; Herzfeld, M.; and Hodges, B. (2001), "Physical effects of artificial destratification in the upper Swan River Estuary," *Hydrological Processes*.

Heinz, G.; Imberger, J.; and Schimmele, M. (1990), "Vertical mixing in Überlinger See, western part of Lake Constance," *Aquat. Sci.*, **52**, 256-68.

Herzfeld, M. (1996), "Sea surface temperature and circulation in the Great Australian bight," Ph.D. Thesis, School of Earth Science, Flinders University, South Australia.

Herzfeld, M. and Hamilton, D. (1997), "A computational aquatic ecosystem dynamics model for the Swan River, Western Australia," *MODSIM '97, International Congress on Modeling and Simulation Proceedings*, 8-11 December, 1997, University of Tasmania, Hobart, **2**, 663-8.

Herzfeld, Michael (May 28, 1999), "Computational aquatic ecosystem dynamics model (CAEDYM), An ecological water quality model designed for coupling with hydrodynamic drivers, Programmer's guide," Centre for Water Research, The University of Western Australia, Nedlands, Australia, 133pp.

Hodges, Ben R. (July 1991), "Pressure-driven flow through an orifice for two stratified, immiscible liquids," M.S. thesis, The George Washington University, School of Engineering and Applied Science.

Hodges, Ben R. (March 1997), "Numerical simulation of nonlinear free-surface waves on a turbulent open-channel flow," Ph.D. dissertation, Stanford University, Dept. of Civil Engineering.

Hodges, Ben R. (June 9, 1998), "Heat budget and thermodynamics at a free surface: Some theory and numerical implementation (revision 1.0c)," Working manuscript, Centre for Water Research, The University of Western Australia, 14pp.

Hodges, Ben R. (1999), "Numerical techniques in CWR-ELCOM," Technical report, Centre for Water Research, The University of Western Australia. (in preparation)

Hodges, Ben R. (2000), "Recirculation and equilibrium displacement of the thermocline in a wind-driven stratified lake," *5th International Symposium on Stratified Flows, (ISSF5)*, Vancouver, July 2000, **1**, 327-30.

Hodges, B.R., Herzfeld, M., and Hamilton, D. (1998), "A computational aquatic ecosystem dynamics model for the Swan River," *EOS Trans. AGU*, **79**(1), Ocean Sciences Meet. Suppl. OS11P-02.

Hodges, B.; Herzfeld, M.; Winters, K.; and Hamilton, D. (1998), "Interactions of a surface gravity waves and a sheared turbulent current," *EOS Trans. AGU*, **79**(1), Ocean Sciences Meet. Suppl. OS53.

Hodges, B.R. and Street, R.L. (1999), "On simulation of turbulent nonlinear free-surface flow," *Journal of Computational Physics*, **151**, 425-57.

Hodges, B.R.; Imberger, J.; Laval, B.; and Appt, J. (2000), "Modeling the hydrodynamics of stratified lakes," *Fourth International conference on HydroInformatics*, Iowa Institute of Hydraulic Research, Iowa City, 23-27 July 2000.

Hodges, B.R. and Imberger, J. (2001), "Simple curvilinear method for numerical methods of open channels," *Journal of Hydraulic Engineering*, **127**(11), 949-58.

Hodges, Ben R. and Street, Robert L. (1996), "Three-dimensional, nonlinear, viscous wave interactions in a sloshing tank," *Proceedings of the Fluid Engineering Summer Meeting 1996*, Vol. **3**, FED-Vol. **238**, ASME, 361-7.

Hodges, Ben R. and Street, Robert L. (1998), "Wave-induced enstrophy and dissipation in a sheared turbulent current," *Proceedings of the Thirteenth Australian fluid Mechanics Conference*, M.C. Thompson and K. Hourigan (eds.), Monash University, Melbourne, Australia, 13-18 December 1998, Vol. **2**, 717-20.

Hodges, B.R., Street, R.L., and Zang, Y. (1996), "A method for simulation of viscous, non-linear, free-surface flows," *Twentieth Symposium on Naval Hydrodynamics*, National Academy Press, 791-809.

Hollan, E. (1998), "Large inflow-driven vortices in Lake Constance," in J. Imberger (ed.), *Physical Processes in Lakes and Oceans. Coastal and Estuarine Studies*, **54,** American Geophysical Union, 123-36.

Hollan, E.; Hamblin, P.F.; and Lehn, H. (1990), "Long-term modeling of stratification in Large Lakes: Application to Lake Constance," in: Tilzer, M.M. and C. Serruya (eds.). *Large Lakes, Ecological Structure and Function***,** Berlin: Springer Verlag, 107-24.

Horn, D.A.; Imberger, J.; and Ivey, G.N. (1999), "Internal solitary waves in lakes – a closure problem for hydrostatic models," *Proceedings of 'Aha Halikoa Hawaiian Winter Workshop*, January 19-22, 1999, University of Hawaii, Manoa.

Horn, D.A.; Imberger, J.; and Ivey, G.N. (1999), "The degeneration of large-scale interfacial gravity waves in lakes," under consideration for publication in *Journal of Fluid Mechanics*.

Horn, D.A.; Imberger, J.; Ivey, G.N.; and Redekopp, L.G. (2000), "A weakly nonlinear model of long internal waves in lakes," *5th International Symposium on Stratified Flows, (ISSF5)*, Vancouver, July 2000, **1**, 331-6.

Imberger, J. (1985), "The diurnal mixed layer," *Limnology and Oceanography,* **30**(4), 737-70.

Imberger, J. (1985), "Thermal characteristics of standing waters: an illustration of dynamic processes," *Hydrobiologia,* **125,** 7-29.

Imberger, J. (1994), "Mixing and transport in a stratified lake," Preprints of *Fourth International Stratified on Flows Symposium,* Grenoble, France, June-July 1994, **3** 1-29.

Imberger, J. (1994), "Transport processes in lakes: a review," in R. Margalef (ed.), *Limnology Now: A Paradigm of Planetary Problems,* Elsevier Science, 99-193.

Imberger, J. (1998), "Flux paths in a stratified lake: A review," in J. Imberger (ed.), *Physical Processes in Lakes and Oceans. Coastal and Estuarine Studies,* **54,** American Geophysical Union, 1-18.

Imberger, J. (1998), "How does the estuary work?" WAERF Community Forum, 25 July 1998, The University of Western Australia.

Imberger, J.; Berman, T; Christian, R.R.; Sherr, E.B.; Whitney, D.E.; Pomeroy, L.R.; Wiegert, R.G.; and Wiebe, W.J. (1983), "The influence of water motion on the distribution and transport of materials in a salt marsh estuary," *Limnology and Oceanography*, **28**, 201-14.

Imberger, J. and Hamblin, P.F. (1982), "Dynamics of lakes, reservoirs, and cooling ponds," *Journal of Fluid Mechanics,* **14**, 153-87.

Imberger, J. and Head, R. (1994), "Measurement of turbulent properties in a natural system," reprinted from *Fundamentals and Advancements in Hydraulic Measurements and Experimentation*.

Imberger, J. and Ivey, G.N. (1991), "On the nature of turbulence in a stratified fluid. Part II: Application to lakes," *Journal of Physical Oceanography,* **21**(5), 659-80.

Imberger, J. and Ivey, G.N. (1993), "Boundary mixing in stratified reservoirs," *Journal of Fluid Mechanics,* **248**, 477-91.

Imberger, J. and Patterson, J.C. (1981), "A dynamic reservoir simulation model – DYRESM: 5," In H.B. Fischer (ed.) *Transport Models for Inland and Coastal Waters,* Academic Press, 310-61.

Imberger, J. and Patterson, J.C. (1990), "Physical limnology," In: *Advances in Applied Mechanics,* **27**, 303-475.

Ivey, G.N. and Corcos, G.M. (1982), "Boundary mixing in a stratified fluid," *Journal of Fluid Mechanics,* **121**, 1-26.

Ivey, G.N. and Imberger, J. (1991), "On the nature of turbulence in a stratified fluid. Part I: The energetics of mixing," *Journal of Physical Oceanography,* **21**(5), 650-8.

Ivey, G.N.; Imberger, J.; and Koseff, J.R. (1998), "Buoyancy fluxes in a stratified fluid," in J. Imberger (ed.), *Physical Processes in Lakes and Oceans. Coastal and Estuarine Studies,* **54,** American Geophysical Union, 377-88.

Ivey, G.N.; Taylor, J.R.; and Coates, M.J. (1995), "Convectively driven mixed layer growth in a rotating, stratified fluid," *Deep-Sea Research I.,* **42**(3), 331-49.

Ivey, G.N.; Winters, K.B; and De Silva; I.P.D. (1998), "Turbulent mixing in an internal wave energized benthic boundary layer on a slope," submitted to *Journal of Fluid Mechanics*.

Jandaghi Alaee, M.; Pattiaratchi, C.; and Ivey, G. (1996), "The three-dimensional structure of an island wake," *8th International Biennial Conference. Physics of Estuaries and coastal Seas (PECS)* 9-11 September 1996, the Netherlands, 177-9.

Javam, A; Teoh, S.G.; Imberger, J.; and Ivey, G.N. (1998), "Two intersecting internal wave rays: a comparison between numerical and laboratory results," in J. Imberger (ed.), *Physical Processes in Lakes and Oceans. Coastal and Estuarine Studies***, 54,** American Geophysical Union, 241-50.

Kurup, R.; Hamilton, D.P.; and Patterson, J.C. (1998), "Modeling the effects of seasonal flow variations on the position of a salt wedge in a microtidal estuary," Estuarine Coastal *and Shelf Science*, **47**(2), 191-208.

Kurup, R.G.; Hamilton, D.P.; and Phillips, R.L. (2000), "Comparison of two 2-dimensional, laterally averaged hydrodynamic model applications to the Swan River Estuary," *Mathematics and Computers in Simulation,* **51**(6), 627-39.

Laval, B.; Hodges, B.R.; and Imberger, J. (2000), "Numerical diffusion in stratified lake," *5th International Symposium on Stratified Flows, (ISSF5)*, Vancouver, July 2000, **1**, 343-8.

Lemckert, C. and Imberger, J. (1995), "Turbulent benthic boundary layers in fresh water lakes," Iutam Symposium on Physical Limnology, Broome, Australia, 409-22.

Maiss, M.; Imberger, J.; and Münnich, K.O. (1994), "Vertical mixing in Überlingersee (Lake Constance) traced by SF6 and heat," *Aquat. Sci.*, **56**(4), 329-47.

Michallet, H. and Ivey, G.N. (1999), "Experiments on mixing due to internal solitary waves breaking on uniform slopes," *Journal of Geophysical Research*, **104**, 13467-78.

Nehru, A; Eckert, W.; Ostrovosky, I.; Geifman, J.; Hadas, O.; Malinsky-Rushansky, N.; Erez, J.; and Imberger, J. (1999), "The physical regime and the respective biogeochemical processes in Lake Kinneret lower water mass," *Limnology and Oceanography*, (in press).

Ogihara, Y.; Zic, K.; Imberger, J.; and Armfield, S. (1996), "A parametric numerical model for lake hydrodynamics," *Ecological Modeling*, **86**, 271-6.

Patterson, J.C; Hamblin, P.F.; and Imberger, J. (1984), "Classification and dynamic simulation of the vertical density structure of lakes," *Limnology and Oceanography*, **29**(4), 845-61.

Pattiaratchi, C.; Backhaus, J.; Abu Shamleh, B.; Jandaghi Alaee, M.; Burling, M.; Gersbach, G.; Pang, D.; and Ranasinghe, R. (1996), "Application of a three-dimensional numerical model for the study of coastal phenomena in south-western Australia," *Proceedings of the Ocean & Atmosphere Pacific International Conference*, Adelaide, October 1995, 282-7.

Riley, G.A., H. Stommel and D.F. Bumpus, "Quantitative ecology of the plankton of the Western North Atlantic," *Bull. Bingham Oceanogr. Coll., 12(3)*, 1-69, 1949.

Robson, B.J.; Hamilton, D.P.; Hodges, B.R.; and Kelsey, P. (2000), "Record summer rainfall induces a freshwater cyanobacterial bloom in the Swan River Estuary," *Australian Limnology Society Annual Congress*, Darwin, 2000.

Saggio, A. and Imberger, J. (1998), "Internal wave weather in a stratified lake," *Limnology and Oceanography*, **43**, 1780-95.

Schladow, S.G. (1993), "Lake destratification by bubble-plume systems: Design methodology," *Journal of Hydraulic Engineering*, **119**(3), 350-69.

Smagorinsky, J. (1963) "General circulation experiments with the primitive equations, ´*Monthly Weather Review*, *91*, 99-152.

Spigel, R.H. and Imberger, J. (1980), "The classification of mixed-layer dynamics in lakes of small to medium size," *Journal of Physical Oceanography,* **10**, 1104-21.

Steele, J.H. (1962), "Environmental control of photosynthesis in the sea," *Limnol. Oceanogr., 7*, 137-150.

Taylor, J.R. (1993), "Turbulence and mixing in the boundary layer generated by shoaling internal waves," *Dynamics of Atmospheres and Oceans,* **19**, 233-58.

Thorpe, S.A. (1995), "Some dynamical effects of the sloping sides of lakes," *IUTAM Symposium on Physical Limnology*, Broome, Australia, 215-30.

Thorpe, S.A. (1998), "Some dynamical effects of internal waves and the sloping sides of lakes," in J. Imberger (ed.), *Physical Processes in Lakes and Oceans. Coastal and Estuarine Studies,* **54,** American Geophysical Union, 441-60.

Thorpe, S.A. and Lemmin, U. (1999), "Internal waves and temperature fronts on slops," *Annales Geophysicae,* **17**(9), 1227-34.

Unlauf, L; Wang, Y.; and Hutter, K. (1999), "Comparing two topography-Following primitive equation models for lake circulation," *Journal of Computational Physics,* **153**, 638-59.

Winter, K.B. and Seim, H.E. (1998), "The role of dissipation and mixing in exchange flow through a contracting channel," submitted to *Journal of Fluid Mechanics*.

Winter, K.B.; Seim, H.E.; and Finnigan, T.D. (1998), "Simulation of non-hydrostatic, density-stratified flow in irregular domains," submitted to *International Journal of Numerical Methods in Fluids*.

Zhu, S. and Imberger, J. (1994) "A three-dimensional numerical model of the response of the Australian North West Shelf to tropical cyclones," in: *J. Austral. Math. Soc. Ser.***, B 36,** 64-100.